Uncertainty After Dark: Evidence from 19 Million Nights of Sleep*

Fotis Grigoris Gill Segal Chao Ying

June 2026

Abstract

Using minute-level wearable-device data on 51,191 adults in the National Institutes of Health's (NIH) *All of Us* Research Program, covering over 19 million person-nights, we show that sleep quality is a high-frequency biomarker of macroeconomic and financial uncertainty. Higher uncertainty predicts lower deep sleep and sleep efficiency for several nights, a "wake-and-see" effect that complements the classic "wait-and-see" channel. The effects are robust to environmental, physiological, and behavioral controls, are stronger for uncertainty than for first-moment market shocks, and are larger in higher-income areas. We also document a reverse channel from physiology to markets: nights of unusually poor sleep predict weaker opening-hour equity returns, lower next-day market liquidity, and higher realized volatility, with stronger effects in retail-dominated stocks. Finally, poor sleep positively relates to the conditional market price of aggregate risk, consistent with lower aggregate risk-bearing capacity. Overall, population sleep provides a high-frequency physiological state variable linking uncertainty, human capital, and market functioning in real time.

Preliminary & Incomplete

Keywords: Uncertainty, Sleep, Health Economics, Behavioral, Macro-Finance

*Grigoris: (fgrigoris@uiowa.edu), Tippie College of Business, University of Iowa; Segal: (Gill_Segal@kenan-flagler.unc.edu), Kenan-Flagler Business School, University of North Carolina at Chapel Hill; Ying: (chaoying@cuhk.edu.hk), Chinese University of Hong Kong. We are grateful for comments from Zhi Da, Umit Gurun, Stefan Nagel, Stijn Van Nieuwerburgh, Jinfei Sheng, and seminar and conference participants at the 2026 FSU Truist Beach Conference, 2026 Kentucky Finance Conference, and the University of Iowa. We thank Hongwei Zhou for excellent research assistance. We gratefully acknowledge All of Us participants for their contributions, without whom this research would not have been possible. We also thank the National Institutes of Health's All of Us Research Program for making available the participant data examined in this study.

"I argue that, in order to move from the idealized homo economicus to modeling a true human (homo experiens), economic theory and empirics need to account for both their minds and bodies to be shaped by past lived experience... concepts from biology, neuropsychiatry, and medicine can guide our model of human decision-making."
— Ulrike Malmendier, 2026 AFA Presidential Address.

Aggregate shocks affect the economy not only by changing prices, constraints, and incentives, but also by changing the state of the agents who make decisions and bear risk. In most macro-finance applications, this human state is latent: it is inferred indirectly from quantities or asset prices rather than measured in the agents themselves. This study provides direct, high-frequency evidence on this latent dimension by showing that aggregate uncertainty leaves a measurable imprint on people's nightly physiology at population scale. Uncertainty plays a major role in macro-finance: it slows investment and hiring through "*wait-and-see*" behavior and depresses valuations. But this standard account misses a more immediate margin. Using minute-level sleep-stage data from 51,191 adults and 19.5 million person-nights in the National Institutes of Health (NIH)'s *All of Us* Research Program,[1] we document that uncertainty systematically predicts lower sleep quality for several nights. We term this a "*wake-and-see*" effect: when uncertainty rises, people lie awake longer and achieve less deep sleep, revealing an immediate health and human-capital cost of these shocks. This physiological response is robust, economically meaningful, and more strongly associated with uncertainty (EPU, VIX) than with market returns. Importantly, sleep quality also predicts next-day market quality and affects the market price of aggregate risk, closing a two-way link between nightly physiology and the financial system.

Our contribution extends beyond documenting a new health consequence of uncertainty. More broadly, this paper addresses a central challenge in macro-finance. Uncertainty is difficult to identify, measure, and map into welfare in real time. It may partly reflect an endogenous response to bad times rather than an exogenous impulse. Because it is unobserved, text-based indices, option-implied measures, realized volatility, and survey disagreement do not always agree. Its welfare consequences may also be immediate and non-pecuniary because uncertainty can spike and resolve faster than consumption or other standard macro quantities move. In asset pricing, it is not always clear whether what is priced is realized

[1]We gratefully acknowledge *All of Us* participants for their contributions, without whom this research would not have been possible. We also thank the National Institutes of Health's All of Us Research Program for making available the participant data examined in this study.

variance risk or forward-looking uncertainty risk. Yet if uncertainty, and more broadly any candidate macro factor, is truly welfare-relevant and priced, it should not appear only in consumption and returns. It should also leave a mark on economic agents. Sleep, and especially deep sleep, is a natural physiological margin through which these effects may operate because it is biologically restorative, objectively measurable at high frequency, and tightly linked to cognition, attention, and risk tolerance. If uncertainty degrades sleep, that non-pecuniary cost can also propagate into pecuniary outcomes by altering investors' capacity to bear risk.

To operationalize this idea, we use minute-level wearable data that record not just total sleep duration, but also time in bed, wake time, and sleep stages. We build daily time series of two standard measures of sleep quality: (i) the proportion of deep (slow-wave) sleep and (ii) sleep efficiency (minutes asleep divided by minutes in bed). We first remove individual fixed effects and then aggregate these measures daily to the cross-sectional median across individuals. We next purge the resulting series of predictable movements due to exogenous environmental factors such as seasonality (day-of-the-week and month-of-the-year effects), weather (sunlight, temperature, rainfall), infectious disease exposure (COVID-19 cases), and broad population mood inferred from social media, and define the residual as *abnormal sleep*. [2] Unlike survey sleep or mood proxies, these measures capture latent physiological responses rather than expressed behavior. The scale and granularity of these data allow us to trace high-frequency physiological responses to shifts in macroeconomic and financial conditions.

Our first set of facts comes from an event study around 50 salient domestic and geopolitical news dates between 2017 and 2023 that capture large and plausibly exogenous events that raise economic and geopolitical uncertainty in the short run (e.g., the COVID-19 pandemic declaration, the U.S. Capitol attack, Russia's invasion of Ukraine, the Silicon Valley Bank collapse). Abnormal sleep falls sharply on the event day, by almost half a standard deviation for both deep-sleep share and sleep efficiency, before reverting over the following days. These patterns show that our abnormal-sleep measure responds to plausibly exogenous shocks and that, unlike macro aggregates, economic news is *immediately* reflected in nightly

[2] As a simple validation exercise, we show that the monthly abnormal-sleep series comove negatively with Google search intensity for terms such as "bad sleep," "can't sleep," and "melatonin." We view this only as validation, not as a substitute for the wearable-based measure. Google searches are expressed behavior, available only at a lower frequency, and reflect attention to sleep problems rather than physiological sleep itself. They cannot recover stage-specific sleep, distinguish deep sleep from sleep efficiency, or trace nightly within-person responses to macro-financial shocks.

physiology.

We then turn to a comprehensive regression analysis to quantify the role of uncertainty. In daily data, a one-standard-deviation rise in economic policy uncertainty (EPU) is associated with a 0.12 standard-deviation decline in deep-sleep share and a 0.22 standard-deviation decline in sleep efficiency, controlling for the full set of environmental, physiological, and behavioral controls. Uncertainty's effects on sleep quality are stable in sign and magnitude across specifications. Controlling for sunlight, temperature, rainfall, physical activity, mood, and other covariates does not materially attenuate the coefficients on uncertainty. In fact, the marginal effect of uncertainty on sleep is on par with the effects of rainfall and mood on these measures. The effects are robust to alternative uncertainty proxies, such as equity volatility (VIX), but do not hold when we substitute uncertainty with first-moment proxies (e.g., daily market returns, the investment-minus-consumption spread, or the intermediary-capital factor). Thus, the physiological response loads on forward-looking second-moment risk rather than on bad realized first-moment outcomes.

To characterize the dynamics of the effect, we estimate VAR-based impulse response functions (IRFs) with recursive identification. A one-standard-deviation uncertainty shock is associated with an immediate reduction in deep-sleep share and sleep efficiency, and each decline persists for several nights. Generalized IRFs and smooth local projections deliver nearly identical IRFs, and the patterns repeat when we replace EPU with equity return volatility. In contrast, we once again show that first-moment shocks to equity returns do not produce comparable changes in sleep quality. Together, these results show that elevated uncertainty, rather than contemporaneous adverse market return realizations, affects the physiological channel. The persistence of these responses implies that even modest nightly effects accumulate into economically meaningful sleep losses over time.

Heterogeneity is economically informative. The IRFs associated with uncertainty shocks are larger in higher-income areas, consistent with greater exposure to or stakes in financial shocks, while they are comparable across racial, gender, and educational groups and are only modestly different by age. This cross-sectional evidence is inconsistent with a narrow sample-composition story (e.g., only select individuals are affected) and indicates a broad population-wide physiological response that scales with economic exposure.

Finally, we show a reverse channel from sleep physiology to financial markets. Nights of unusually poor sleep at the population level predict deterioration in measures of market quality on the following trading day. Lower abnormal sleep quality, and particularly reduced deep sleep, predicts weaker early-session equity returns, higher realized market volatility, more downside relative to upside semivariance, and lower market liquidity (higher Amihud illiquidity) the next day. The effects are concentrated in the first 60 to 180 minutes of trading and taper off afterward, consistent with sleep-impaired attention and slower information processing at the market open. These findings hold after controlling for the lagged effects of prior-day EPU and close-to-open returns that capture overnight news. The effects are generally stronger among stocks where trading is more retail-dominated.

We also connect our population-level sleep metrics to standard asset-pricing theory by examining whether sleep quality scales the conditional market price of aggregate risk, thereby serving as a proxy for the representative agent's risk aversion and capacity to bear risk. We specify a stochastic discount factor where the price of risk is a function of sleep quality and estimate the model using a Generalized Method of Moments estimator across a comprehensive set of test assets, including portfolios sorted by size, momentum, profitability, and industry returns. Our results reveal that improvements in aggregate sleep have a consistently negative and statistically significant effect on the market price of risk. Economically, this suggests that a well-rested population exhibits a higher risk-bearing capacity, leading to lower required risk premiums. In contrast, sleep deprivation can act as a friction that increases marginal utility and the compensation required for bearing systematic risk, above and beyond the conventional quantity-of-risk effect captured by volatility.

Economic magnitude. How large are these effects in economic terms? We evaluate this using both relative benchmarking and absolute pecuniary costs. First, the OLS evidence suggests that the physiological response to second-moment risk is substantially larger than the response to tangible environmental shocks. In absolute terms, the impact of uncertainty on sleep efficiency is about 4 times (0.22 / 0.05) larger than the impact of a comparable shock to rainfall (see Table 2).

Second, we contextualize these relative physiological costs in terms of pecuniary losses. Following Bloom (2009), we focus on the effects of a two-standard-deviation shock to uncertainty. Our impulse response estimation shows that sleep efficiency cumulatively declines by 1.16 standard deviations in the week following such a shock. Scaling this standardized effect in a conservative manner, vis-a-vis existing literature, yields an implied loss of roughly

33.4 to 51.7 minutes of sleep per capita in the week following the shock.[3] Aggregating this average effect across the 51,191 individuals in the cohort suggests that the shock is related to a total sleep time reduction of roughly 28,500 to 44,100 hours.

Finally, Gibson and Shrader (2018) find that a 1-hour increase in weekly sleep raises worker earnings by about 1.1% in the short run. Applying this elasticity indicates that a two-standard-deviation uncertainty shock that under a cautious calibration trims, on average, approximately 42.6 minutes of sleep per week implies nearly a 0.8% decline in short-run earnings ($(42.6/60) \times 1.1\%$). While such pecuniary calculations inherently rely on prior literature-based tuning, this exercise illustrates how our estimated physiological friction systematically impairs human capital exactly when market conditions demand peak cognitive capacity.[4]

In sum, sleep metrics provide a high-frequency and objective welfare measure that links uncertainty to real-time human-capital depreciation. For macroeconomics, the results reveal a new welfare margin: uncertainty shocks not only depress investment through "*wait-and-see*" but also tax nightly restoration through "*wake-and-see*," impairing cognition and productivity before those costs appear in standard aggregates. Because uncertainty is latent and its proxies often disagree, abnormal sleep also provides a model-free biomarker of second-moment risk. For finance, our results document a two-way link between markets and physiology: uncertainty worsens sleep, poor sleep degrades next-day market quality, and sleep scales the conditional market price of risk by shifting aggregate risk-bearing capacity. More broadly, population-scale wearable data give macro-finance a new empirical object with which to study whether proposed shocks and candidate factors are truly welfare relevant and potentially priced, broadening welfare measurement beyond prices, quantities, and consumption to the biological channels through which risk is experienced.

Related Literature. Existing research shows that uncertainty is welfare decreasing, with theoretical and empirical evidence that it depresses real economic growth (see, e.g., Gilchrist, Sim and Zakrajšek, 2014; Jurado, Ludvigson and Ng, 2015; Fernández-Villaverde,

[3] Footnote 15 on Page 28 contains the calculations underlying these figures.

[4] RAND Europe estimates that insufficient sleep costs the U.S. economy up to $411 billion (about 2% of GDP) and 1.23 million working days per year, underscoring the plausibility that repeated uncertainty-driven sleep losses lead to large output costs (see https://www.rand.org/pubs/research_reports/RR1791.html). The CDC also recommends at least seven hours of sleep for adults, so even modest repeated disruptions push a large share of the population further below healthy thresholds (see https://www.cdc.gov/sleep/data-research/facts-stats/adults-sleep-facts-and-stats.html).

Guerrón-Quintana, Kuester and Rubio-Ramírez, 2015; Arellano, Bai and Kehoe, 2019; Basu and Bundick, 2017), while also lowering valuations and raising risk premia (see, e.g., Bansal and Yaron, 2004; Boguth and Kuehn, 2013; Buraschi, Trojani and Vedolin, 2014; Kung and Schmid, 2015; Johannes, Lochstoer and Mou, 2016; Ai and Kiku, 2016; Bretscher, Hsu and Tamoni, 2023; Bekaert, Engstrom and Xu, 2022). Real-options models such as McDonald and Siegel (1986) and, more recently, Bloom, Bond and Van Reenen (2007), Bloom (2009), and Alfaro, Bloom and Lin (2024) link these negative effects of uncertainty to "*wait-and-see*" behavior. Firms pause investment and hiring, thereby generating short-run contractions. We complement this literature by uncovering a "*wake-and-see*" channel: uncertainty shocks register on people's bodies by reducing deep sleep and sleep efficiency for several nights. These effects load on risk (policy uncertainty and return volatility) rather than first-moment market fluctuations, revealing a new welfare margin through which uncertainty imposes immediate human-capital costs. More generally, this evidence suggests that population sleep can serve as a high-frequency physiological state variable that reveals when macroeconomic shocks are experienced as welfare-relevant by economic agents.

Our focus on deep sleep and sleep efficiency as economically relevant, high-frequency health metrics is grounded in sleep medicine research. Irish, Kline, Gunn, Buysse and Hall (2015) review evidence that stress exposure is associated with lower sleep quality. Banks and Dinges (2007) review experimental evidence that sleep restrictions carry behavioral and physiological costs, including attention lapses and reduced cognitive performance. Regarding deep sleep, slow-wave sleep supports learning and memory consolidation (Rasch and Born, 2013), and suppressing slow-wave sleep for just a few nights measurably worsens insulin sensitivity, despite unchanged total sleep time (Tasali, Leproult, Ehrmann and Van Cauter, 2008).

Our paper is also related to a broader body of evidence linking adverse macroeconomic conditions to worsened mental health. Following the 2008 crash, older U.S. adults experienced significant increases in depressive symptoms and antidepressant use (McInerney, Mellor and Nicholas, 2013). Parmar, Stavropoulou and Ioannidis (2016) and Chang, Stuckler, Yip and Gunnell (2013) document higher rates of anxiety, depression, and suicide during the Great Recession. Engelberg and Parsons (2016) show more broadly that adverse stock returns can trigger an uptick in hospital admissions, particularly for the treatment of psychological conditions. The aforementioned studies either focus on a specific episode (e.g., the 2008 financial crisis) or on health outcomes after bad first-moment shocks have already materialized. By contrast, we show an anticipatory physiological response: uncertainty itself (before negative outcomes are realized) degrades nightly sleep, even after controlling for market return realizations. Moreover, our results suggest that the health costs of poor economic conditions are more widespread than previously thought: whereas hospitalizations are triggered by extreme left-tail events and only affect a small fraction of the population, sleep quality responds even to diffusive shocks and is continuously borne by all individuals, thereby creating a channel for a feedback effect onto the real and financial economy.

Economic uncertainty, in particular, can impact health measures. Higher U.S. suicide rates have been associated with economic policy uncertainty (Antonakakis and Gupta, 2017); and uncertainty correlates with unhealthy choices consistent with self-control costs, such as greater consumption of alcohol and cigarettes (Kalcheva, McLemore and Sias, 2021). Importantly, these studies rely on *aggregate and low-frequency* outcomes (suicides, health-care utilization, or annually reported lifestyle behaviors) that are informative but cannot capture immediate physiological responses or day-to-day heterogeneity.[5] In contrast, we use wearable device data to show that uncertainty registers within nights, and we quantify the persistence and economic magnitude of these effects.

Socioeconomic disparities in sleep are well documented. Poor sleep quality is prevalent among lower-income and minority groups (Patel, Grandner, Xie, Branas and Gooneratne, 2010; Grandner, Patel, Gehrman, Xie, Sha, Weaver and Gooneratne, 2010). Studies also show that sleep duration declines with income both across countries and across income groups within countries (Jara, Perez and Wagner, 2025). While most of this work characterizes static or long-run differences, we study *dynamic* sleep responses to economic shocks. Notably, the sleep of affluent households is more adversely affected by rising uncertainty.

Finally, our analysis linking nightly physiology to next-day market quality connects to research on sentiment and attention in financial markets. Non-economic shocks that affect

[5] We note that sleep data are also available from the American Time Use Survey (ATUS). However, relative to the *All of Us* data, the ATUS relies on a single-day, telephone time-diary recall of minutes "sleeping," which is subjectively measured, whereas the *All of Us* data provides objective measures from wearable devices (i.e., Fitbits). Moreover, ATUS is primarily cross-sectional, with respondents interviewed once about the prior 24 hours, with annual samples on the order of approximately seven to 13 thousand individuals per year. This means that the ATUS data cannot track day-to-day dynamics within an individual. By contrast, *All of Us* now includes longitudinal Fitbit data for about 50 thousand participants, many of whom provide months or years of daily records. Finally, ATUS records sleep duration only and thus cannot capture stage-specific physiology (e.g., changes in deep sleep) that is central to our analysis.

mood move prices and liquidity: national soccer defeats predict next-day market declines (Edmans, García and Norli, 2007); daylight-saving transitions (with potential sleep loss) may be followed by abnormally low returns and poorer household financial decision-making (Kamstra, Kramer and Levi, 2000; Pinegar, 2002; Freed, 2022; Gonzalez and Li, 2024); sunshine correlates with higher returns (Hirshleifer and Shumway, 2003); later local sunsets, which proxy for sleep disruption and reduced mental alertness, are associated with lower abnormal returns on retail investors' trades (Han, Hirshleifer, Sheng and Sun, 2025); and distracting events lead investors to underreact to earnings news (Hirshleifer, Lim and Teoh, 2009).[6] Broader sentiment measures also forecast returns and trading activity (e.g., Baker and Wurgler (2007) and Da, Engelberg and Gao (2015)).

We differ from these earlier studies by uniquely combining (i) direct wearable-based sleep measures, which reveal a *continuous* high-frequency impact of lowered sleep, rather than isolated-event effects, (ii) the effects of sleep on *aggregate* market outcomes, rather than individual-specific trades or firm-specific gains, and (iii) *unexpected time-series* variation in sleep, above and beyond environmental factors, rather than predictable cross-sectional sleep variation driven by geography or daylight cycles. Our focus on *deep*-sleep dynamics, rather than sleep duration or timing, reveals a distinct physiological pathway through which attention and risk processing affect market quality.

The rest of the paper is organized as follows. Section 1 describes and summarizes the data. Section 2 shows empirical results related to the impact of uncertainty on sleep. Section 3 explores the converse relationship between sleep and market quality, while Section 4 concludes.

1 Data

1.1 Primary Database

We source all health-related data from the *All of Us* Research Program that is administered by the US National Institutes of Health (NIH). This research program, which was launched in 2015 and is described by All of Us Research Program Investigators (2019), aims to accelerate

[6]Other sentiment-based effects on valuations include Cao and Wei (2005); Da, Engelberg and Gao (2011); Goetzmann, Kim, Kumar and Wang (2015); Stambaugh, Yu and Yuan (2012); Antoniou, Doukas and Subrahmanyam (2013); Hillert, Jacobs and Müller (2014); Peress (2014); Hirshleifer, Jiang and DiGiovanni (2020).

health and medical breakthroughs by gathering comprehensive and granular health care data from a diverse population in the United States. As of October 2025, the program has enrolled more than 597,000 individuals who have completed the initial steps required to join (e.g., agreeing to share their electronic health records and providing at least one biospecimen to be stored at the program's biobank). The dataset is continuously expanding and includes anonymized health records, genomic data, survey responses that capture social, environmental, and lifestyle characteristics, as well as real-time health measurements from wearable devices for a subset of individuals.[7]

Our analysis specifically leverages the wearable device data available for 51,191 adults included in the *All of Us* cohort. These data are made available through a partnership between the NIH and Fitbit, a leading manufacturer of wearable devices that was acquired by Google in January 2021. This partnership allows Fitbit owners who are registered with the *All of Us* Research Program to consent to contribute their data from the wearable device to the research program. Users can provide their wearable device data via either the Bring Your Own Device (BYOD) program or the Wearables Enhancing *All of Us* Research (WEAR) study, which provides Fitbit devices to individuals who identify with communities that are underrepresented in medical research.[8]

For the purpose of our study, the data from these wearable devices include granular (minute-level) data on sleep. Beyond recording the total amount of time each individual sleeps each night, these devices also record (i) the amount of time spent in bed, which captures the combination of how long it takes to fall asleep, as well as the actual time spent asleep and the time spent awake during the night, and (ii) the number of minutes spent in the light, rapid-eye movement (REM), and deep (slow wave) stages of sleep. These granular data allow us to capture the length and quality of each individual's sleep on a daily basis. Moreover, the wearable device data also include details on the user's physical activity (e.g., minutes engaged in physical activity) and heart rate (e.g., beats per minute).

We employ data from Version 8 of the Controlled Tier of the *All of Us* Curated Data Repository. This version runs from March 26, 2017, through October 1, 2023. In pre-processing the data for our study, we only include observations for which the data's "is_main_sleep" flag

[7] More detailed summary statistics related to the *All of Us* database are available online at https://www.researchallofus.org/data-tools/data-snapshots/.

[8] See additional details on this WEAR initiative online at https://allofus.nih.gov/article/announcement-all-of-us-adds-data-from-50-more-participants-in-largest-data-expansion-to-date.

is set to one: we focus on each individual's main sleep event each day, dropping entries in the dataset that are related to naps. Overall, these filters provide us with sleep data on 19,542,781 person-nights across 51,191 unique individuals included in the sample.

1.2 Individual Measures

Motivated by the importance of an individual's deep sleep and sleep duration for both short-term outcomes, such as cognitive performance and productivity, and long-term effects, such as cardiovascular risks and mortality, we use the individual-level sleep data to construct two main variables of interest, deep sleep and sleep efficiency, that are defined as

$$\text{DeepSleep}_{i,t} = \frac{\text{Minutes of Deep Sleep}_{i,t}}{\text{Minutes of Sleep}_{i,t}}, \tag{1}$$

and

$$\text{SleepEfficiency}_{i,t} = \frac{\text{Minutes of Sleep}_{i,t}}{\text{Minutes in Bed}_{i,t}}. \tag{2}$$

Here, $(\text{Minutes of Sleep})_{i,t}$ captures the total number of minutes (i.e., the sum of light, REM, and deep minutes) that individual i spent sleeping on day t, $(\text{Minutes of Deep Sleep})_{i,t}$ captures the number of minutes the individual spends in slow-wave sleep, and $(\text{Minutes in Bed})_{i,t}$ reflects the number of minutes an individual spends in bed. We set the sleep day t to correspond to the date on which the individual falls into their main sleep, rather than the date on which the individual wakes up from their main sleep. For example, if an individual goes to sleep at 10:00pm on Wednesday, February 8, 2023, and wakes up at 7:00am on Thursday, February 9, 2023, then sleep date t corresponds to Wednesday, February 8.

Measurement Limitation. When utilizing commercial wearable technology, it is important to distinguish between the measurement of sleep efficiency and deep sleep. Sleep efficiency is measured via actigraphy, which uses an accelerometer to detect movement and classify binary awake-versus-asleep states. Because errors in actigraphy are akin to classical white noise, the econometric implications depend on how sleep efficiency is deployed in our specifications: when sleep efficiency is used as an outcome variable (Section 2), the measurement error inflates residual variance and attenuates statistical significance; when sleep efficiency is used as a predictor (Section 3), it induces standard attenuation bias, meaning our results represent a conservative *lower bound* of the true relation between sleep efficiency disruption and subsequent market outcomes.

Conversely, measuring deep (slow-wave) sleep without measurement noise requires electroencephalography (EEG). Because wearables lack EEG capabilities, they estimate sleep stages using photoplethysmography to track resting heart rate (HR) and heart rate variability (HRV), alongside movement. A potential econometric concern is that uncertainty shocks induce acute psychological stress, which biologically elevates heart rate and autonomic arousal. Consequently, a wearable algorithm may classify an uncertainty-induced state of high physiological arousal as a reduction in deep sleep. We note that (i) even if elevated heart rate is misclassified as reduced deep sleep, it is still indicative that economic factors raise physiological stress; (ii) we provide sensitivity analysis in Appendix IA.B to show that the bias induced by misclassification is economically inconsequential.

1.3 Summary Statistics

Panel A in Table 1 provides summary statistics related to these two proxies of sleep quality. The data show that, on average, an individual spends 15.2% of their sleep time in deep sleep. These figures are in line with the notion that deep sleep should comprise approximately 10% to 20% of a healthy adult's total sleep time. The data also show that the average adult has a sleep efficiency of 87.5%, in line with the view that a healthy adult should spend 85% or more of their time in bed asleep.

Panel B of Table 1 reports personal characteristics for the participants in our sample. The majority of individuals identify as White (81.2%), while 3.3%, 4.7%, and 10.7% identify as Asian, Black, or another race, respectively. Most participants (91.7%) are non-Hispanic, with 6.7% identifying as Hispanic and 1.6% identifying as another ethnicity. The sample is also skewed toward females, who comprise 69.7% of participants. The average age of participants is 54 years, with a median of 55 years. Five percent of individuals are 27 years of age or younger, while another five percent are 77 years of age or older.

The *All of Us* Research Program also provides demographic characteristics related to each participant's geographic location in the U.S., measured at the three-digit ZIP code level. These measures are drawn from the annual American Community Survey (ACS) administered by the Census Bureau. On average, participants reside in areas where 88.5% of individuals have obtained at least a high school degree, and the mean annual income is $66,000. Educational attainment shows relatively little variation across geographies, with 90% of participants living in areas where between 80.2% and 94.5% of residents have com-

Table 1: Summary statistics: Sleep, individual, and demographic characteristics
The table reports summary statistics for the two measures of sleep quality (Panel A) and the sample's individual and demographic characteristics (Panel B). Panel A summarizes the distribution of deep sleep, defined in equation (1), and sleep efficiency, defined in equation (2), across all individual-day observations. We report the mean, standard deviation, median, and the 5th, 10th, 25th, 75th, 90th, and 95th percentiles of these variables. In Panel B, each individual's race, ethnicity, and sex are self-reported upon their enrollment in the *All of Us* Research Program. We express these variables as the share of individuals reporting each category. Birth date, also collected upon onboarding, is used to compute each individual's age (in years). We report the mean, median, standard deviation, and the 5th, 10th, 25th, 75th, 90th, and 95th percentiles of age. The remaining demographic variables come from the American Community Survey (ACS) and are mapped to each participant on the basis of their location, defined at the three-digit ZIP-code level. "Education," "Income," and "Assistance" denote, respectively, the share of adults with at least a high-school diploma, the median household income (in thousands of dollars), and the share of households receiving income assistance in the corresponding area. "Vacant" denotes the percentage of vacant households. "Deprivation" reflects the value of an area-level deprivation index at the three-digit ZIP-code level. A complete definition of each variable is provided in Section IA.A of the Internet Appendix.

Panel A: Sleep-Related Characteristics									
	Mean	Std	p5	p10	p25	Median	p75	p90	p95
Deep sleep	0.152	0.036	0.094	0.106	0.126	0.152	0.177	0.199	0.211
Sleep efficiency	0.875	0.018	0.844	0.852	0.864	0.876	0.887	0.897	0.902
Panel B: Individual and Demographic Characteristics									
	Asian	Black	White	Other					
Race	0.033	0.047	0.812	0.107					
	Hispanic	Non-Hispanic	Other						
Ethnicity	0.067	0.917	0.016						
	Female	Male	Other						
Sex	0.697	0.300	0.004						
	Mean	Std	p5	p10	p25	Median	p75	p90	p95
Age (Years)	53.856	16.385	27.132	31.168	40.214	55.233	68.256	74.292	77.292
Education	88.493	4.834	80.150	82.824	86.003	89.307	91.913	93.789	94.487
Income ($k)	66.015	17.232	45.696	47.874	54.647	61.390	74.163	88.430	99.513
Assistance	13.284	5.394	5.998	7.276	9.643	12.637	16.193	20.172	22.939
Poverty	14.451	5.107	6.669	8.160	10.958	13.982	17.715	20.588	22.654
Deprivation	31.066	5.869	21.919	24.027	27.592	30.322	34.779	38.846	40.578

pleted high school. By contrast, income varies more substantially: the standard deviation is \$17,000 per annum, and 90% of participants live in areas where average income ranges from \$45,700 to \$99,500 per year.

The average person lives in an area where 13.3% of households received income assistance benefits in the past 12 months, and 14.5% of households lived below the federal poverty line in the previous year. Finally, the typical individual lives in a location where the Nationwide Community Deprivation Index of Brokamp, Beck, Goyal, Ryan, Greenberg and Hall (2019), a multifaceted measure of community material deprivation constructed from ACS data, is 31.1%. This is broadly in line with the national mean value of this index and suggests that individuals represented by the data live in similar locations to those of the typical U.S. household.

We emphasize that the wearable subcohort is not designed to be nationally representative, and it is likely more health-engaged than the U.S. population as a whole. Our objective is therefore not to recover exact population sleep levels, but to test whether high-frequency physiological responses to uncertainty are detectable in a large national cohort. In that sense, the time-series relations we study are informative about mechanism even if the cohort differs from the population in levels.

1.4 Aggregate Measures

1.4.1 Sleep Quality at the Aggregate

Although our data includes detailed biometric information on over 50 thousand *unique* individuals, we are primarily interested in how the *typical* individual's sleep quality varies with adverse economic conditions. As such, we aggregate the raw data on approximately 19 million person-day sleep records into two time series, DeepSleep_t and SleepEfficiency_t, that represent the typical individual's sleep quality on each day of the sample period. We obtain these time series through the steps outlined below.

First, an analysis of variance (ANOVA) test shows that about 30% of the variation in sleep quality arises between individuals. Thus, we remove individual fixed effects from all health metrics of interest to eliminate across-individual differences and cleanly isolate within-individual variation in sleep quality. We then aggregate the *individually-demeaned* data for $\text{DeepSleep}_{i,t}$ and $\text{SleepEfficiency}_{i,t}$ across all individuals i in the sample by computing their daily median value. The median is used to minimize sensitivity to any outlier observations, although similar results are obtained by computing daily across-individual averages.

Second, we only retain aggregate observations if the underlying cross-section is sufficiently large. Although the wearables data begin on March 26, 2017, days prior to April 26, 2017 feature fewer than 1,000 unique individuals per day. As such, we set the start date of the aggregate time series to April 26, 2017. Figure IA.D.1 in the Internet Appendix shows how coverage, measured in thousands of participants per day, evolves over the remainder of the sample period. The figure shows that the number of participants in the *All of Us* program is steadily increasing over time, leading to potential time trends. For instance, the left panel of Figure IA.D.2 in the Internet Appendix shows that the raw median values of DeepSleep and SleepEfficiency trend down over time. To ensure stationarity, we linearly detrend each of the time series (see the right panel of the same figure). We ensure that our baseline results are robust to this detrending.

Lastly, we winsorize the aggregate sleep series at the 1% level to reduce the influence of a small number of extreme but predictable calendar-related outliers, most notably around the onset of Daylight Saving Time. Figure IA.D.5 plots the raw and winsorized series, and the Internet Appendix reports robustness to alternative preprocessing choices, including specifications without winsorization.

1.4.2 Abnormal Sleep Quality

We define abnormal sleep as sleep quality that cannot be explained by observed physiological conditions, environmental conditions, or broad population mood. Specifically, abnormal sleep quality on day t is the residual of the projection:

$$\text{SleepQuality}_t = \beta_0 + \delta_t + \mu_t + \boldsymbol{x}_t'\boldsymbol{\beta} + \varepsilon_t, \tag{3}$$

where $\text{SleepQuality}_t \in \{\text{DeepSleep}_t, \text{ SleepEfficiency}_t\}$, δ_t are day-of-the-week fixed effects, μ_t is a month-of-the-year fixed effect, and $\boldsymbol{x}_t$ is a vector of control variables that includes typical determinants of sleep that are exogenous to any given individual. We include $\boldsymbol{\delta}_t$ and $\boldsymbol{\mu}_t$ in this regression to account for the fact that sleep quality exhibits both intra-week and intra-year seasonality. For instance, Figure IA.D.3 in the Internet Appendix shows that the proportion of deep sleep tends to peak in the middle of the week but sharply declines between Friday and Sunday. Similarly, sleep efficiency tends to peak on Friday night but drops on both Saturday and Sunday.[9] Similarly, Figure IA.D.4 in the Internet Appendix shows that sleep patterns tend to vary over the course of the year, with deep sleep (sleep efficiency) being highest (lowest) in the summer months of the year.

The vector of control variables $\boldsymbol{x}_t$ includes typical and time-varying determinants of sleep that are exogenous to any given individual. These controls include the amount of sunlight (measured in hours per day), average daily temperature (measured in degrees Celsius), daily rainfall (measured in millimeters per day), newly diagnosed COVID-19 cases (per one million people), and general happiness (proxied by the language-based Hedonometer index of Dodds, Harris, Kloumann, Bliss and Danforth (2011) and Dodds, Clark, Desu, Frank, Reagan, Williams, Mitchell, Harris, Kloumann, Bagrow *et al.* (2015)).

The definitions of all control variables are provided in Section IA.A of the Internet Appendix, and their summary statistics are reported in Table IA.C.1 of the Internet Appendix. We scale each variable by its unconditional standard deviation to account for the different units of measurement of the controls included in $\boldsymbol{x}_t$ and estimate this projection using daily data from April 26, 2017, to May 26, 2023 (the last day all control variables are available).

The key variable of interest in equation (3) is the residual ε_t. For each measure of sleep quality, it reflects an abnormal variation in sleep that is orthogonal to the comprehensive set of controls and fixed effects.

1.5 Validation vis-à-vis Google Search

If the residuals from projection (3) capture meaningful unexpected variation in sleep quality that is orthogonal to the known determinants of sleep included in $\boldsymbol{x}_t$, such as temperature and the amount of daylight, then they should covary with the intensity with which individuals search for sleep-related terms on Google. This validation test is inspired by Da *et al.* (2015), who use Google search volumes to measure market-wide sentiment.

We implement this test using data on the intensity with which U.S. households search the internet for terms that include "can't sleep" and "bad sleep," catch-all phrases for poor sleep, and "melatonin," a common sleep-related supplement that households may search for when

[9] By eliminating these predictable patterns in sleep quality, we ensure that our findings do not merely capture weekly seasonality in the news cycle. Empirical evidence shows that, in corporate disclosures, bad news is often released on Fridays, as reviewed in Gersen and O'Connell (2009).

experiencing difficulty sleeping. We obtain this data from Google, which provides search intensity for these terms from May 2017 through May 2023.[10] The search intensity index for each term is normalized to equal 100 in the day when the term was most popular within the sample. Accordingly, a value of 25, for instance, on another day d indicates that the term's popularity in that day was one-quarter of its peak popularity during the full sample period.

We aggregate the daily residuals from equation (3) to the weekly frequency by computing their average value within each week. We denote the weekly value of this residual by $\varepsilon_t^{(W)}$. We then apply the same weekly aggregation to the Google Trends series after aligning the daily sleep residuals and Google Trends data by date. To remove remaining low-frequency seasonal variation in search behavior, we residualize the weekly Google Trends series with respect to month-of-year fixed effects. We then estimate the association between changes in abnormal sleep quality and changes in residualized Google search volume at the weekly frequency. The association between the weekly measure of abnormal sleep quality and Google search volume (GSV) is estimated via:

$$\Delta\omega_w^{(W)} = \rho_0 + \rho_1 \Delta\widetilde{GSV}_w + \vartheta_w, \tag{4}$$

where $\omega_w^{(W)}$ denotes the weekly-aggregated residuals from equation (3) obtained when SleepQuality_t is proxied using either the proportion of deep sleep or sleep efficiency, and $\widetilde{GSV}_w$ is the weekly Google Trends index for one of the three search terms, "can't sleep," "bad sleep," or "melatonin," after residualizing the weekly search series on month-of-year fixed effects. We estimate projection (4) using the first difference of each variable, such that a positive change in $\omega_w^{(W)}$ represents an improvement in abnormal sleep quality between week $w-1$ and week w, while a positive change in $\widetilde{GSV}_w$ represents increased residualized search interest over the same period. We standardize both the dependent and independent variables, such that ρ_1 represents the correlation between the two.

Figure 1 presents the results using scatterplots. The top row displays the results when sleep quality is measured using abnormal deep sleep, while the bottom row displays the results when sleep quality is measured using abnormal sleep efficiency. The first, second, and third columns report the results when the search terms are "can't sleep," "bad sleep," and "melatonin," respectively. Each scatterplot also shows the best linear fit for the association

[10]See the Google Trends website for further details on this dataset.

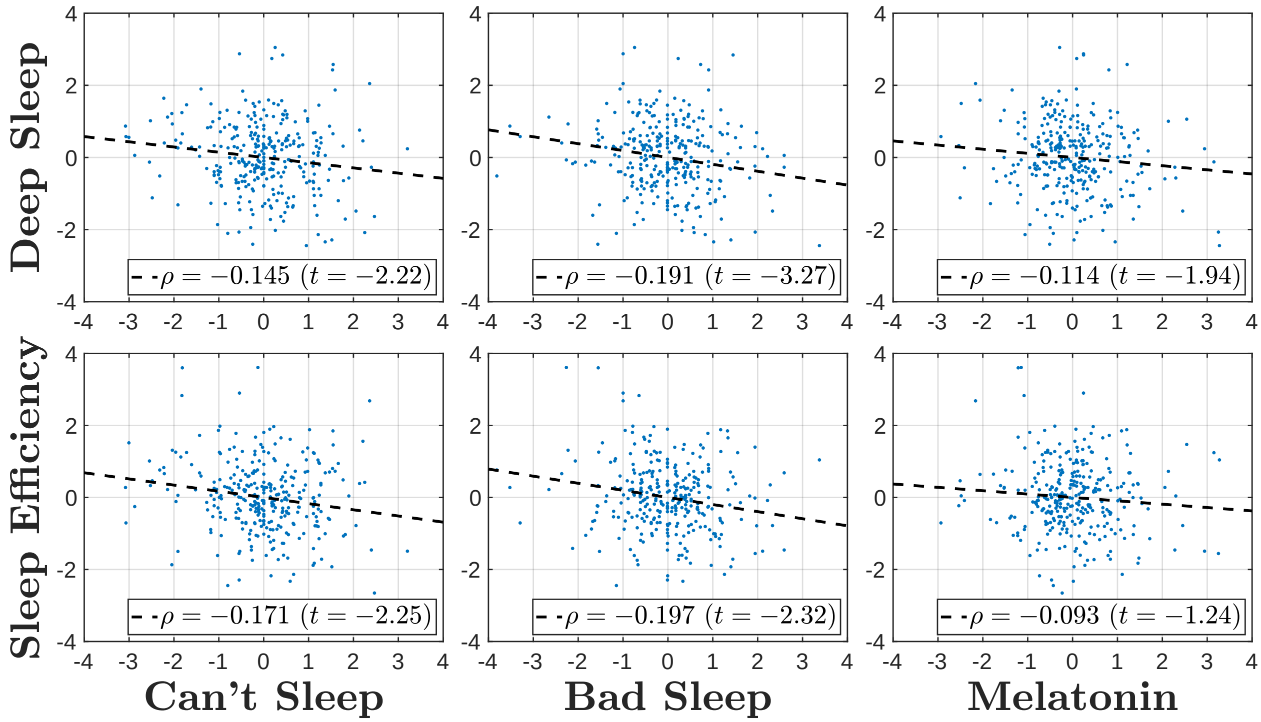

Figure 1: Association with internet search activity

The figure shows how abnormal sleep quality comoves with Google search interest in "Can't Sleep," "Bad Sleep," and "Melatonin." We obtain these results by (i) filtering each measure of sleep quality through equation (3) to obtain our proxy for abnormal sleep, (ii) aligning daily abnormal sleep with daily Google Trends data, (iii) averaging both series within each week, (iv) residualizing the weekly Google Trends series on month-of-year fixed effects, and (v) relating weekly changes in abnormal sleep to weekly changes in residualized search intensity via equation (4). Each subpanel plots the scatterplot of standardized weekly changes with the fitted OLS line and reports the slope, which corresponds to the Pearson correlation coefficient, along with its Newey and West (1987) t-statistic that is computed using five lags. The top row measures sleep quality via the proportion of deep sleep (equation (1)), while the bottom row measures sleep quality via sleep efficiency (equation (2)). Columns correspond to the three keywords: "Can't Sleep," "Bad Sleep," and "Melatonin." The sample ranges from May 2017 through May 2023.

between these variables, with a slope of ρ_1.

The figure reveals a clear negative relation between innovations in abnormal sleep quality and the popularity of sleep-related searches. Weeks characterized by heightened search activity for "can't sleep," "bad sleep," and "melatonin" among U.S. households coincide with deteriorations in abnormal sleep quality. The correlations are uniformly negative across all six panels. The magnitudes are largest for "bad sleep" for both deep sleep and sleep efficiency. Overall, the evidence supports the interpretation that the residuals from equation (3) capture meaningful variation in sleep quality rather than merely reflecting seasonal, weather-related, or other predictable determinants of sleep.

2 Wake-and-See: The Imprint of Uncertainty on Sleep

In this section, we demonstrate that uncertainty shocks leave a real-time imprint on sleep quality, making abnormal sleep an *implicit physiological barometer of when uncertainty shocks are experienced as welfare-relevant.* In Section 2.1 we employ an event study methodology, showing that large and arguably exogenous events associated with higher geopolitical uncertainty coincide with immediate declines in sleep quality. In Section 2.2 we employ projection analysis, showing that policy uncertainty systematically predicts lower sleep, and the economic magnitude is as large as that of other environmental factors. In Section 2.3 we use recursive identification to extract uncertainty shocks, showing the dynamic persistent effect of uncertainty on sleep quality. Lastly, in Section 2.4 we study the heterogeneity in the imprint of uncertainty on sleep, depending on several demographic dimensions.

2.1 Event Study

We demonstrate that part of the variation in abnormal sleep quality is driven by individuals' physiological reactions to large exogenous shocks that, beyond any first-moment effects, also elevate uncertainty regarding social, political, and economic conditions. We disentangle the reaction to first- versus second-moment shocks in later subsections.

Specifically, we study how sleep quality fluctuates around a set of salient domestic and global events that received broad coverage in U.S. media and plausibly raised short-run economic or geopolitical uncertainty between May 2017 and April 2023. Table IA.C.2 reports the resulting 50 events and their descriptions. The events range from disasters, violence, and terrorist attacks (e.g., the Grenfell Tower fire that killed 72 individuals in London in June 2017 and the assassination of former Japanese Prime Minister Shinzo Abe in July 2022) to financial and political events (e.g., the collapse of Silicon Valley Bank in March 2023, the United States Capitol attack of January 2021, and the midterm elections of November 2022). Other prominent events include the outbreak of the COVID-19 virus in early 2020, the murder of George Floyd in May of the same year, and many of the geopolitical events that are highlighted by Caldara and Iacoviello (2022) during the sample period.

We examine how the residuals from equation (3) evolve in the nine-day window around each event. Specifically, we treat each event date as time zero and track the residuals from

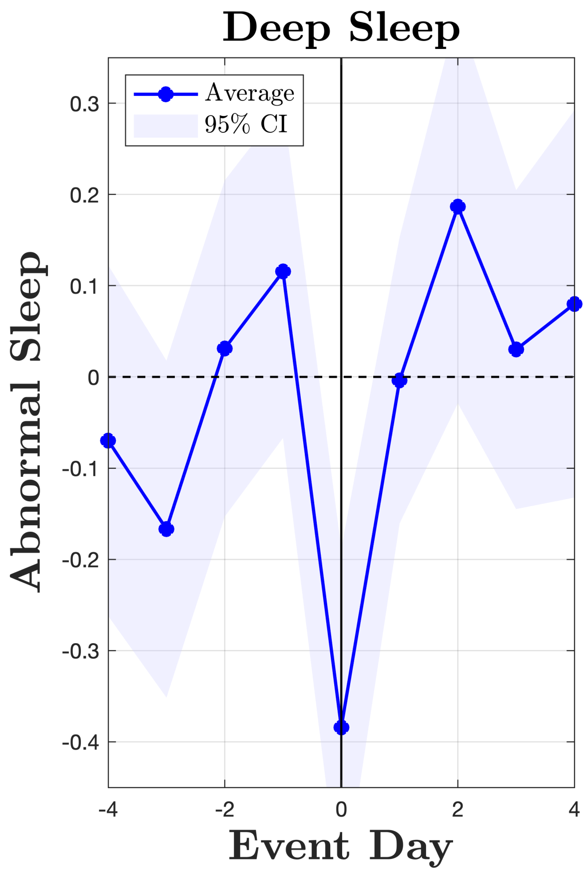

Figure 2: Event study
The figure reports the results of event studies in which the average value of abnormal sleep quality, obtained by filtering each measure of sleep quality through equation (3), is displayed around 50 prominent domestic and geopolitical news days that are relevant for U.S. households between May 2017 and April 2023. A list of these 50 events is provided in Table IA.C.2 of the Internet Appendix. We record how each measure of abnormal sleep quality behaves in the 9-day window centered around each event (i.e., from four days before the event to four days after). The solid blue line then reports the average value of abnormal sleep on each event date, while the blue-shaded region represents the 95% confidence interval associated with this cross-event average. The standard errors underlying this confidence interval are computed in accordance with White (1980). The left panel reports the results obtained when sleep quality is measured using the proportion of deep sleep from equation (1), while the right panel reports the results obtained using the measure of sleep efficiency from equation (2).

four days before to four days after the event. Finally, we compute the average value of the residual across all events and plot the resulting values in Figure 2 alongside the 95% confidence intervals.

The results in both panels of Figure 2 indicate that both deep sleep and sleep efficiency drop sharply on days with salient national and geopolitical news. The magnitude of the decline amounts to about half a standard deviation of these metrics across these 50 event days. This large decline in sleep quality on the event date is statistically significant at the

5% level but is relatively short-lived, as both deep sleep and sleep efficiency rebound to their pre-event baseline in the days following the typical event. Nonetheless, in Section 2.3 we use impulse-response analysis to show that the effect of *uncertainty* shocks persists for several days. The lack of persistence in our event study could either reflect the fact that the sample of events is small or the fact that it blends the reaction to both first- and second-moment variation, whereas only the latter induces a significant effect on abnormal sleep (while the former induces a *transitory* effect; see Section 2.2).

In all, the analysis reaffirms that the residuals underlying equation (3) reflect the unexpected components of sleep quality and that large geopolitical shocks register in individuals' sleep in real-time and without a lag. We view the event-study evidence as descriptive validation rather than the main identification strategy, since some salient events may affect sleep through channels other than uncertainty. Our core identification instead comes from the continuous-proxy evidence and from the fact that sleep loads much more strongly on second-moment measures than on first-moment market realizations, as shown in the next subsections.

2.2 Projections

Motivated by the evidence that abnormal sleep declines around salient geopolitical events, we hypothesize that sleep quality is systematically related to daily variation in macroeconomic and financial uncertainty. The focus on uncertainty is driven by two notions. First, unlike realized large first-moment shocks, which are either backward-looking or infrequent, uncertainty is highly persistent and forward-looking by nature. The prospects of large future shocks, governed by greater jump intensity or a spike in the conditional volatility of Gaussian shocks, have a large economic impact (see, e.g., Bloom, 2009; Ludvigson, Ma and Ng, 2021; Anschukov, Bhamra and Kuehn, 2024). Second, if economic shocks affect individuals' sleep, they may also be related to sentiment. Uncertainty and sentiment interact and reinforce one another: Garcia (2013) finds that the sensitivity of investors to news is highest during recessions, characterized by elevated volatility; Dicks and Fulghieri (2021) show that investor sentiment depends on uncertainty about the fundamentals; Birru and Young (2022) show that higher uncertainty enhances the role of sentiment in affecting asset prices.

Uncertainty has many facets, each having potentially different implications for the macroeconomy. For our benchmark analysis, we consider the prominent measure of economic policy uncertainty of Baker, Bloom and Davis (2016), a widely adopted measure of economic uncertainty based on textual analysis of news content. In robustness, we also consider forms of financial uncertainty: VIX, equity market volatility (Baker, Bloom, Davis and Kost, 2026), and macroeconomic uncertainty (Bekaert *et al.*, 2022), obtaining similar results.[11]

To verify our hypothesis, we start with the following contemporaneous projection:

$$\text{SleepQuality}_t = \beta_0 + \boldsymbol{\delta}_t + \boldsymbol{\mu}_t + \beta_1 \text{EPU}_t + \boldsymbol{x}_t' \boldsymbol{\beta} + \varepsilon_t \tag{5}$$

where EPU_t denotes the natural logarithm of the Economic Policy Uncertainty (EPU) index of Baker *et al.* (2016) on day t, SleepQuality refers either to the aggregate DeepSleep or SleepEfficiency, as constructed in Section 1.4.1, and the vector of control variables in (3) is augmented to include other measures of an individual's physiological conditions beyond the existing set of exogenous environment controls. These additional physiological controls include average daily activity, measured by the number of "very active" minutes from the physical activity Fitbit data provided by *All of Us*, and heart rate, measured via the average individual's heart rate, measured in beats per minute.

In the context of the projection, it is important to distinguish between second-moment and first-moment effects. Specifically, the regression includes two proxies for the latter: (i) the realized market returns; (ii) the daily Hedonometer index (Dodds *et al.*, 2011). The inclusion of this broad sentiment index ensures that the partial effect of the uncertainty proxy is not simply capturing anticipated first-moment effects, generalized bad news, or broad societal pessimism. This language-based sentiment measure acts as a high-frequency, forward-looking proxy for first-moment macro expectations and general mood, beyond any first-moment effects captured by realized market returns.

We standardize all variables in this equation to have a unit standard deviation. As such, each slope coefficient reports how many standard deviations each measure of sleep quality changes for a one-standard-deviation change in a predictor of interest. Table 2 provides the results.

Columns (1) and (5) in Table 2 report univariate regressions that document the association between the EPU index and each proxy of sleep quality. Column (1) shows that a

[11] We do not claim that any single proxy isolates a pure structural uncertainty shock. Rather, our claim is comparative: across specifications and proxies, sleep responds systematically more strongly to second-moment uncertainty measures than to first-moment realizations of bad economic outcomes.

Table 2: Projection results

The table reports the results of estimating equation (5) when sleep quality is measured using the proportion of deep sleep from equation (1) (Panel A) or sleep efficiency from equation (2) (Panel B). The projection includes combinations of the following predictor variables: the logarithmic daily value of the Economic Policy Uncertainty (EPU) index of Baker *et al.* (2016), the total amount of sunlight per day, the average daily temperature and amount of rainfall, the number of newly diagnosed COVID-19 cases per one million residents, the amount of physical activity, the daily value of the Hedonometer of Dodds *et al.* (2011), referred to as "Happy," and the average beats per minute of the typical individual's heart rate. In the final column of each panel, we also control for the excess market return on each trading day, which is denoted by MKTRF. A complete definition of each variable is provided in Section IA.A of the Internet Appendix. Each variable is standardized by its unconditional standard deviation and the t-statistic associated with each slope coefficient, reported in parentheses, is constructed using Newey and West (1987) standard errors that are computed using nine lags. The regression is estimated using daily data that begins on April 26, 2017 and runs through May 26, 2023.

Variable	Panel A: Deep Sleep				Panel B: Sleep Efficiency			
	(1)	(2)	(3)	(4)	(5)	(6)	(7)	(8)
EPU	-0.09		-0.12	-0.14	-0.30		-0.22	-0.21
	(-4.11)		(-6.28)	(-4.94)	(-10.44)		(-7.60)	(-5.90)
Sunlight		0.01	0.00	-0.09		0.28	0.27	0.12
		(0.06)	(0.04)	(-0.58)		(1.61)	(1.71)	(0.63)
Temperature		0.16	0.17	0.31		-0.62	-0.60	-0.59
		(2.16)	(2.45)	(3.29)		(-5.41)	(-5.48)	(-4.73)
Rainfall		-0.07	-0.07	-0.11		-0.05	-0.05	-0.06
		(-4.39)	(-4.47)	(-4.79)		(-2.50)	(-2.64)	(-2.41)
COVID-19		0.02	0.07	0.08		-0.12	-0.03	-0.03
		(0.98)	(3.74)	(3.87)		(-3.21)	(-0.93)	(-0.73)
Happy		0.08	0.04	0.05		0.27	0.19	0.24
		(3.33)	(1.54)	(1.89)		(9.24)	(7.18)	(7.80)
Activity		0.17	0.18	0.12		0.10	0.11	0.08
		(4.98)	(5.41)	(2.97)		(2.02)	(2.59)	(1.52)
Heart rate		0.13	0.13	0.10		0.03	0.02	0.01
		(5.33)	(5.63)	(3.71)		(0.93)	(0.65)	(0.15)
MKTRF				0.02				0.00
				(1.03)				(0.19)
N	2221	2221	2221	1533	2221	2221	2221	1533
R^2	0.58	0.62	0.62	0.53	0.48	0.51	0.53	0.51

one-standard-deviation increase in economic uncertainty is associated with a 0.09 standard-deviation reduction in the median individual's proportion of deep sleep. Similarly, Column (5) shows that the same change in EPU results in a 0.30 standard-deviation reduction in sleep efficiency (i.e., more time spent awake in bed).

Together, these results provide preliminary support for our hypothesis. They point to a new non-pecuniary cost of uncertainty: whereas extant literature discusses the welfare loss in terms of reduced economic growth due to "wait-and-see" effects (McDonald and Siegel, 1986), the projection points to a complementary welfare loss in terms of economic agents' health due to a "wake-and-see" effect—the loss of restorative sleep due to economic-based stressors—which could be converted to productivity losses as in Gibson and Shrader (2018).

Next, Columns (2) and (6) report how the control variables in equation (3) are related to each outcome variable. While longer daylight hours are largely unrelated to sleep quality, higher temperatures tend to improve deep sleep but reduce sleep efficiency, while a greater incidence of COVID-19 cases also tends to improve deep sleep while reducing sleep efficiency. Increases in rainfall reduce both measures of sleep quality, while happiness increases both measures of sleep quality. Finally, increases in physical activity improve both measures of sleep.

Columns (3) and (7) report the results of incorporating the EPU index alongside the full suite of physiological and environmental controls. The estimates confirm that spikes in uncertainty remain negatively and significantly associated with both measures of sleep quality. Remarkably, the magnitude of this uncertainty penalty is highly competitive with direct physical disruptions. Column (3) demonstrates that a one-standard-deviation increase in uncertainty is associated with a reduction in the median deep-sleep share of 0.12 standard deviations, an effect comparable in absolute value to the disruption caused by heavy rainfall or shifts in general happiness. Even more strikingly, Column (7) shows that a one-standard-deviation increase in EPU is related to a 0.22 standard deviation reduction in sleep efficiency, an impact that is roughly four times larger than that of rainfall. Importantly, this physiological impairment is not merely a contemporaneous reaction to news flow: as the next subsection demonstrates, uncertainty shocks are followed by persistent dynamic responses over subsequent days.

Finally, Columns (4) and (8) of Table 2 show that the negative uncertainty-sleep relation remains when we control for equity market returns. Although including market returns restricts our sample to trading days only, thus reducing the total number of observations by about 700 days, we continue to find an economically large and negative association between increases in economic uncertainty and reductions in sleep quality. Interestingly, the slope coefficient on the market return is statistically insignificant. In robustness checks, we confirm that other first-moment proxies do not predict sleep quality, in contrast to a broad range of uncertainty metrics. Sleep, it seems, responds to higher-order forward-looking information rather than to realized first-moment shocks.[12]

2.2.1 Robustness

We verify that the negative relation between economic uncertainty and sleep quality persists across (i) alternative methodologies for constructing the aggregate sleep-quality series, (ii) a range of subsample analyses, including excluding the COVID-19 recession and focusing only on the more recent sample period, and (iii) alternative measures of economic uncertainty.

Table IA.C.3 in the Internet Appendix shows that the results materially persist if we do not apply a linear time trend to our aggregate measures of sleep (Panel A), consider the cross-sectional *average* individual each day rather than the *median* individual (Panel B), or do not remove day-of-the-week or month-of-the-year seasonality (Panel C). Panel D shows that the results are materially unchanged when we do not winsorize the data but control for sharp changes in sleep quality around predictable public holidays, public events, and Daylight Saving Time changes via a comprehensive set of fixed effects. Finally, Panel E documents that we obtain similar results if we simply do not winsorize the data, but ignore the predictable effects of holidays.

Our baseline sample analysis overlaps with the COVID-19 recession. Although the onset of the pandemic in 2020 generated unprecedented disruptions to daily routines, it also constitutes the largest and most plausibly exogenous aggregate uncertainty shock in our sample. A natural concern is that the observed deterioration in sleep quality during this period reflects the mechanical effects of lockdowns or disruptions to daily schedules rather than economic uncertainty itself. To address this concern, our baseline specification controls for the daily incidence of COVID-19 cases to absorb direct health-related distress. Moreover, Table IA.C.4 in the Internet Appendix shows that our results remain robust after excluding the COVID-19 recession (Panel A).

We also consider the possibility that changes in the composition of the *All of Us* sample

[12]It is important to stress that the insignificant relation between the market return and sleep does not indicate that the market factor is not priced by the representative agent. In our framework, marginal utility is a function of both pecuniary and non-pecuniary states: First, the pecuniary effects of market returns are well established; Second, a factor is priced not if its *realized* return affects sleep, but rather if its *expected* return—or the ex-ante risk associated with it—affects sleep. We document precisely that: the VIX, a well-established measure of the quantity of market risk and a predictor of short-term market returns, significantly disrupts sleep (see section 2.2.1). The fact that the ex-ante quantity of market risk imposes a direct physiological toll strongly implies that the market is indeed a priced factor.

over time, as well as improvements in wearable fitness-tracking technology, may affect the sleep quality measurements. To account for this, Panel B of Table IA.C.4 repeats the baseline analysis using only the more recent (and stable) portion of the sample period. The results remain qualitatively unchanged.

Similarly, Table IA.C.5 in the Internet Appendix shows that our results remain robust when we replace the EPU index with alternative proxies for economic uncertainty. In particular, we continue to find a negative relation between uncertainty and sleep quality when uncertainty is measured using the risk-neutral VIX index in Panel A, the realized equity market volatility index in Panel B, or the daily measure of economic uncertainty from Bekaert *et al.* (2022) in Panel C.

To further address concerns related to intrinsic persistence of the EPU index, we estimate an AR(1) model for EPU and use the residuals as model-based innovations. We then repeat the baseline projection when the level of EPU is replaced with either these innovations in Panel D, or with only positive innovations to EPU, capturing strictly unexpected positive shocks to uncertainty in Panel E. In both cases, increases in uncertainty remain associated with declines in sleep quality.

Finally, we continue to find little evidence that first-moment shocks explain meaningful variation in sleep quality. For example, fluctuations in neither the investment-minus-consumption spread of Papanikolaou (2011) (Panel G) nor the intermediary capital factor of He, Kelly and Manela (2017) (Panel H) consistently explain changes in sleep quality.

2.3 Structural VAR and Impulse Response Functions

The preceding analysis was confined to static effects. We now study the dynamic propagation of policy uncertainty and sleep quality using a recursively identified vector autoregression (VAR). Specifically, we model these variables as following an autoregressive law of motion with exogenous regressors:

$$\boldsymbol{y}_t = \boldsymbol{c} + \boldsymbol{A}_1 \boldsymbol{y}_{t-1} + \boldsymbol{B}\boldsymbol{X} + \boldsymbol{u}_t. \tag{6}$$

Here, $\boldsymbol{y}_t$ is a $(K \times 1)$ vector that includes all the variables of interest described below, $\boldsymbol{c}$ is a $(K \times 1)$ vector of intercept terms, $\boldsymbol{A}_1$ is a $(K \times K)$ matrix of autoregressive coefficients, $\boldsymbol{B}$ is a matrix of coefficients associated with the day-of-the-week and month-of-the-year dummies included in the matrix $\boldsymbol{X}$, and $\boldsymbol{u}_t$ is a $(K \times 1)$ vector of reduced-form innovations with $\mathbb{E}[\boldsymbol{u}_t] = \boldsymbol{0}$ and a symmetric, positive definite covariance matrix $\boldsymbol{\Sigma}_u = \mathbb{E}[\boldsymbol{u}_t \boldsymbol{u}_t']$. These properties of the covariance matrix allow us to write $\boldsymbol{\Sigma}_u = \boldsymbol{P}\boldsymbol{P}'$, where $\boldsymbol{P}$ is a lower triangular matrix with positive diagonal elements obtained through Cholesky factorization.

On each day t of the sample period, $\boldsymbol{y}_t$ includes the following nine variables that are placed in the following order: the duration of sunlight, the average daily temperature, the amount of precipitation, the number of newly diagnosed cases of the COVID-19 virus, the level of the Hedonometer of Dodds *et al.* (2011), the value of the EPU index, the amount of physical activity, the quality of sleep measured using either DeepSleep or SleepEfficiency as constructed in Section 1.4.1, and within-day average heart rate.

Placing the variables in this order provides us with structural (orthogonal) shocks to each variable in equation (6) via $\boldsymbol{\epsilon}_t = \boldsymbol{P}^{-1}\boldsymbol{u}_t$. Our identifying assumptions are that (i) meteorological variables are contemporaneously exogenous to the rest of the system; (ii) COVID-19 cases can contemporaneously respond to weather, but not to happiness, EPU, or physiological outcomes on the same day; (iii) happiness and economic uncertainty can react to environmental shocks but not to physiological outcomes; and (iv) physiological outcomes can respond instantaneously to all preceding shocks but do not contemporaneously influence those earlier variables.[13]

The dynamic system described by equation (6), along with the identifying assumptions outlined above, allows us to trace impulse response functions (IRFs) that examine how a structural shock to economic uncertainty propagates through this dynamic system and impacts the quality of sleep.[14] We obtain these IRFs by estimating (6) on an equation-by-equation basis using OLS. We then compute the Cholesky decomposition of $\hat{\boldsymbol{\Sigma}}_u$, and use estimates of $\boldsymbol{A}_1$ and $\boldsymbol{P}$ to construct the impulse responses for $h = 0, \ldots, 15$ days ahead. Statistical inference associated with these IRFs is conducted using a residual bootstrap with 1000 draws from the estimated values of $\hat{\boldsymbol{u}}_t$. We interpret the resulting IRFs as informative about timing and persistence under a transparent ordering identification scheme.

[13]Figure IA.D.6 in the Internet Appendix shows that our results are essentially unchanged if we augment this VAR by placing the excess market return, investment-minus-consumption spread of Papanikolaou (2011), and the intermediary capital factor of He *et al.* (2017) before EPU, so that uncertainty shocks are orthogonal to the contemporaneous first-moment effect.

[14]The $(K \times K)$ matrix of impulse responses for forecast horizon $h = 0, \ldots, H$ is denoted by $\boldsymbol{\Theta}_h$. Column j of this matrix records the responses of all variables to a structural shock to variable j at time 0. The IRF for forecast horizon h can be found via $\boldsymbol{\Theta}_h = \boldsymbol{P}$ for $h = 0$ and $\boldsymbol{\Theta}_h = \boldsymbol{A}_1^h \boldsymbol{P}$ for $h \geq 1$.

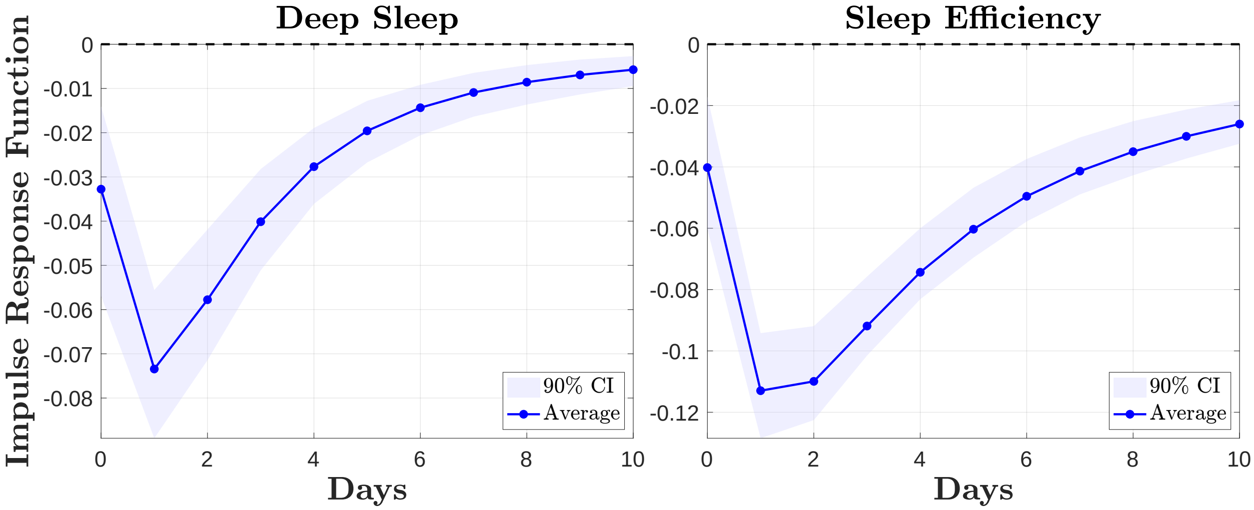

Figure 3: Impulse response functions: Baseline
The figure reports impulse response functions (IRFs) that display how a structural shock to economic uncertainty, measured using the natural logarithm of the daily Economic Policy Uncertainty (EPU) index of Baker *et al.* (2016), propagates to the proportion of deep sleep (left panel), measured via equation (1), and sleep efficiency (right panel), measured via equation (2). These IRFs are obtained by estimating the vector autoregression presented by equation (6) and employing the recursive (Cholesky-based) identification of structural shocks. The solid blue line in each panel represents the average effect, and the 90% confidence interval represented by the blue-shaded region is obtained using a residual bootstrap with one thousand draws from the estimated residuals. Finally, the analysis uses daily data and runs from April 26, 2017 through May 26, 2023.

Figure 3 displays the IRFs from the baseline specification. The panels show how a one–standard-deviation structural shock to economic policy uncertainty (EPU) affects deep sleep (left) and sleep efficiency (right). In the left panel, higher uncertainty is associated with a 0.07-standard-deviation reduction in the median proportion of time spent in deep sleep on the night following the uncertainty shock. The same shock implies a 0.11–standard-deviation decline in sleep efficiency the following night. Although these one-day effects are modest, they are statistically significant and persist for several subsequent nights. As a result, the *cumulative* impulse-response over a span of one week is quite substantial, amounting to about a 0.28 standard deviation reduction for deep sleep and a 0.58 standard deviation reduction for sleep efficiency. This is sizable: a two-standard-deviation Cholesky shock to uncertainty reduces total sleep time by over 42 minutes over the next week.[15][16]

2.3.1 Robustness

We implement a battery of robustness checks to verify that the IRFs presented in Figure 3 are not driven by specific identification assumptions or methodological choices. These tests confirm that the baseline IRFs are not materially affected by (i) the order of variables in (6) that drive the Cholesky decomposition associated with equation (6); (ii) using local projections (Jordà, 2005) rather than a VAR to estimate the IRFs; (iii) using an alternative measure of economic uncertainty in place of the EPU index; and (iv) considering several methodological variations in how the sleep quality measures are constructed in the data.

First, we consider the *generalized* IRFs described by Pesaran and Shin (1998). These IRFs do not depend on the order of variables included in $\boldsymbol{y}_t$. These generalized IRFs are defined by $\boldsymbol{\Theta}_h^{(G)} = \boldsymbol{\Psi}_h \boldsymbol{\Sigma} \boldsymbol{D}^{-1/2}$ for $h = 0, \ldots, H$, where $\boldsymbol{\Psi}_h$ represents the matrix of moving-average (MA) coefficients for the h^{th} lag from the MA representation of equation (6) and $\boldsymbol{D} = \operatorname{diag} \boldsymbol{\Sigma}$ represents a $(K \times K)$ matrix that retains the diagonal elements of $\boldsymbol{\Sigma}$. While

[15]Because sleep efficiency is a ratio, translating a decline in the ratio into minutes of sleep loss requires a distinction between the extensive margin (time spent in bed) and the intensive margin (the efficiency of sleep during that time). Large-scale empirical studies demonstrate that bedtime screen use reduces actual sleep duration by an average of 24 minutes per night (see, e.g., Hjetland, Skogen, Hysing, Gradisar and Sivertsen (2025)). To be highly conservative, we deliberately evaluate a baseline range where heightened uncertainty prompts individuals to delay time in bed by only five to eight minutes per night. Let B denote time spent in bed, S denote minutes asleep, and E denote sleep efficiency. The change in sleep minutes (ΔS) is given by:

$$\Delta S = E_0 \Delta B + B_0 \Delta E + \Delta E \Delta B$$

We apply the cumulative intensive margin shock observed in our impulse responses, scaled by the standard deviation of the raw aggregate sleep efficiency series (0.5%), yielding $\Delta E = -1.16 \times 0.005 = -0.0058$. Given our sample's baseline sleep efficiency of $E_0 = 0.875$, an assumed 8 hour baseline in bed (B_0), and an average sleep delay of $\Delta B = -6.5$ minutes, aggregating this identity over the post-shock week yields:

$$\Delta S_{\text{Weekly}} \approx -42.6 \text{ minutes.}$$

Bounding the daily sleep delay between 5 and 8 minutes implies a total weekly sleep loss of 33.4 to 51.7 minutes. This is an especially conservative range, given that our aggregation method for sleep efficiency uses the median. In the tails of the distribution, the individual effect could be considerably larger.

[16]The persistence of the IRF likely reflects both the persistence of the physiological response to the initial uncertainty shock and the persistence of subsequent movements in EPU itself. To obtain a *lower bound* that isolates the effects of a one-time shock to EPU, we provide two supplementary computations. First, under the assumption that a single event affects physiology for only three days (see, e.g., Kim and Dimsdale (2007)), we consider a cumulative effect over three days, which amounts to a 0.35 standard deviation drop. Second, in an untabulated result, we re-estimate the VAR by replacing the level of EPU with its innovations obtained from an AR(1) model. In this case, the impulse response reverts to the baseline after approximately three days and the cumulative IRF amounts to a 0.15 standard deviation decrease in sleep quality.

these GIRFs retain the observed contemporaneous correlation among innovations and do not admit a structural interpretation of shocks, they provide a means to assess the sensitivity of the IRFs to variable ordering. Figure IA.D.7 in the Internet Appendix shows that these generalized IRFs are almost identical to the baseline (orthogonalized) IRFs considered above. Moreover, Figures IA.D.8 and IA.D.9 show that the results are qualitatively similar when the variables in the VAR are reordered to place the EPU index or sleep quality last, respectively. Collectively, these results highlight that our conclusions are largely insensitive to the order in which variables are included in $\boldsymbol{y}_t$.

Second, Figure IA.D.10 in the Internet Appendix repeats the analysis using equity market volatility in place of the EPU index of Baker *et al.* (2016). The results show that a structural shock to uncertainty continues to display a negative, persistent, and statistically significant association with both deep sleep and sleep efficiency.

Next, the negative and persistent effects of uncertainty on sleep quality persist if we (i) compute the daily average value of sleep quality across individuals in the *All of Us* data instead of the daily median (Figure IA.D.11), (ii) do not linearly detrend the aggregate measures of sleep quality (Figure IA.D.12), (iii) do not winsorize the aggregate measures to reduce the impact of outlier days, such as the start of Daylight Saving Time (Figures IA.D.13 and IA.D.14), and (iv) do not remove day-of-the-week or month-of-the-year fixed effects to account for predictable calendar-time variation in sleep quality (Figure IA.D.15).

Finally, Figure IA.D.16 indicates that the negative response of sleep to uncertainty is not driven by the sharp spike in uncertainty during the COVID-19 pandemic. Removing the COVID-19 recession from the sample period continues to produce a negative and statistically significant decline in sleep. Moreover, we focus on the recent half of the sample period in Figure IA.D.17 and show that a significant decline in sleep quality continues to persist.

2.4 Cross-Sectional Heterogeneity

We examine how the impact of uncertainty on sleep quality differs across demographics of interest. Namely, we examine whether the estimated uncertainty-sleep relation differs by income, age, race, sex, and education.

We obtain each individual's characteristics through surveys completed as part of the onboarding process to join the *All of Us* Research Program. While age, race, and sex are individual-specific traits, the remaining demographic characteristics (e.g., income and education) are collected as part of the Census Bureau's annual ACS initiative and are not individual-specific. Rather, these statistics reflect survey responses from households in the same three-digit ZIP code location as the individuals in the *All of Us* Research Program.

We analyze *relative* heterogeneity along each dimension by estimating the IRFs implied by the VAR represented by equation (6). Instead of measuring sleep quality using the median person's deep sleep or sleep efficiency on a given day t, we consider the *difference* in sleep quality on day t between (i) individuals with a high level of a given characteristic, such as income, and (ii) individuals with a low level of the same characteristic. This captures how sleep quality on a given day changes between the two populations of interest. In constructing these cohort-level time series, we explicitly do not absorb individual fixed effects. Because a subject's cohort classification is entirely time-invariant over our high-frequency sample, individual fixed effects would perfectly subsume the cross-sectional variation required to identify the baseline wedge between the groups. By preserving the non-demeaned data, we are able to accurately measure the unconditional spread in sleep quality across these distinct populations over time. When the characteristic of interest is continuous, such as age or income, we use the 80^{th} and 20^{th} percentiles of the cross-sectional distribution of that characteristic to delineate members of the high and low groups. When the characteristic is defined in a binary manner (e.g., "white" or "non-white"), we split individuals into two groups on the basis of this binary variable. The results are reported in Figures 4 and 5.

Figure 4 shows how sleep quality differentially reacts to structural economic uncertainty shocks across the wealth distribution. We proxy for wealth in one of four ways. The top row of the figure divides individuals into groups based on the median household income in their residential area. The second row compares the differential sleep response between individuals living in areas with lower use of income assistance (wealthier locations) and areas with higher use of income assistance (less wealthy locations). The third row splits individuals based on an area's deprivation index. This composite index combines several variables in the ACS into a single metric of a location's socioeconomic conditions, with higher values indicating greater hardship. The final row reports the differential response between individuals living in areas with low poverty rates (i.e., fewer households in the same three-digit ZIP code living below the federal poverty line) versus those living in areas with high poverty rates.

By and large, the figure indicates that individuals living in higher-income or less-deprived

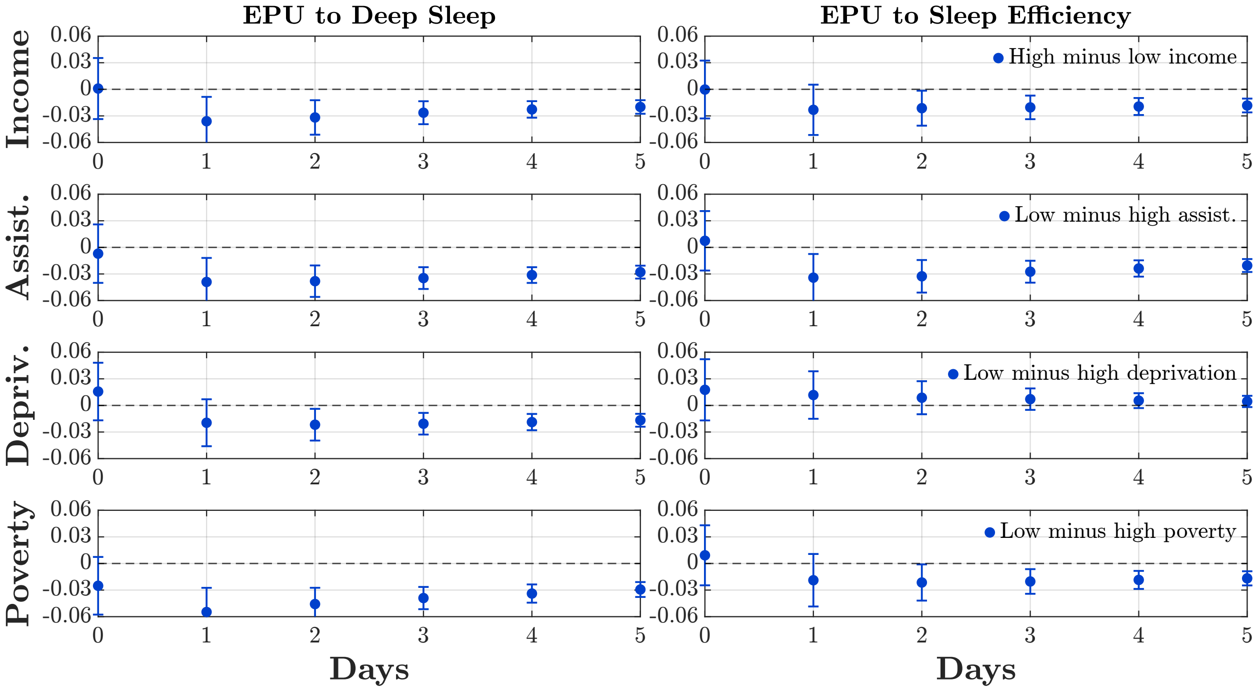

Figure 4: Impulse response functions: Heterogeneity by wealth
The figure reports impulse response functions (IRFs) that display how a structural shock to economic uncertainty, measured using the natural logarithm of the daily Economic Policy Uncertainty (EPU) index of Baker *et al.* (2016), propagates to the difference in one of the two measures of sleep quality between two populations of interest. In the left panel, we measure sleep quality using the proportion of deep sleep, obtained via equation (1), while the right panel focuses on efficiency (right panel), obtained via equation (2). The first row corresponds to the difference in sleep quality between individuals living in areas with the top versus bottom quintile of household income. The second row corresponds to the difference in sleep quality between individuals living in areas in the bottom versus top quintile of income assistance. The third row looks at the difference in sleep quality between individuals living in areas in the bottom versus top quintile of the deprivation index of Brokamp *et al.* (2019). The bottom row looks at the difference in sleep quality between individuals living in areas in the bottom versus top quintile of poverty rates. A definition of each of these variables is provided in Section IA.A of the Internet Appendix. IRFs are obtained by estimating the vector autoregression presented by equation (6) and employing the recursive (Cholesky-based) identification of structural shocks. The solid blue line in each panel represents the average effect, and the 90% confidence interval represented by the blue-shaded region is obtained using a residual bootstrap with one thousand draws from the estimated residuals. Finally, the analysis uses daily data and runs from April 26, 2017 through May 26, 2023.

areas tend to exhibit more negative sleep-quality responses to economic uncertainty shocks than less wealthy households. In particular, the future impact of uncertainty on either deep sleep or sleep efficiency is more sizable for wealthier households. Wealthier households tend to experience a 0.05-standard-deviation *excess* reduction in sleep quality, suggesting that the overall impact on their sleep is about 1.5 times as large as that of the median household, as reported in Figure 3. These effects tend to be statistically significant at the 10% level and

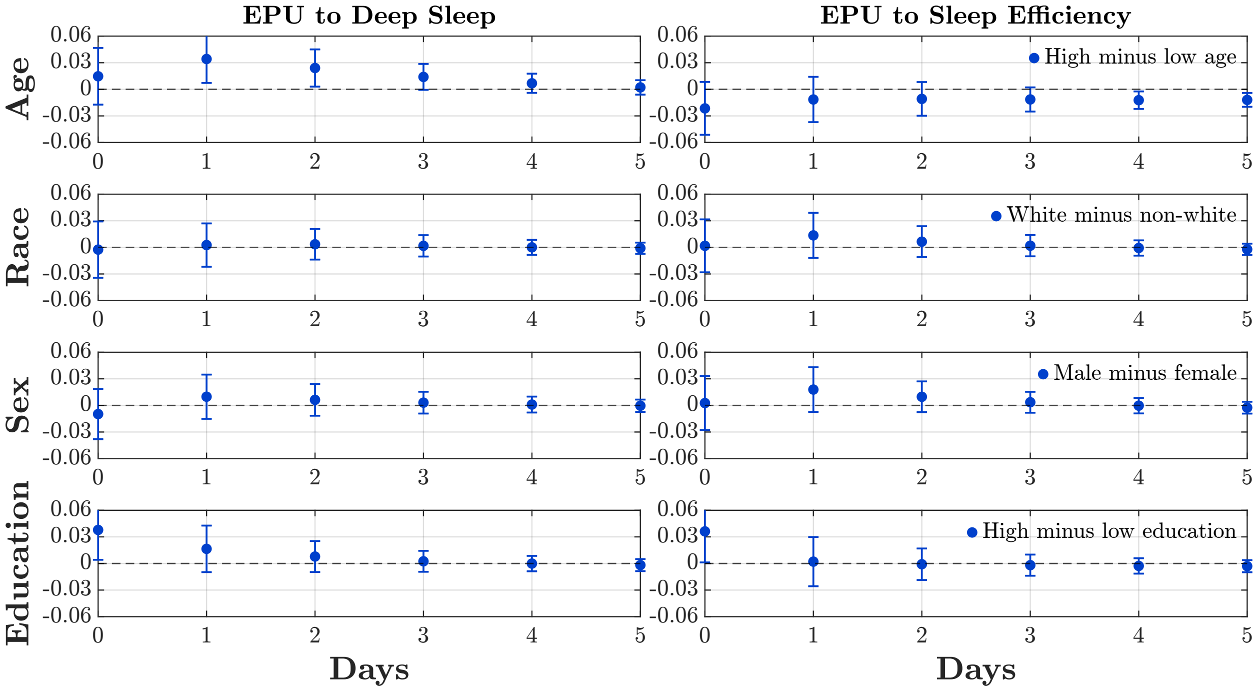

Figure 5: Impulse response functions: Heterogeneity by age, race, education, and sex The figure reports impulse response functions (IRFs) that display how a structural shock to economic uncertainty, measured using the natural logarithm of the daily Economic Policy Uncertainty (EPU) index of Baker *et al.* (2016), propagates to the difference in one of the two measures of sleep quality between two populations of interest. In the left panel, we measure sleep quality using the proportion of deep sleep, obtained via equation (1), while the right panel focuses on efficiency (right panel), obtained via equation (2). The first row looks at the difference in sleep quality between individuals in the top versus bottom quintile of age. The second row looks at the difference in sleep quality between white versus non-white individuals. The third row looks at the difference in sleep quality between male versus female individuals. The bottom row looks at the difference in sleep quality between individuals living in areas in the top versus bottom quintile of high school completion rates. A definition of each of these variables is provided in Section IA.A of the Internet Appendix. IRFs are obtained by estimating the vector autoregression presented by equation (6) and employing the recursive (Cholesky-based) identification of structural shocks. The solid blue line in each panel represents the average effect, and the 90% confidence interval represented by the blue-shaded region is obtained using a residual bootstrap with one thousand draws from the estimated residuals. Finally, the analysis uses daily data and runs from April 26, 2017 through May 26, 2023.

persist for multiple days.

In contrast to the wealth-related results, Figure 5 shows relatively muted differential effects associated with age, race, sex, and education (as proxied by the percentage of residents in a given three-digit ZIP code location who have completed high school or a higher level of education). The top row shows that individuals in the top quintile of age (i.e., those around 70 years and older) tend to sleep slightly better after an uncertainty shock than those in the bottom quintile of age (i.e., those around 35 years and younger). This is consistent with the notion that uncertainty shocks are likely to have a bigger effect on working individuals rather than on retired individuals. This age-related effect is, however, statistically insignificant. The middle two panels show essentially no differences across racial groups or across sexes, and the bottom panel shows no effects based on education rates.[17]

We interpret these heterogeneity patterns as suggestive rather than causal. Because income, deprivation, and education are measured at the area level, they likely proxy for a broader bundle of correlated exposures, local conditions, and portfolio stakes. The key fact for our purposes is that the response is not concentrated in a narrow demographic subset and is stronger in groups plausibly more exposed to financial risk.

3 The Imprint of Sleep on Equity Markets

In this section, we examine the reverse relation: whether sleep quality predicts next-day financial-market outcomes. We examine whether poor sleep spills over into equity markets through two channels:

Hypothesis 1. *Given that sleep quality affects cognitive performance, better sleep should be associated with investors' greater capacities to process and act on information, leading to higher liquidity and enhanced market stability.*

Hypothesis 2. *Because abnormal sleep is a nightly population-level physiological state variable linked to mood and risk-bearing capacity, improvements in abnormal sleep should predict higher short-run market returns.*[18]

Section 3.1 provides empirical evidence supporting these conjectures, while Section 3.2 shows that these effects are more pronounced for stocks dominated by retail trading.

[17] This muted effect of education is consistent with the lack of variation in high school education rates across the United States. The typical three-digit ZIP code sees around 88% of individuals complete high school, and 50% of locations in the United States see between 86% and 92% of individuals graduate from high school.

[18] We do not interpret our observed sleep time-series literally as the sleep of the marginal trader. Rather, in the same spirit as aggregate sentiment or attention measures, it is a population-level state variable that is correlated with the cognitive and affective state of marginal investors.

3.1 Market Evidence

This section examines whether abnormal sleep quality, the component of sleep quality unexplained by exogenous environmental factors, predicts next-day intraday market quality using a projection-based framework. We examine market outcomes measured from the market open on trading day t through to minute τ of the same trading day, where $\tau \in \{60, 120, 180, 300, 390\}$ minutes. Specifically, we estimate the following projection:

$$y_{t,(Open \to \tau)} = \beta_0 + \beta_1 \text{Abnormal DeepSleep}_{t-1} + x'_{t-1}\gamma + \delta_t + \mu_t + \epsilon_{t,\tau} \tag{7}$$

Here, $y_{t,(\text{Open} \to \tau)}$ denotes a market-level outcome from the market's open on day t to minute τ of the same trading day. The dependent variables we consider span multiple dimensions of market conditions and include: (i) intraday price dynamics, measured via cumulative log returns (denoted by "Return"); (ii) realized volatility constructed from high-frequency returns (denoted by "RV"); (iii) volatility asymmetry, measured as the difference between the positive and negative semi-volatilities of returns (denoted by "RV^{+}-RV^{-}"); and (iv) the Amihud (2002) illiquidity measure (denoted by "Amihud"); and (v) the average relative bid-ask spread (denoted by "Spread"). We construct each variable using high-frequency returns on the SPDR S&P 500 ETF (SPY) as a proxy for the aggregate market.

The key explanatory variable in equation (7) is $\text{AbnormalDeepSleep}_{t-1}$, which captures the abnormal component of deep sleep on the night preceding trading day t. Consistent with the construction described by equation (3), this variable isolates variation in deep sleep that is orthogonal to exogenous environmental conditions, such as the amount of sunlight each day.

To account for persistence in the dependent variable, the control vector $\boldsymbol{x}_{t-1}$ includes the lagged dependent variable, y_{t-1}. Although the timing of the regression already helps alleviate concerns that overnight news could simultaneously affect sleep quality and next-day market conditions (i.e., because information arriving after an individual has fallen asleep cannot mechanically influence measured sleep that night), we also include three additional controls in $\boldsymbol{x}$: the previous day's economic policy uncertainty index, the previous day's open-to-close return, and the overnight return, defined as the return from the market close on day $t-1$ to the market open on day t. Taken together, these controls help absorb the effects of overnight information shocks that may otherwise confound the relation between sleep quality and next-day market outcomes. All regressions include day-of-week ($\boldsymbol{\delta_t}$) and month-of-year ($\boldsymbol{\mu}_t$) fixed effects, and variables are standardized to facilitate the interpretation of slope coefficients.

Accordingly, the coefficient on abnormal sleep in equation (7) can be interpreted as capturing the variation in market quality associated with the population's physiological state, conditional on public information observed by the time of the market's open. This equation provides a direct test of our primary conjectures as, under Hypothesis 1, we expect improved sleep to enhance market stability and reduce execution costs, implying $\beta_1 < 0$ when the outcome variables of interest represent measures of illiquidity or realized risk. Similarly, the detrimental effects of downside risk are likely to be less severe following high-quality sleep. Likewise, under Hypothesis 2, better sleep quality could enhance the population's cognitive ability or risk-bearing capacity and result in higher cumulative returns. This suggests that $\beta_1 > 0$ when the outcome variable of interest represents returns.

Table 3 reports the results. We focus on the effects of deep sleep—the core restorative component—on market-wide outcomes, but report the results for sleep efficiency in Table IA.C.6 of the Internet Appendix. The analysis reveals that abnormal deep sleep serves as a statistically and economically significant predictor of intraday returns. For all intraday horizons τ, the estimated coefficients of β_1 in equation (7) are positive and statistically significant. For returns, the coefficient peaks at the 120-minute horizon. While the cumulative effect remains evident over the full trading day, its magnitude levels off after the first two hours of trading. This pattern is consistent with Hypothesis 2: restorative sleep may improve mood, enabling well-rested traders to push prices toward higher values during the high-volume opening hours of the market, rather than generating a steady upward drift throughout the day.

Beyond directional price movements, higher deep sleep is associated with lower market volatility and a reduced prevalence of downside tail risk. The coefficients on overall realized volatility are negative and significant across all forecast horizons, implying a persistent stabilizing effect of well-rested market participants. In contrast, the effect on volatility asymmetry, denoted by "RV^{+}-RV^{-}," is short-lived. Deep sleep significantly predicts an increase in the upside variance relative to downside variance during the first 180 minutes of trading, but this effect dissipates as the market approaches the close. The effect is strongest during the morning session, when uncertainty resolution is greatest, and is consistent with a combination of physiological buffering against panic selling and enhanced risk-bearing capacity, both of which are central to Hypothesis 2.

The predictive relation between deep sleep and market outcomes also extends to measures of market quality, especially during the opening hours of trading. Improvements in deep sleep are associated with enhanced market liquidity and lower execution costs. Notably, the coefficients on the Amihud illiquidity measure are negative and statistically significant for the first 120 minutes. The bid–ask spread coefficients are also negative and economically largest early in the trading day (120–180 minutes). These results corroborate Hypothesis 1: sleep-deprived investors may struggle to provide liquidity during the market open, a period demanding peak cognitive processing speed and attention. However, these constraints may become less binding as trading slows and information flow normalizes over the course of the day.

As a robustness check, we also estimate these projections using abnormal sleep efficiency. The results, reported in Table IA.C.6 of the Internet Appendix, lead to similar conclusions regarding market stability and market quality, particularly through the relation with realized volatility and selected liquidity measures. However, the predictive content for directional prices (returns) and tail-risk asymmetry appears to be specific to deep sleep quality. In other words, while sleep efficiency appears to support market liquidity and overall volatility, the relation between sleep and returns seems to operate primarily through deep sleep, a dimension of sleep quality that is not directly observable in survey-based data.[19] For additional robustness, the Internet Appendix also reports the baseline analysis excluding the COVID-recession period (Table IA.C.8). The results remain broadly similar to the full-sample analysis.

A natural concern is that our predictive results are driven by scheduled macroeconomic announcements. First, the results may reflect favorable pre-open macroeconomic news. To address this possibility, we augment the baseline specification by controlling for pre-open macroeconomic information shocks. In the Internet Appendix we include dummy variables for good macroeconomic news releases (e.g., GDP, initial jobless claims, unemployment rate, and industrial production) announced prior to the market open. The results, reported in Table IA.C.7, remain quantitatively and statistically similar to the baseline. Second, sched-

[19]Moreover, we check whether daily Google search changes for the keywords described in Section 1.5 predict similar market outcomes as deep sleep. While the sign of the results aligns with the effects of deep sleep, we document insignificant results for all terms. For example, increased Google searches for the term "melatonin" predicts lower next day open-to-close returns of only 2 basis points (t-statistic of -0.88) and mildly greater Amihud illiquidity (t-statistic of 0.28). Once again, this underscores the importance of the restorative component of sleep for driving sentiment and cognition, rather than pure revealed sleep distress.

Table 3: Deep Sleep and Intraday Market Responses

This table reports regressions in which the dependent variables are intraday market outcomes measured from the market open on day t through to horizon τ on the same trading day, where $\tau \in \{60, 120, 180, 300\}$ minutes, as well as over the full open-to-close trading day, which corresponds to $\tau = 390$ minutes. The dependent variables capture several dimensions of intraday market quality: (i) intraday price dynamics, measured by cumulative returns over the corresponding window (*Return*); (ii) realized volatility constructed from high-frequency returns (RV); (iii) intraday volatility asymmetry, measured as the difference between positive and negative realized volatility components ($RV^+ - RV^-$); and (iv) liquidity and trading-cost measures, including the Amihud illiquidity measure, defined as the absolute return divided by dollar trading volume, and the average relative bid–ask spread (*Spread*). Detailed definitions, construction procedures, and timing conventions for all dependent variables are provided in Section IA.A. The key explanatory variable is the abnormal component of deep sleep on night $t-1$, that is, the night between the close of trading day $t-1$ and the open of trading day t. This variable is obtained by filtering the deep-sleep measure defined in equation (1) through equation (3). All regressions include the previous trading day's open-to-close return, the overnight return, lagged economic policy uncertainty (EPU_{t-1}), and the lagged dependent variable (y_{t-1}) as controls. All variables are standardized. The sample spans April 26, 2017 to May 26, 2023. t-statistics based on Newey and West (1987) standard errors are reported in brackets.

Minutes (τ)	60	120	180	300	Close
Return	0.06	0.07	0.06	0.05	0.05
	[2.78]	[3.02]	[2.74]	[1.99]	[2.25]
$\bar{R}^2$	0.01	0.03	0.01	0.01	0.01
RV	-0.02	-0.03	-0.03	-0.03	-0.02
	[-1.95]	[-2.86]	[-3.09]	[-2.91]	[-2.75]
$\bar{R}^2$	0.72	0.74	0.75	0.77	0.78
RV^+-RV^-	0.06	0.06	0.05	0.03	0.03
	[2.77]	[2.50]	[2.13]	[1.14]	[1.50]
$\bar{R}^2$	0.03	0.07	0.05	0.06	0.06
Amihud	-0.06	-0.05	-0.04	-0.04	-0.05
	[-2.23]	[-2.05]	[-1.32]	[-1.41]	[-1.85]
$\bar{R}^2$	0.04	0.03	0.02	0.02	0.02
AvgRelSpread	-0.05	-0.05	-0.04	-0.03	-0.02
	[-1.33]	[-1.66]	[-1.98]	[-1.85]	[-1.82]
$\bar{R}^2$	0.30	0.55	0.67	0.71	0.68
Controls	Yes	Yes	Yes	Yes	Yes
N	1531	1531	1531	1531	1531

uled announcements may affect sleep through anticipation. Under this hypothesis, expected news induces anxiety and poor sleep, followed by a market reaction when the news is released.[20] To address this concern, we exclude macroeconomic news days (i.e., days when major macroeconomic reports such as GDP, CPI, and nonfarm payrolls are released prior to the market open) and find that the results remain unchanged (see Table IA.C.9). In addition, we include the absolute value of the overnight return—a proxy of pre-open news uncertainty—and obtain similar findings (see Table IA.C.10).

3.2 Retail-Based Cross-Sectional Evidence

To the extent that abnormal sleep is a sentiment-related variable, the effects of sleep on returns should matter most in segments of the market where discretionary, attention-constrained trading is most important. Retail investors are a natural candidate because retail trading is more likely to reflect limited attention, slower information processing, and variation in risk taking that may be related to physiological state. We therefore test whether the sleep–market-quality relations are stronger for stocks with greater exposure to retail trading.

We use the WRDS TAQ-based Intraday Indicator Data, which is constructed from TAQ trades and quotes data during regular market hours, to measure both (i) trading intensity by trader type and (ii) standard intraday market-quality characteristics. Retail trading is measured as the total number of trades in stock i on day t that are classified as retail-initiated trades. WRDS also provides the number of trades that exceed a dollar size of \$50,000 per stock-day. We use this latter variable as a proxy for institutional trading activity.

Using these variables, we define a proxy variable for the relative importance of retail traders for stock i on trading day t as the (log) difference between the total number of retail- and institutional-initiated trades. This construction intentionally captures *relative* retail dominance. Higher values indicate that, on that day, a stock's trading is more retail-heavy relative to large institutional trades. With the same TAQ-based data, we also track four complementary dimensions of intraday market quality: (i) the *effective bid-ask spread*, which proxies for execution costs; (ii) *intraday volatility*, which proxies for within-day price

[20] Conceptually, this anticipation effect could attenuate, not amplify, our estimates. Anticipation of major news inherently heightens uncertainty and suppresses deep sleep, regardless of whether the subsequent news realization turns out to be favorable or unfavorable for the market. This dynamic generates instances of poor sleep paired with positive market returns, which mechanically biases our positive predictive coefficient downward.

instability; (iii) *dollar price impact*, which proxies for market depth/resiliency; and (iv) *absolute buy–sell imbalance*, which captures one-sided order flow pressure versus balanced flow.

At the end of each month, we sort stocks into three portfolios based on the relative importance of retail trade activity using the 30th and 70th percentiles as breakpoints. Using these portfolio assignments, we then form daily time series of each portfolio's open-to-close returns and each of the four TAQ-based characteristics described above.

Table 4: Sleep and market outcomes: Heterogeneity by relative retail dominance
The table reports the results of sorting stocks each month into three portfolios based on the 30th and 70th percentiles of the retail-trading measure. This measure is defined as the log difference between the number of retail trades in stock i on day t and the number of institutional trades, defined as trades with a dollar size that exceeds \$50,000. We then construct daily equal-weighted portfolio series for open-to-close returns and TAQ-based measures of market quality. For each portfolio, we estimate the predictive regressions in equation (7). H–L denotes the difference in the sleep coefficient between the high- and low-retail portfolios. Newey and West (1987) t-statistics are reported in brackets. For the market-quality measures, lower values indicate better liquidity and stability, so a negative H–L implies that sleep improves market quality more strongly in the high-retail portfolio. For readability, coefficients are scaled to correspond to conventional magnitudes; for example, returns, price impact, and imbalance are multiplied by 100.

	P1 (Low)	P2	P3 (High)	H–L
Return	0.06	0.08	0.11	0.05
	[1.24]	[1.65]	[2.26]	[2.07]
Effective spread	0.18	0.04	-0.04	-0.22
	[2.39]	[0.98]	[-1.65]	[-3.14]
Intraday volatility	0.17	-0.47	-0.04	-0.21
	[1.50]	[-0.89]	[-1.24]	[-1.97]
Dollar price impact	0.21	0.08	0.06	-0.15
	[2.53]	[1.96]	[1.32]	[-1.75]
Absolute buy–sell imbalance	0.09	0.06	0.01	-0.08
	[2.98]	[3.58]	[0.85]	[-2.80]

We then estimate portfolio-level predictive regressions of next-day outcomes on abnormal sleep, mirroring the baseline specification in equation (7). Specifically, for each portfolio p, we regress the daily open-to-close returns and TAQ-based market-quality characteristics on the previous night's abnormal sleep. We maintain the exact same control vector used in the aggregate market analysis alongside the same day-of-week and month-of-year fixed effects. Table 4 summarizes the results. We report the estimated slope for each portfolio, which captures the degree to which better deep sleep is associated with the outcome of interest, and the cross-sectional difference in these measures between the stocks with the least retail-initiated trades (the low portfolio) and the most retail-initiated trades (the high portfolio).

First, the aggregate market return predictability documented in Table 3 masks substantial heterogeneity across firms. While intraday open-to-close returns rise for all stocks in response to higher abnormal sleep, the effect increases monotonically from 6 basis points in the low-retail portfolio to 11 basis points in the high-retail portfolio (double the market-wide effect), yielding a statistically significant high-minus-low spread in returns. Because retail investors' risk-taking is sensitive to their physiological states, better sleep is consistent with more favorable next-day valuation pressure in retail-heavy stocks.

Second, for effective spreads, measuring the actual execution costs incurred by traders, the effect of deep sleep flips from positive in the low-retail portfolio (0.18) to negative in the high-retail portfolio (-0.04), generating a strong cross-sectional spread. This suggests that the liquidity relation is strongest in retail-heavy stocks. For instance, cognitively restored retail traders may trade more actively, whereas lower sleep quality may be associated with reduced participation, which would be consistent with wider effective spreads.

Intraday volatility also appears to be lower in the retail-dominated portfolio after unusually high deep sleep, as reflected by the negative spread between the volatility of the high portfolio versus the low portfolio. That said, this pattern is not strictly monotonic across the three portfolios. This pattern is consistent with evidence that sleep disruption impairs retail investors' attention and information processing, leading to poorer trading performance (see, e.g., Han *et al.* (2025)). When retail traders are well-rested, this noise-driven turbulence subsides, leading to much lower intraday volatility for retail-dominated stocks.

Third, dollar price impact, or Kyle's lambda, also improves for the high-retail portfolio. This variable, which captures market depth and measures how much a trade moves the price, is significantly lower for the retail-dominated portfolio. The -0.15 difference between the dollar price impact of the high-minus-low portfolio is statistically significant at the 10% level. This could reflect, for instance, how the diminished cognitive capacity of retail traders results in shallower order books, causing incoming trades to have a steeper impact on prices.

Finally, the absolute buy–sell imbalance provides indirect evidence consistent with a sleep-related information-processing channel. The high-minus-low difference is significantly negative, suggesting that abnormal sleep leads to a much more balanced order flow in retail stocks. Sleep deprivation can increase the likelihood that retail investors will simply herd or react uniformly to salient news. Restorative sleep promotes independent, heterogeneous decision-making, which reduces one-sided order-flow pressure.

Taken together, the evidence in Table 4 shows that better sleep is systematically associated with stronger market-quality outcomes and, exactly as an attention- and cognition-based theory would predict, these improvements are overwhelmingly concentrated in the stocks most exposed to retail investors.

3.3 Sleep and the Conditional Market Price of Risk

To connect our population-level sleep metrics to the standard asset-pricing language, we also examine whether sleep scales the conditional market price of risk, thereby acting as a proxy for the representative agent's capacity to bear risk. Specifically, motivated by Zhang (2005) and İmrohoroğlu and Tüzel (2014), we specify the stochastic discount factor (SDF) as:

$$M_t = 1 - \lambda_t \, MKT_t, \tag{8}$$

$$\ln \lambda_t = b_0 + b_1 SLEEP_t + b_2 VOL_t. \tag{9}$$

$SLEEP_t$ is one of the two measures of abnormal sleep innovations (i.e., deep sleep or sleep efficiency), measured during the night preceding the trading day t, and VOL_t denotes the innovation to uncertainty, measured as the log first difference of the EPU index. Because λ_t is the strictly-positive time-varying market factor risk premium, the specification implies that either sleep, uncertainty, or both could impact the marginal utility of investors. Notably, $\partial \ln \lambda_t / \partial SLEEP_t = b_1$ captures the influence of sleep quality on the marginal utility, while $\partial \ln \lambda_t / \partial VOL_t = b_2$ reflects the relation between uncertainty and the marginal utility.[21]

Table 5 reports the optimal GMM estimates for the parameters (b_0, b_1, b_2) using the moment condition $\mathbb{E}[M_t R^e_{i,t}] = 0$, where $R^e_{i,t}$ denotes the excess returns of test-asset i on trading day t. The menu of test assets includes the value-weighted returns of 25 portfolios sorted on size and book-to-market, size and investment, size and profitability, size and long-term reversals, book-to-market and investment, book-to-market and profitability, and 38

[21]The SDF specification is deliberately parsimonious. First, while daily data are sufficient to identify any comovement between sleep and the market, we avoid proposing sleep as a standalone risk factor in the SDF due to a short sample period. Second, the SDF is not intended to serve as a comprehensive pricing model for the cross-section of all anomalies. Rather, we are only interested in the robustness and significance of b_1.

Table 5: Sleep, volatility, and the conditional market price of risk
SDF specification: $M_t = 1 - \exp(b_0 + b_1\, SLEEP_t + b_2\, VOL_t)\, MKT_t$. Parameters are estimated by optimal GMM using moments $\mathbb{E}[M_t R^e_{i,t}] = 0$ on the following set of daily value-weighted test asset returns: 25 portfolios sorted on size and book-to-market, size and investment, size and profitability, size and long-term reversals, book-to-market and investment, book-to-market and profitability, and 38 industry portfolios. t-statistics are reported in parentheses.

	Deep Sleep		Sleep Efficiency	
b_0	-2.944	-1.116	-2.274	-1.027
	(-4.558)	(-7.172)	(-4.353)	(-5.486)
b_1 (Sleep)	-1.613	-0.319	-1.804	-0.462
	(-4.685)	(-1.974)	(-2.466)	(-2.593)
b_2 (Volatility)		1.125		1.086
		(9.856)		(7.661)

industry portfolios. This constitutes a comprehensive set aimed at breaking any strong factor structure inherent in a small set of assets (Lewellen, Nagel and Shanken, 2010).

Across both measures of sleep quality, we find that the coefficient b_1 is negative and significant at least at the 10% level. In other words, improvements in sleep lower the price per unit of aggregate risk. This is consistent with the notion that well-rested investors have a greater risk-bearing capacity or lower effective risk aversion. The negative slope coefficient on sleep quality is also consistent with the evidence from Table 3 that improved sleep leads intraday to higher upside volatility relative to downside volatility, and to a reduction in the realized variance overall. Conversely, the positive uncertainty coefficient ($b_2 > 0$) implies a higher price of aggregate risk in turbulent, high-volatility states, aligning with the standard asset-pricing notion whereby a greater quantity of risk should amplify the risk premium. Importantly, the effect of sleep on the marginal utility remains negative regardless of whether we include fundamental uncertainty in the SDF, suggesting that sleep affects conditional risk premia beyond the conventional quantity of risk effect.

4 Conclusion

Economic uncertainty is reflected not only in macroeconomic aggregates and asset prices but also in nightly physiology. In this sense, population sleep acts as a high-frequency physiological state variable that helps measure a welfare-relevant margin of macro-financial risks before they appear in conventional macroeconomic aggregates. Using novel minute-level sleep data for a national cohort, we show that increases in uncertainty are associated with a reduction in deep sleep and sleep efficiency for several nights. This "*wake-and-see*" response is robust to environmental, physiological, and behavioral controls, is more tightly linked to second-moment risk than to first-moment market movements, and is economically meaningful in the aggregate. We then close the loop by showing that population-level sleep quality predicts next-day market quality. Nights of unusually poor sleep foreshadow weaker opening-hour returns, higher realized volatility, more downside relative to upside semivariance, and lower liquidity, with effects concentrated early in the trading day and stronger in retail-dominated stocks. Poor sleep also relates to a higher conditional market price of aggregate risk, consistent with lower aggregate risk-bearing capacity. Taken together, the evidence reveals a two-way link between financial markets and physiological restoration.

Our broader contribution is to show how biometric time series can be used to identify whether candidate macro-financial factors are truly welfare-relevant and potentially priced. Because uncertainty is latent, difficult to measure, and hard to map into welfare in real time, our approach complements traditional indicators with a high-frequency physiological measure linked to attention, cognition, productivity, and risk-bearing capacity. In doing so, we identify a novel non-pecuniary channel through which uncertainty imposes costs: lost deep sleep and reduced sleep efficiency that accumulate across nights and individuals and plausibly translate into lower labor productivity and foregone output. More broadly, the results suggest that population-scale wearable data can extend macro-finance beyond prices, quantities, and consumption by helping quantify the biological channels through which risk is experienced.

The analysis also points to several directions for future research. First, sleep can be modeled as a state variable that shifts risk-bearing capacity or the ability to process information, allowing theories with state-dependent risk aversion or information-processing frictions to be disciplined with daily physiological data and intraday market outcomes. Second, nightly restoration can be embedded directly in preferences or in the accumulation of cognitive capital to study how uncertainty propagates to consumption, investment, and labor supply when restorative resources are depleted. Third, as wearable time series in *All of Us* lengthen and coverage deepens, it will become possible to test whether population sleep directly forecasts lower-frequency macroeconomic outcomes such as productivity, spending, and employment. Each of these directions would connect human physiology more tightly to the macro-finance cycle and help quantify the welfare costs of risk beyond conventional pecuniary margins.

References

Ai, H. and Kiku, D. (2016). Volatility risks and growth options. *Management Science*, **62** (3), 741–763.

Alfaro, I., Bloom, N. and Lin, X. (2024). The finance uncertainty multiplier. *Journal of Political Economy*, **132** (2), 577–615.

All of Us Research Program Investigators (2019). The "all of us" research program. *New England Journal of Medicine*, **381** (7), 668–676.

Amihud, Y. (2002). Illiquidity and stock returns: Cross-section and time-series effects. *Journal of Financial Markets*, **5** (1), 31–56.

Anschukov, A., Bhamra, H. S. and Kuehn, L.-A. (2024). Leverage dynamics and learning about economic crises. *Available at SSRN 4898492*.

Antonakakis, N. and Gupta, R. (2017). Is Economic Policy Uncertainty related to suicide rates? evidence from the United States. *Social Indicators Research*, **133** (2), 543–560.

Antoniou, C., Doukas, J. A. and Subrahmanyam, A. (2013). Cognitive dissonance, sentiment, and momentum. *Journal of Financial and Quantitative Analysis*, **48** (1), 245–275.

Arellano, C., Bai, Y. and Kehoe, P. J. (2019). Financial frictions and fluctuations in volatility. *Journal of Political Economy*, **127** (5), 2049–2103.

Baker, M. and Wurgler, J. (2007). Investor sentiment in the stock market. *Journal of Economic Perspectives*, **21** (2), 129–151.

Baker, S. R., Bloom, N. and Davis, S. J. (2016). Measuring economic policy uncertainty. *Quarterly Journal of Economics*, **131** (4), 1593–1636.

—, —, — and Kost, K. (2026). Policy news and stock market volatility. *Journal of Financial Economics*, **175**, 104187.

Banks, S. and Dinges, D. F. (2007). Behavioral and physiological consequences of sleep restriction. *Journal of Clinical Sleep Medicine*, **3** (5), 519–528.

Bansal, R. and Yaron, A. (2004). Risks for the long run: A potential resolution of asset pricing puzzles. *Journal of Finance*, **59** (4), 1481–1509.

Basu, S. and Bundick, B. (2017). Uncertainty shocks in a model of effective demand. *Econometrica*, **85** (3), 937–958.

Bekaert, G., Engstrom, E. C. and Xu, N. R. (2022). The time variation in risk appetite and uncertainty. *Management Science*, **68** (6), 3975–4004.

Birru, J. and Young, T. (2022). Sentiment and uncertainty. *Journal of Financial Economics*, **146** (3), 1148–1169.

Bloom, N. (2009). The impact of uncertainty shocks. *Econometrica*, **77** (3), 623–685.

—, Bond, S. and Van Reenen, J. (2007). Uncertainty and investment dynamics. *Review of Economic Studies*, **74**, 391–415.

Boguth, O. and Kuehn, L.-A. (2013). Consumption volatility risk. *Journal of Finance*, **68** (6), 2589–2615.

Bretscher, L., Hsu, A. and Tamoni, A. (2023). The real response to uncertainty shocks: The risk premium channel. *Management Science*, **69** (1), 119–140.

Brokamp, C., Beck, A. F., Goyal, N. K., Ryan, P., Greenberg, J. M. and Hall, E. S. (2019). Material community deprivation and hospital utilization during the first year of life: An urban population–based cohort study. *Annals of Epidemiology*, **30**, 37–43.

Buraschi, A., Trojani, F. and Vedolin, A. (2014). When uncertainty blows in the orchard: Comovement and equilibrium volatility risk premia. *Journal of Finance*, **69** (1), 101–137.

Caldara, D. and Iacoviello, M. (2022). Measuring geopolitical risk. *American economic review*, **112** (4), 1194–1225.

Cao, M. and Wei, J. (2005). Stock market returns: A note on temperature anomaly. *Journal of Banking & Finance*, **29** (6), 1559–1573.

Chang, S., Stuckler, D., Yip, P. and Gunnell, D. (2013). Impact of 2008 global economic crisis on suicide: Time trend study in 54 countries. *BMJ*, **347**, f5239.

Da, Z., Engelberg, J. and Gao, P. (2011). In search of attention. *Journal of Finance*, **66** (5), 1461–1499.

—, — and — (2015). The sum of all fears: Investor sentiment and asset prices. *Review of Financial Studies*, **28** (1), 1–32.

Dicks, D. and Fulghieri, P. (2021). Uncertainty, investor sentiment, and innovation. *Review of Financial Studies*, **34** (3), 1236–1279.

Dodds, P. S., Clark, E. M., Desu, S., Frank, M. R., Reagan, A. J., Williams, J. R., Mitchell, L., Harris, K. D., Kloumann, I. M., Bagrow, J. P. *et al.* (2015). Human language reveals a universal positivity bias. *Proceedings of the National Academy of Sciences*, **112** (8), 2389–2394.

—, Harris, K. D., Kloumann, I. M., Bliss, C. A. and Danforth, C. M. (2011). Temporal patterns of happiness and information in a global-scale social network: Hedonometrics and twitter. *PLoS ONE*, **6** (12), e26752.

Edmans, A., García, D. and Norli, Ø. (2007). Sports sentiment and stock returns. *Journal of Finance*, **62** (4), 1967–1998.

Engelberg, J. and Parsons, C. A. (2016). Worrying about the stock market: Evidence from hospital admissions. *The Journal of Finance*, **71** (3), 1227–1250.

Fernández-Villaverde, J., Guerrón-Quintana, P., Kuester, K. and Rubio-Ramírez, J. (2015). Fiscal volatility shocks and economic activity. *American Economic Review*, **105** (11), 3352–3384.

Freed, P. G. (2022). Insufficient sleep and intra-day financial decision-making. *Available at SSRN 4535348*.

Garcia, D. (2013). Sentiment during recessions. *Journal of Finance*, **68** (3), 1267–1300.

Gersen, J. E. and O'Connell, A. J. (2009). Hiding in plain sight? timing and transparency in the administrative state. *The University of Chicago Law Review*, pp. 1157–1214.

Gibson, M. and Shrader, J. (2018). Time use and labor productivity: The returns to sleep. *Review of Economics and Statistics*, **100** (5), 783–798.

Gilchrist, S., Sim, J. W. and Zakrajšek, E. (2014). Uncertainty, financial frictions, and investment dynamics, working Paper, National Bureau of Economic Research.

Goetzmann, W. N., Kim, D., Kumar, A. and Wang, Q. (2015). Weather-induced mood, institutional investors, and stock returns. *Review of Financial Studies*, **28** (1), 73–111.

Gonzalez, A. and Li, X. (2024). Let me sleep on it: Sleep and investor reactions to earnings surprises. *The European Journal of Finance*, **30** (12), 1327–1344.

Grandner, M. A., Patel, N. P., Gehrman, P. R., Xie, D., Sha, D., Weaver, T. and Gooneratne, N. (2010). Who gets the best sleep? ethnic and socioeconomic factors related to sleep complaints. *Sleep Medicine*, **11** (5), 470–478.

Haghayegh, S., Khoshnevis, S., Smolensky, M. H., Diller, K. R. and Castriotta, R. J. (2019). Accuracy of wristband fitbit models in assessing sleep: systematic review and meta-analysis. *Journal of medical Internet research*, **21** (11), e16273.

Han, H. S., Hirshleifer, D., Sheng, J. and Sun, Z. (2025). *Trading in Twilight: Sleep, Mental Alertness, and Stock Market Trading*. NBER Working Paper 33477, National Bureau of Economic Research.

He, Z., Kelly, B. and Manela, A. (2017). Intermediary asset pricing: New evidence from many asset classes. *Journal of Financial Economics*, **126** (1), 1–35.

Hillert, A., Jacobs, H. and Müller, S. (2014). Media makes momentum. *Review of Financial Studies*, **27** (12), 3467–3501.

Hirshleifer, D., Jiang, D. and DiGiovanni, Y. M. (2020). Mood beta and seasonalities in stock returns. *Journal of Financial Economics*, **137** (1), 272–295.

—, Lim, S. S. and Teoh, S. H. (2009). Driven to distraction: Extraneous events and underreaction to earnings news. *Journal of Finance*, **64** (5), 2289–2325.

— and Shumway, T. (2003). Good day sunshine: Stock returns and the weather. *Journal of Finance*, **58** (3), 1009–1032.

Hjetland, G. J., Skogen, J. C., Hysing, M., Gradisar, M. and Sivertsen, B. (2025). How and when screens are used: comparing different screen activities and sleep in norwegian university students. *Frontiers in psychiatry*, **16**, 1548273.

İmrohoroğlu, A. and Tüzel, Ş. (2014). Firm-level productivity, risk, and return. *Management science*, **60** (8), 2073–2090.

Irish, L. A., Kline, C. E., Gunn, H. E., Buysse, D. J. and Hall, M. H. (2015). The role of sleep hygiene in promoting public health: A review of empirical evidence. *Sleep Medicine Reviews*, **22**, 23–36.

Jara, C., Perez, F. and Wagner, R. (2025). Sleep hours fall as income rises: Macro and micro evidence on sleep inequality around the world. *Economics & Human Biology*, **58**, 101496.

Jetté, M., Sidney, K. and Blümchen, G. (1990). Metabolic equivalents (mets) in exercise testing, exercise prescription, and evaluation of functional capacity. *Clinical Cardiology*, **13** (8), 555–565.

Johannes, M., Lochstoer, L. A. and Mou, Y. (2016). Learning about consumption dynamics. *Journal of Finance*, **71** (2), 551–600.

Jordà, Ò. (2005). Estimation and inference of impulse responses by local projections. *American Economic Review*, **95** (1), 161–182.

Jurado, K., Ludvigson, S. C. and Ng, S. (2015). Measuring uncertainty. *American Economic Review*, **105** (3), 1177–1216.

Kalcheva, I., McLemore, P. and Sias, R. D. (2021). Economic Policy Uncertainty and self-control: Evidence from unhealthy choices. *Journal of Financial and Quantitative Analysis*, **56** (4), 1446–1475.

Kamstra, M. J., Kramer, L. A. and Levi, M. D. (2000). Losing sleep at the market: The daylight saving anomaly. *American Economic Review*, **90** (4), 1005–1011.

Kim, E.-J. and Dimsdale, J. E. (2007). The effect of psychosocial stress on sleep: a review of polysomnographic evidence. *Behavioral sleep medicine*, **5** (4), 256–278.

Kung, H. and Schmid, L. (2015). Innovation, growth, and asset prices. *Journal of Finance*, **70** (3), 1001–1037.

Lewellen, J., Nagel, S. and Shanken, J. (2010). A skeptical appraisal of asset pricing tests. *Journal of Financial economics*, **96** (2), 175–194.

Ludvigson, S. C., Ma, S. and Ng, S. (2021). Uncertainty and business cycles: Exogenous impulse or endogenous response? *American Economic Journal: Macroeconomics*, **13** (4), 369–410.

McDonald, R. and Siegel, D. (1986). The value of waiting to invest. *Quarterly Journal of Economics*, **101** (4), 707–727.

McInerney, M., Mellor, J. M. and Nicholas, L. H. (2013). Recession depression: Mental health effects of the 2008 stock market crash. *Journal of Health Economics*, **32** (6), 1090–1104.

Newey, W. K. and West, K. D. (1987). A simple, positive semi-definite, heteroskedasticity and autocorrelation consistent covariance matrix. *Econometrica*, **55** (3), 703–708.

Papanikolaou, D. (2011). Investment shocks and asset prices. *Journal of Political Economy*, **119** (4), 639–685.

Parmar, D., Stavropoulou, C. and Ioannidis, J. P. A. (2016). Health outcomes during the 2008 financial crisis in europe: Systematic literature review. *BMJ*, **354**, i4588.

Patel, N. P., Grandner, M. A., Xie, D., Branas, C. C. and Gooneratne, N. (2010). "Sleep Disparity" in the Population: Poor sleep quality is strongly associated with poverty and ethnicity. *BMC Public Health*, **10**, 475.

Peress, J. (2014). The media and the diffusion of information in financial markets: Evidence from newspaper strikes. *Journal of Finance*, **69** (5), 2007–2043.

Pesaran, H. H. and Shin, Y. (1998). Generalized impulse response analysis in linear multivariate models. *Economics Letters*, **58** (1), 17–29.

Pinegar, J. M. (2002). Losing sleep at the market: Comment. *American Economic Review*, **92** (4), 1251–1256.

Rasch, B. and Born, J. (2013). About sleep's role in memory. *Physiological Reviews*, **93** (2), 681–766.

Stambaugh, R. F., Yu, J. and Yuan, Y. (2012). The short of it: Investor sentiment and anomalies. *Journal of Financial Economics*, **104** (2), 288–302.

Tasali, E., Leproult, R., Ehrmann, D. A. and Van Cauter, E. (2008). Slow-wave sleep and the risk of type 2 diabetes in humans. *Proceedings of the National Academy of Sciences*, **105** (3), 1044–1049.

White, H. (1980). A heteroskedasticity-consistent covariance matrix estimator and a direct test for heteroskedasticity. *Econometrica*, pp. 817–838.

Zhang, L. (2005). The value premium. *The Journal of Finance*, **60** (1), 67–103.

Internet Appendix

IA.A Variable Descriptions

Activity. Data on activity is obtained from the NIH's *All of Us* Research Program. Specifically, we use data on each individual's number of "very active minutes" per day of the sample period. These are the number of minutes the individual engaged in activities with metabolic equivalents (METs) of six or greater, where METs are defined in line with Jetté, Sidney and Blümchen (1990). These minutes only start accruing after 10 minutes of exercise at this level of intensity. After obtaining this data, we calculate the cross-sectional median value of active minutes across all individuals in the data. This provides us with a daily time series of activity that ranges from January 5, 2013 through October 1, 2023.

Age. The age of an individual is calculated by computing the number of years between (i) the individual's date of birth, as reported through the onboarding process of the *All of Us* Research Program and (ii) the date of each sleep event associated with the individual.

Amihud illiquidity. The Amihud illiquidity measure is computed as the absolute value of the cumulative return divided by the total dollar-trading volume within each intraday window. Specifically, for each trading day t and horizon $\tau \in \{60, 120, 180, 300, \text{Close}\}$ minutes,

$$\text{Amihud}_{t,\tau} = \frac{|\text{CumRet}_{\text{open}_t \to \tau_t}|}{\text{DollarVolume}_{\text{open}_t \to \tau_t}},$$

where $\tau = \text{ALL}$ denotes the full open-to-close trading session. Both cumulative returns and trading volumes are constructed for the SPY ETF using the NYSE Trade and Quote (TAQ) database, which aggregates trade and quote information at a one-minute frequency during regular trading hours (9:30 a.m.–4:00 p.m. EST). This variable captures the price impact per dollar traded and serves as an inverse proxy for market liquidity.

Spread. To measure the level of intraday trading costs and market liquidity, we compute the simple (unweighted) average *relative* bid–ask spread within each intraday window. Specifically, for each trading day t and horizon $\tau \in \{60, 120, 180, 300, \text{Close}\}$ minutes, the cumulative average relative spread is defined as

$$\text{Spread}_{t,\tau} = \frac{1}{M_{t,\tau}} \sum_{i=1}^{M_{t,\tau}} \text{RelSpread}_{t,i},$$

where $M_{t,\tau}$ denotes the number of one-minute intervals observed from the market open through horizon τ or until the official market close, whichever comes first. For $\tau = \text{ALL}$, the measure aggregates all available one-minute observations during the regular trading session of that day. The one-minute relative bid–ask spread for minute i is defined as

$$\text{RelSpread}_{t,i} \equiv \frac{\text{Ask}_{t,i} - \text{Bid}_{t,i}}{\text{Mid}_{t,i}}, \qquad \text{Mid}_{t,i} = \frac{\text{Ask}_{t,i} + \text{Bid}_{t,i}}{2}.$$

These measures are constructed using one-minute bid and ask quotes for the SPY ETF from the TAQ database. This variable summarizes the typical relative trading cost faced by market participants, assigning equal weight to each minute within the specified window. By scaling bid–ask spreads by the prevailing mid-quote, $\text{AvgRelSpread}_{t,\tau}$ expresses trading costs in percentage terms and captures the average level of liquidity over the trading window.

COVID-19. The number of new COVID-19 cases diagnosed each day per one million people in the United States between March 3, 2020 and December 31, 2023 is obtained from the Center for Systems Science and Engineering (CSSE) at Johns Hopkins University at the following link: https://github.com/CSSEGISandData/COVID-19/.

Cumulative return. Cumulative market returns are computed from one-minute log returns measured from the market open on day t through each intraday horizon $\tau \in \{60, 120, 180, 300, \text{Close}\}$ minutes. Specifically, for each day t and horizon τ,

$$\text{CumRet}_{t,\tau} = \sum_{j=1}^{M_{t,\tau}} r_{t,j},$$

where $r_{t,j}$ denotes the one-minute log return of the SPY ETF in minute j of trading day t, and $M_{t,\tau}$ denotes the number of one-minute intervals observed from the market open through horizon τ or until the official market close, whichever comes first (with $\tau = \text{ALL}$ representing the full trading session). The one-minute price series used to construct these returns are obtained from the NYSE Trade and Quote (TAQ) database, which aggregates trade and quote information at the one-minute frequency during regular trading hours (9:30 a.m.–4:00 p.m. EST).

Deep Sleep. Data on deep sleep is constructed using data provided by the *All of Us* Research Program. The construction of this variable is provided in the discussion related to equation (1) in the main text.

Deprivation index. The Nationwide Community Deprivation Index is constructed by following Brokamp *et al.* (2019) and is disseminated through the *All of Us* Research Program. This variable is constructed from responses to the annual American Community Survey (ACS) administered by the United States Census Bureau and reflects the first principal component of six measures of socioeconomic conditions captured by the ACS. This principal component, which explains about 50% to 60% of the variation in the underlying measures, is referred to as the "Deprivation index" and is scaled to take values between zero (low deprivation) and one (high deprivation). The *All of Us* Research Program reports the value of this index that corresponds to the three-digit ZIP code associated with an individual's location in the United States.

Education. Education refers to the fraction of the population at the three-digit ZIP code level that are 25 years of age or older with an educational attainment of at least high school graduation or equivalent (e.g., have successfully completed the General Educational Development (GED) test). This variable is constructed from responses to the annual American Community Survey (ACS) administered by the United States Census Bureau. The *All of Us* Research Program reports the value of this variable that corresponds to the three-digit ZIP code associated with an individual's location in the United States.

Ethnicity. Ethnicity refers to the self-reported ethnicity of an individual included in the *All of Us* Research Program. Selections include "Hispanic, Latino, or Spanish," and "Non-Hispanic," among other possible selections (including choosing not to answer). Complete information on the coding of this variable is available online via the *All of Us* documentation.

Good Macro News Dummies. Data on macroeconomic announcements are obtained from standard economic release calendars and include four major indicators: the unemployment rate (UNRATE), initial jobless claims (ICSA), real gross domestic product (GDPC1), and industrial production (INDPRO). For each release, we collect both the realized value and the corresponding consensus forecast from "www.investing.com". We then construct directionally consistent surprise measures by comparing actual outcomes to forecasts, taking into account the economic interpretation of each variable. Specifically, for variables where lower values indicate stronger economic conditions (UNRATE and ICSA), realizations below the forecast are classified as good news, while realizations above the forecast are classified as bad news. For variables where higher values indicate stronger economic conditions (GDPC1 and INDPRO), realizations above the forecast are classified as good news, while realizations below the forecast are classified as bad news. Based on these classifications, we construct four pre-open good-news indicator variables: *UNRATE Good*, *ICSA Good*, *GDPC1 Good*, and *INDPRO Good*.

All four macroeconomic series are released prior to the U.S. equity market open (9:30 a.m. ET) on trading day t, with GDP, initial jobless claims, and the unemployment rate released at 8:30 a.m. ET, and industrial production released at 9:15 a.m. ET. In the C1.5 specification, these four good-news dummies are included jointly as contemporaneous pre-open controls. They are aligned with trading day t, so that they capture macroeconomic information shocks arriving after the sleep period on night $t-1$ but before the market opens on day t.

Happy. Happiness is measured using the daily language-based hedonometer index that is made available on hedonometer.org. This index is constructed following the methodology described by Dodds *et al.* (2011) and Dodds *et al.* (2015).

HR. The heart rate (HR) is constructed using data from the NIH *All of Us* Research Program. Specifically, on each day of the sample period, we compute the average value of each individual's heart rate using minute-level heart rate data. We then take the median heart rate across all individuals in the data on the given day. This provides us with a daily time series of heart rates that ranges from January 21, 2015 through October 1, 2023.

Income. Income refers to the median household income in the past 12 months in 2015 inflation-adjusted dollars. This variable is constructed from responses to the annual American Community Survey (ACS) administered by the United States Census Bureau. The *All of Us* Research Program reports the value of this variable that corresponds to the three-digit ZIP code associated with an individual's location in the United States.

Income assistance. Income assistance refers to fraction of households in a three-digit ZIP code area that have received public assistance income or food stamps or Supplemental Nutrition Assistance Program (SNAP) benefits in the past 12 months. This variable is constructed from responses to the annual American Community Survey (ACS) administered by the United States Census Bureau. The *All of Us* Research Program reports the value of this variable that corresponds to the three-digit ZIP code associated with an individual's location in the United States.

Poverty. Poverty refers to the fraction of households in a three-digit ZIP code area that have a household income in the last 12 months that is below the federal poverty level. This variable is constructed from responses to the annual American Community Survey (ACS) administered by the United States Census Bureau. The *All of Us* Research Program reports the value of this variable that corresponds to the three-digit ZIP code associated with an individual's location in the United States.

Race. Race refers to the self-reported race of an individual included in the *All of Us* Research Program. Selections include "White," "Black," and "Asian," among other possible selections (including choosing not to answer). Complete information on the coding of this variable is available online via the *All of Us* documentation.

Rainfall. Data on the average daily rainfall, measured in millimeters, is obtained from Meteostat (https://meteostat.net/en/), one of the largest vendors of open climate and weather data. Meteostat aggregates weather data from a variety of sources, including the NOAA, to provide data on the weather at each of the thousands of weather stations located in the United States. We then compute the average amount of rainfall across all of these weather stations on each day of the sample period.

Realized volatility (RV). Intraday realized volatility is constructed from one-minute log returns of the SPDR S&P 500 ETF (SPY) using high-frequency trade prices from the NYSE Trade and Quote (TAQ) database. For each trading day t and intraday horizon $\tau \in \{60, 120, 180, 300, \text{Close}\}$ minutes, realized volatility is defined as the square root of the cumulative sum of squared one-minute log returns:

$$\text{RV}_{t,\tau} = \sqrt{\sum_{j=1}^{M_{t,\tau}} r_{t,j}^2},$$

where $r_{t,j}$ denotes the one-minute log return of SPY in minute j of trading day t, and $M_{t,\tau}$ denotes the number of one-minute intervals observed from the market open through horizon τ or until the official market close, whichever comes first. To capture directional components of volatility, we further decompose realized volatility into negative and positive components, $\text{RV\_neg}_{t,\tau}$ and $\text{RV\_pos}_{t,\tau}$, by restricting the summation to negative ($r_{t,j} < 0$) and positive ($r_{t,j} > 0$) one-minute returns, respectively. All realized volatility measures are computed using intraday data during regular trading hours (9:30 a.m.–4:00 p.m. EST).

Realized volatility asymmetry ($RV^+ - RV^-$). To capture asymmetries between upside and downside intraday volatility, we construct a realized-volatility gap measure based on one-minute semivariances. For each trading day t and intraday horizon $\tau \in \{60, 120, 180, 300, \text{Close}\}$ minutes, the volatility asymmetry measure is defined as

$$RV^{+}_{t,\tau} - RV^{-}_{t,\tau},$$

where $RV^{+}_{t,\tau}$ and $RV^{-}_{t,\tau}$ denote the cumulative positive and negative realized volatility components (defined as square roots of restricted sums) computed from one-minute log returns up to horizon τ or the market close. A positive value of $RV^{+}_{t,\tau} - RV^{-}_{t,\tau}$ indicates that upside price movements contribute more to total volatility than downside movements during the corresponding intraday window.

Sex. Sex refers to the self-reported sex of an individual included in the *All of Us* Research Program. Selections include "Male" and "Female" among other possible selections (including choosing not to answer). Information on the coding of this variable is available online via the *All of Us* documentation.

Sleep Efficiency. Data on sleep efficiency is constructed using data provided by the *All of Us* Research Program. The construction of this variable is provided in the discussion related to equation (2) in the main text.

Sunlight. Data on the average amount of sunlight each day, measured in hours, is provided by the National Oceanic and Atmospheric Administration (NOAA) agency of the U.S. Department of Commerce. This data, which is collected and disseminated by NOAA's Global Monitoring Laboratory, reports the daily average sunlight duration across 21 U.S. main cities from January 1, 2015 through December 31, 2023. The data are available via the following link: https://gml.noaa.gov/grad/solcalc/.

Temperature. Data on the average daily temperature is obtained from Meteostat (https://meteostat.net/en/), one of the largest vendors of open climate and weather data. Meteostat aggregates weather data from a variety of sources, including the NOAA, to provide data on the weather at each of the thousands of weather stations located in the United States. We then compute the average temperature, recorded in degrees Celsius, across all of these weather stations on each day between January 1, 2014 and December 3, 2023.

WRDS TAQ Millisecond Intraday Indicators: Retail participation and market quality

Retail participation variables and stock-level market-quality characteristics are obtained from the WRDS TAQ Millisecond Tools *Millisecond Intraday Indicators* (daily stock-level indicators computed during regular market hours).

Absolute buy–sell imbalance (BS_RATIO_NUM). The absolute percent order imbalance based on the number of trades. Higher values indicate more one-sided trading (either buy- or sell-dominated), while lower values indicate more balanced order flow.

Dollar price impact (DOLLARPRICEIMPACT_LR_AVE). The simple averaged dollar price impact based on the Lee–Ready classification. Higher values indicate that signed order flow moves prices more (lower depth / worse resiliency).

Effective spread (EFFECTIVESPREAD_PERCENT_AVE). The simple averaged percent effective spread based on the Lee–Ready classification. Higher values indicate a larger effective bid–ask spread and thus higher execution costs / worse liquidity.

Intraday volatility (IVOL_T). The trade-based intraday volatility measure computed during market hours. Higher values indicate greater intraday price variation / lower intraday stability.

Relative retail participation (TOTAL_TRADE_RETAIL_REL). Defined as the difference between the number of retail trades (`TOTAL_TRADE_RETAIL`) and the number of 50K institutional trades (`TOTAL_TRADE_INST50K`). A higher value indicates that a stock's trading activity is more retail-dominated relative to the large-trade institutional proxy on that day.

Total 50K institutional trades (TOTAL_TRADE_INST50K). The total number of trades in the WRDS "50K Institutional" category during market hours. This category is a size-cutoff proxy provided by WRDS and should be interpreted as a large-trade institutional proxy rather than a literal measure of all institutional trading.

Total retail trades (TOTAL_TRADE_RETAIL). The total number of trades classified as retail during market hours in the WRDS Millisecond Intraday Indicators.

IA.B Measurement Error in Deep Sleep from Wearable Devices

A natural concern is that consumer wearable devices may not measure the amount of time spent in deep sleep without error. Unlike polysomnography (PSG), which directly measures brain activity and is considered the clinical gold standard for sleep-stage classification, commercial fitness trackers infer sleep stages using proprietary algorithms based on movement and physiological signals from heart rate. Prior validation studies show that wearable devices generally perform well in measuring total sleep duration and sleep-wake states, but are less accurate in classifying specific sleep stages, including deep sleep (e.g., Haghayegh, Khoshnevis, Smolensky, Diller and Castriotta (2019)). Several studies further document that wearable devices often understate deep sleep and overstate light sleep on average, although the direction and magnitude of the bias can vary across devices, populations, and sleep conditions. Because our baseline specifications include individual fixed effects, such time-invariant, device-specific biases are absorbed.

To assess whether our baseline results are driven by plausible time-varying measurement error in wearable measures of deep sleep, we conduct a sensitivity analysis that allows measured deep sleep to be contaminated by heart-rate-related misclassification. Specifically, we construct an adjusted measure of deep sleep:

$$\text{DeepSleep}_t^{\text{Adj.}}(\lambda) = \frac{\text{Minutes of Deep Sleep}_t + \lambda \cdot \text{HR}_t^{\text{Adj.}}}{\text{Minutes of Sleep}_t}, \tag{IA.B.1}$$

where $\text{HR}_t^{\text{Adj.}}$ denotes either demeaned or standardized heart rate. The scalar λ, which is measured in minutes of deep sleep per unit of heart rate, governs the magnitude of the correction. Positive values of λ correct for the continuous inverse relationship assumed by wearable algorithms: the adjustment adds minutes back on nights when elevated heart rate causes the device to understate true deep sleep (implicitly assuming these minutes were erroneously assigned to lighter sleep stages, thereby keeping total time asleep fixed). Symmetrically, it subtracts artificially inflated minutes on nights when heart rate is unusually low. We then re-estimate the baseline daily regression of sleep quality on economic policy uncertainty for a broad grid of values of λ, while holding the underlying regression sample and control variables fixed across specifications.

Figure IA.B.1 reports the estimated coefficient on economic policy uncertainty across alternative values of λ. The left panel uses demeaned heart rate, while the right panel uses standardized heart rate. Across a wide range of conservative calibrations, adjusting for potential heart-rate misclassification yields coefficients that are even more negative than our baseline. Moreover, the associated confidence intervals remain robustly below zero. While the estimated effect eventually attenuates toward zero at extreme values of λ, reaching this threshold requires assuming an implausibly large algorithmic penalty that far exceeds the error margins documented in clinical validation studies. This indicates that if wearable algorithms are indeed penalizing deep sleep for stress-induced heart rate elevations, our unadjusted baseline estimates serve as a conservative lower bound for the true physiological effect, rather than being driven by mismeasurement.

Overall, the results suggest that our baseline findings are robust to a broad class of measurement-error corrections motivated by the sleep-tracking literature.

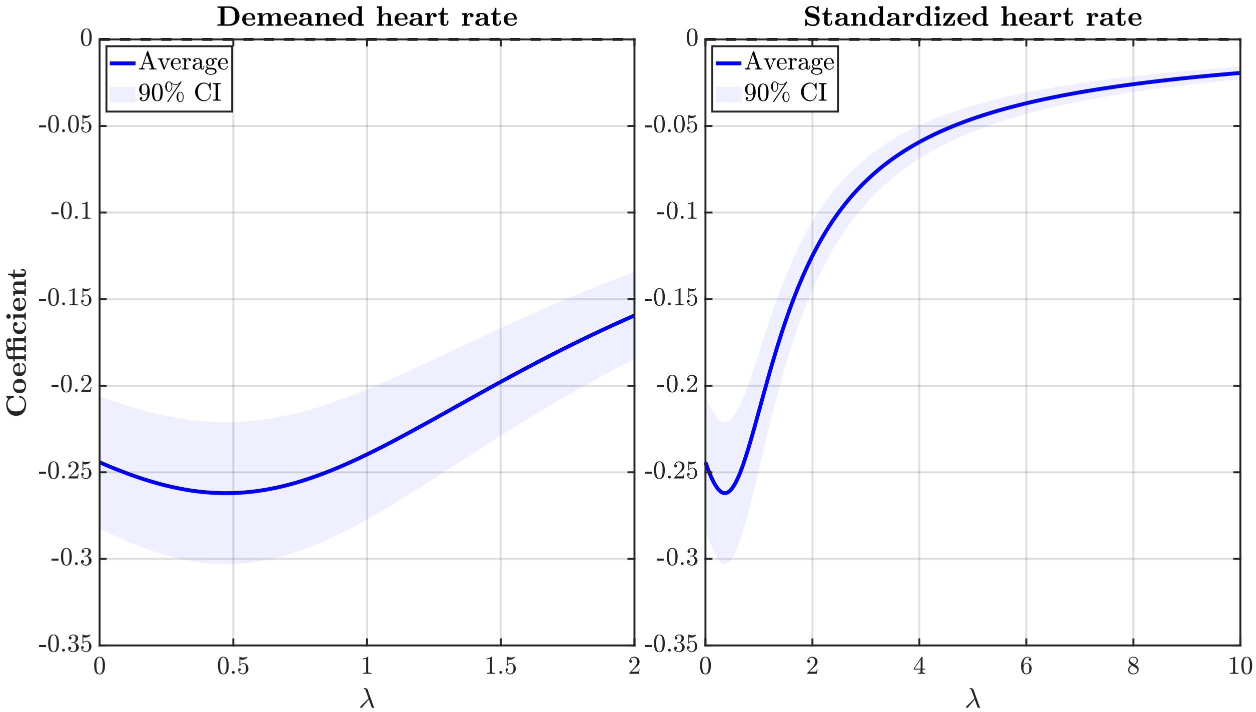

Figure IA.B.1: Sensitivity to measurement error
The figure reports the estimated sensitivity of sleep quality to the Economic Policy Uncertainty (EPU) index of Baker *et al.* (2016) after adjusting deep sleep for potential heart-rate-related measurement error. For each value of λ, adjusted deep sleep is constructed as the average minutes of deep sleep, measured at the aggregate level, plus λ times the corresponding heart-rate adjustment, per equation (IA.B.1). Here, the average heart rate is also measured at the aggregate level. The figure then re-estimates the baseline daily regression of adjusted deep sleep on the EPU index from equation (5) and plots the resulting coefficient on EPU across the λ grid. The left-hand panel adjusts deep sleep using demeaned heart rate, while the right-hand panel adjusts deep sleep by the standardized heart rate. Standard errors are computed using Newey and West (1987) with nine lags. The sample period underlying this analysis ranges from April 26, 2017 through May 26, 2023.

Table IA.C.1: Summary statistics: Other variables

The table reports summary statistics for the control variables used in the main analyses: the natural logarithm of the daily Economic Policy Uncertainty (EPU) index (Baker *et al.*, 2016); daylight duration (hours), which is referred to as "Sunlight;" average daily temperature (degrees Celsius); and average daily precipitation (millimeters). We also report the daily number of newly diagnosed COVID-19 cases per million people and the Hedonometer's daily happiness score (Dodds *et al.*, 2011). Finally, we construct two additional variables from using *All of Us* data: daily physical activity (measured in minutes of "very active" physical activity) and each individual's heart rate, expressed in beats per minute (BPM). For each variable, the table reports the mean, median, standard deviation, and the 5th, 10th, 25th, 75th, 90th, and 95th percentiles. Complete variable definitions appear in Section IA.A of the Internet Appendix. The sample ranges from April 26, 2017 through May 26, 2023.

	Mean	Std	p5	p10	p25	Median	p75	p90	p95
EPU	4.80	0.62	3.89	4.07	4.40	4.75	5.16	5.63	5.96
Sunlight (Hours)	12.23	1.96	9.37	9.51	10.33	12.28	14.13	14.85	14.97
Temperature (Celsius)	12.82	8.35	0.14	1.90	5.57	12.95	21.16	23.57	24.16
Rainfall (mm)	2.31	1.45	0.51	0.69	1.21	2.03	3.04	4.33	5.21
COVID	1.49	2.17	0.00	0.00	0.00	0.64	2.08	4.88	6.51
Activity (Mins)	3.70	1.63	1.00	1.00	3.00	4.00	5.00	6.00	6.00
Happy	5.98	0.06	5.88	5.92	5.96	5.99	6.02	6.04	6.06
HR (BPM)	73.98	0.77	72.81	72.99	73.40	73.91	74.56	75.03	75.23

IA.C Additional Tables

Table IA.C.2: Key domestic and geopolitical news days

The table presents a set of 50 prominent domestic and geopolitical news events that are relevant for U.S. households between May 2017 and April 2023. We initially screened events using a large language model and then manually verified and curated the final set according to prominence, U.S. relevance, and plausible short-run uncertainty content.

Number	Date	Event Description
1	2017-06-01	Trump announces U.S. withdrawal from Paris Climate Agreement
2	2017-06-14	Grenfell Tower fire in London kills 72, prompts safety overhaul debate
3	2017-07-04	North Korea launches its first ICBM (Hwasong-14)
4	2017-08-17	ISIS-inspired van attacks in Barcelona and Cambrils kill 16
5	2017-10-01	Las Vegas shooting becomes deadliest in modern U.S. history
6	2017-10-27	Catalan parliament declares independence; Spain imposes direct rule
7	2017-12-08	Tensions with North Korea increase following test of Hwasong-15 ICBM
8	2017-12-22	Trump signs $1.5 tn Tax Cuts and Jobs Act into law
9	2018-01-06	Nation-wide anti-government protests crest across Iran
10	2018-03-04	Nerve-agent attack on Skripals strains U.K.–Russia relations
11	2018-04-07	Suspected chlorine-gas attack hits Douma, Syria
12	2018-04-12	Syrian crisis escalates after chemical attack on civilians
13	2018-04-14	U.S., U.K., France launch missile strikes on Syrian regime sites
14	2018-10-02	Saudi journalist Jamal Khashoggi murdered inside Istanbul consulate
15	2018-11-06	U.S. midterm elections flip House control to Democrats
16	2018-11-25	Russia seizes Ukrainian vessels in Kerch Strait
17	2018-12-22	Longest U.S. federal shutdown begins over border-wall funding
18	2019-01-25	Record 35-day U.S. government shutdown ends
19	2019-03-22	Mueller delivers Russia-probe report to U.S. Attorney General
20	2019-05-10	U.S. hikes tariffs on $200 bn of Chinese goods—trade-war apex
21	2019-06-20	Iran shoots down U.S. RQ-4 drone over Strait of Hormuz
22	2019-09-14	Drone/missile attack cripples Saudi Aramco oil facilities at Abqaiq
23	2019-10-09	Turkey launches offensive against Kurdish forces in Syria
24	2019-12-18	U.S. House impeaches President Trump for abuse of power
25	2020-01-03	U.S. drone strike kills Iranian general Qasem Soleimani
26	2020-01-23	Wuhan locks down as novel coronavirus spreads globally
27	2020-03-11	WHO declares COVID-19 a global pandemic
28	2020-04-12	OPEC+ finalises historic oil-production cuts
29	2020-05-25	Murder of George Floyd sparks worldwide protests
30	2020-06-30	China imposes sweeping national-security law on Hong Kong
31	2020-07-01	US/Iran tensions escalate
32	2020-07-22	U.S. orders closure of China's Houston consulate; Beijing retaliates
33	2020-08-09	Belarus election triggers mass protests against Lukashenko
34	2020-11-07	Joe Biden projected winner of U.S. presidential election
35	2020-11-10	Pfizer reports 90 % efficacy in first COVID-19 vaccine data
36	2021-01-06	U.S. Capitol insurrection shocks American democracy
37	2021-06-24	Surfside condominium tower collapses in Florida
38	2021-07-07	Haitian President Jovenel Moïse assassinated
39	2021-08-03	Afghan Crisis escalates following Taliban attacks on urban areas
40	2022-04-14	Ukraine sinks Russia's Black Sea flagship Moskva
41	2022-05-14	White-supremacist shooting kills 10 in Buffalo, New York
42	2022-06-24	U.S. Supreme Court overturns Roe v. Wade
43	2022-07-08	Former Japanese PM Shinzo Abe assassinated
44	2022-09-16	Death of Mahsa Amini ignites nationwide protests in Iran
45	2022-11-13	Bombing in tourist region of Istanbul killed 6 and injured 81
46	2022-12-07	Peru's President Castillo ousted after failed self-coup
47	2022-12-22	Historic Arctic blast cripples U.S. infrastructure and travel
48	2023-02-06	Magnitude-7.8 earthquake devastates Turkey and Syria
49	2023-03-10	Silicon Valley Bank collapse triggers banking turmoil
50	2023-04-15	Sudan civil war erupts between army and Rapid Support Forces

Table IA.C.3: Projections: Robustness to the construction of the sleep measures
The table presents a series of robustness tests related to the projection analysis associated with equation (5), described in Section 2.2. Specifically, the table reports robustness to various aspects of the aggregation procedure described in Section 1.4.1. Panels A and B report the results obtained after reconstructing the aggregate measures of sleep quality without detrending the data and by taking the cross-sectional average rather than median each day, respectively. Panel C reports the results obtained by estimating equation (3) without including any day-of-the-week or month-of-the-year fixed effects. Next, Panel D reports the results obtained if the data are not winsorized but a comprehensive set of holiday fixed effects is included in the regression analysis. These fixed effects capture differences in sleep quality on (i) the days that Daylight Saving Time starts and ends, (ii) Federal holidays, (iii) Easter, (iv) Federal election dates, (v) and holidays, including New Year, July 4, Christmas, Thanksgiving, and Labor Day. Finally, Panel E reports the results obtained if we do not winsorize the data. Odd-numbered columns report the results of univariate regressions, while even-numbered columns also include the comprehensive set of control variables underlying equation (5). Finally, t-statistics, reported in parentheses, are constructed using Newey and West (1987) standard errors that are constructed using nine lags. The sample period runs from April 26, 2017 through May 26, 2023.

Variable	Deep Sleep		Sleep Efficiency	
	(1)	(2)	(3)	(4)
Panel A: No time trend				
EPU	-0.19	-0.23	-0.37	-0.31
	(-7.85)	(-11.41)	(-14.87)	(-11.98)
R^2	0.49	0.64	0.43	0.59
Panel B: Cross-sectional average				
EPU	-0.10	-0.12	-0.30	-0.21
	(-4.71)	(-6.99)	(-9.89)	(-6.99)
R^2	0.63	0.68	0.46	0.51
Panel C: No day or month fixed effects				
EPU	-0.19	-0.22	-0.34	-0.29
	(-6.95)	(-9.43)	(-11.62)	(-11.21)
R^2	0.04	0.39	0.11	0.38
Panel D: No winsorization with holiday fixed effects				
EPU	-0.09	-0.11	-0.06	-0.04
	(-4.07)	(-5.90)	(-10.32)	(-7.44)
R^2	0.58	0.63	0.98	0.98
Panel E: No winsorization				
EPU	-0.09	-0.12	-0.03	-0.01
	(-4.09)	(-6.34)	(-1.90)	(-0.50)
R^2	0.57	0.62	0.04	0.05
Controls	No	Yes	No	Yes

Table IA.C.4: Projections: Sub-sample analysis

The table presents a series of robustness tests related to the sample period of data used to estimate equation (5), described in Section 2.2. While the sample period underlying the baseline regressions runs from April 26, 2017 through May 26, 2023, this table considers two alternative sample periods. To begin, Panel A repeats the baseline regressions after removing the NBER recession that ranged from February 2020 through April 2020. Next, Panel B repeats the baseline regressions in the recent half of the sample period, which ranges from May 10, 2020 through May 26, 2023. Odd-numbered columns report the results of univariate regressions, while even-numbered columns also include the comprehensive set of control variables underlying equation (5). Finally, t-statistics, reported in parentheses, are constructed using Newey and West (1987) standard errors with nine lags.

Variable	Deep Sleep		Sleep Efficiency	
	(1)	(2)	(3)	(4)
Panel A: Drop NBER recession				
EPU	-0.04	-0.09	-0.20	-0.15
	(-1.82)	(-4.66)	(-6.65)	(-5.32)
R^2	0.57	0.62	0.49	0.54
Panel B: Sub-sample analysis				
EPU	-0.13	-0.08	-0.26	-0.14
	(-4.39)	(-2.82)	(-7.13)	(-4.93)
R^2	0.62	0.68	0.60	0.67
Controls	No	Yes	No	Yes

Table IA.C.5: Projections: Robustness to economic conditions

The table presents a series of robustness tests related to the projection analysis associated with equation (5), described in Section 2.2. Specifically, the table reports robustness to using alternative measures of economic conditions in the projection, in place of the Economic Policy Uncertainty (EPU) index. Panel A replaces the daily value of the EPU index with the daily value of the VIX index. Likewise, Panels B and C measure the daily level of uncertainty using the equity market volatility index (VOL) and the Bekaert *et al.* (2022) (BEX) measure of economic uncertainty, respectively. Panel D replaces the level of the EPU index with its innovation, obtained from an AR(1) model. Similarly, Panel E replaces the level of the EPU index with its positive innovations. Negative innovations to the EPU index are replaced with a zero. Panel F measures economic conditions using daily excess market returns, while Panels G and H measure the level of economic conditions using the investment-minus-consumption (IMC) spread of Papanikolaou (2011) and the intermediary capital factor (INT) of He *et al.* (2017), respectively. Odd-numbered columns report the results of univariate regressions, while even-numbered columns also include the comprehensive set of control variables underlying equation (5). Finally, t-statistics, reported in parentheses, are constructed using Newey and West (1987) standard errors that are computed using nine lags. The sample period runs from April 26, 2017 through May 26, 2023.

Variable	Deep Sleep		Sleep Efficiency	
	(1)	(2)	(3)	(4)
Panel A: VIX	-0.06	-0.08	-0.27	-0.16
	(-1.86)	(-2.43)	(-6.21)	(-4.22)
R^2	0.47	0.52	0.41	0.50
Panel B: VOL	-0.04	-0.05	-0.19	-0.11
	(-2.15)	(-2.71)	(-5.24)	(-3.96)
R^2	0.57	0.62	0.43	0.51
Panel C: BEX	-0.15	-0.13	-0.28	-0.16
	(-7.14)	(-5.60)	(-8.02)	(-4.96)
R^2	0.49	0.53	0.41	0.50
Panel D: EPU AR(1) residuals	-0.02	-0.03	-0.10	-0.04
	(-1.47)	(-2.21)	(-3.64)	(-2.46)
R^2	0.57	0.62	0.41	0.51
Panel E: Positive EPU AR(1) residuals	-0.03	-0.03	-0.12	-0.07
	(-1.80)	(-1.91)	(-4.24)	(-3.64)
R^2	0.57	0.62	0.41	0.51
Panel F: MKTRF	0.02	0.03	0.03	0.02
	(1.15)	(1.56)	(0.83)	(0.86)
R^2	0.46	0.52	0.34	0.48
Panel G: IMC	0.01	0.01	0.00	-0.01
	(0.36)	(0.41)	(0.22)	(-0.30)
R^2	0.46	0.52	0.34	0.48
Panel H: INT	0.02	0.03	0.02	0.00
	(0.99)	(1.47)	(0.67)	(0.22)
R^2	0.46	0.52	0.34	0.48
Controls	No	Yes	No	Yes

Table IA.C.6: Sleep Efficiency and Intraday Market Responses
This table reports regressions in which the dependent variables are intraday market responses measured from the market open of day t through horizon τ of the same trading day, where $\tau \in \{60, 120, 180, 300\}$ minutes, as well as the full open-to-close trading day. The dependent variables span multiple dimensions of intraday market quality, including: (i) intraday price dynamics, measured by cumulative market returns over the same windows; (ii) realized volatility (RV) constructed from high-frequency returns; (iii) measures of intraday volatility asymmetry, captured by the difference between positive and negative realized volatility components ($RV^+ - RV^-$); and (iv) liquidity and trading cost measures, including the Amihud illiquidity measure (computed as the absolute return divided by dollar trading volume) and the average relative bid–ask spread (AvgRelSpread). Detailed definitions, construction procedures, and timing conventions for all dependent variables are provided in Section IA.A. The key explanatory variable is the abnormal component of sleep efficiency on night $t-1$ (i.e., the night following the close of trading day $t-1$), obtained by filtering sleep efficiency, defined in equation (2), through equation (3). All regressions include the following controls: the previous trading day's open-to-close return and overnight return, the lagged economic policy uncertainty (EPU_{t-1}), and the lagged dependent variable (y_{t-1}). All variables are standardized. The sample covers April 26, 2017 through May 26, 2023. t-statistics based on Newey and West (1987) standard errors are reported in brackets.

Minutes (τ)	60	120	180	300	Close
Return	0.01	0.01	-0.03	-0.01	-0.02
	[0.16]	[0.19]	[-0.73]	[-0.27]	[-0.43]
$\bar{R}^2$	0.01	0.02	0.01	0.01	0.01
RV	-0.05	-0.03	-0.02	-0.02	-0.02
	[-2.26]	[-1.78]	[-1.25]	[-1.19]	[-1.17]
$\bar{R}^2$	0.72	0.74	0.75	0.77	0.78
RV^+-RV^-	-0.01	-0.00	-0.03	-0.02	-0.02
	[-0.26]	[-0.09]	[-0.80]	[-0.61]	[-0.63]
$\bar{R}^2$	0.03	0.06	0.05	0.06	0.06
Amihud	-0.09	-0.11	-0.12	-0.07	-0.10
	[-2.49]	[-2.85]	[-3.22]	[-2.06]	[-2.65]
$\bar{R}^2$	0.04	0.03	0.03	0.02	0.02
AvgRelSpread	-0.07	-0.05	-0.03	-0.02	-0.02
	[-1.66]	[-1.39]	[-1.27]	[-0.89]	[-1.24]
$\bar{R}^2$	0.30	0.55	0.67	0.71	0.68
Controls	Yes	Yes	Yes	Yes	Yes
N	1532	1532	1532	1532	1532

Table IA.C.7: Deep Sleep and Intraday Market Responses with Pre-Open Macro News Controls

This table reports regressions in which the dependent variables are intraday market outcomes measured from the market open on day t through to horizon τ on the same trading day, where $\tau \in \{60, 120, 180, 300\}$ minutes, as well as over the full open-to-close trading day, which corresponds to $\tau = 390$ minutes. The dependent variables capture several dimensions of intraday market quality: (i) intraday price dynamics, measured by cumulative returns over the corresponding window (*Return*); (ii) realized volatility constructed from high-frequency returns (RV); (iii) intraday volatility asymmetry, measured as the difference between positive and negative realized volatility components ($RV^+ - RV^-$); and (iv) liquidity and trading-cost measures, including the Amihud illiquidity measure, defined as the absolute return divided by dollar trading volume, and the average relative bid–ask spread (*Spread*). Detailed definitions, construction procedures, and timing conventions for all dependent variables are provided in Section IA.A. The key explanatory variable is the abnormal component of deep sleep on night $t-1$, that is, the night between the close of trading day $t-1$ and the open of trading day t. This variable is obtained by filtering the deep-sleep measure defined in equation (1) through equation (3). All regressions include the previous trading day's open-to-close return, the overnight return, lagged economic policy uncertainty (EPU_{t-1}), and the lagged dependent variable (y_{t-1}) as controls. In addition, we include four dummy variables indicating pre-open good macroeconomic news releases on day t, corresponding to GDP, initial jobless claims, unemployment rate, and industrial production, as described in Section IA.A. All variables are standardized. The sample spans April 26, 2017 to May 26, 2023. t-statistics based on Newey and West (1987) standard errors are reported in brackets.

Minutes (τ)	60	120	180	300	Close
Return	0.06***	0.07***	0.06***	0.04**	0.05**
	[2.79]	[3.05]	[2.75]	[1.96]	[2.19]
$\bar{R}^2$	0.01	0.03	0.01	0.01	0.01
RV	-0.02**	-0.03***	-0.03***	-0.03***	-0.02***
	[-2.02]	[-2.87]	[-3.07]	[-2.92]	[-2.74]
$\bar{R}^2$	0.72	0.74	0.75	0.77	0.78
RV^+-RV^-	0.06***	0.06**	0.05**	0.03	0.03
	[2.77]	[2.50]	[2.11]	[1.09]	[1.44]
$\bar{R}^2$	0.03	0.06	0.05	0.06	0.06
Amihud	-0.05**	-0.05**	-0.04	-0.04	-0.05*
	[-2.23]	[-2.07]	[-1.36]	[-1.45]	[-1.96]
$\bar{R}^2$	0.04	0.03	0.02	0.02	0.02
Spread	-0.05	-0.05	-0.04**	-0.03*	-0.02*
	[-1.31]	[-1.64]	[-1.96]	[-1.82]	[-1.80]
$\bar{R}^2$	0.30	0.55	0.67	0.71	0.68
Controls	Yes	Yes	Yes	Yes	Yes
N	1532	1532	1532	1532	1532

Table IA.C.8: Deep Sleep and Intraday Market Responses Excluding COVID Days This table reports regressions in which the dependent variables are intraday market outcomes measured from the market open on day t through to horizon τ on the same trading day, where $\tau \in \{60, 120, 180, 300\}$ minutes, as well as over the full open-to-close trading day, which corresponds to $\tau = 390$ minutes. The dependent variables capture several dimensions of intraday market quality: (i) intraday price dynamics, measured by cumulative returns over the corresponding window (*Return*); (ii) realized volatility constructed from high-frequency returns (RV); (iii) intraday volatility asymmetry, measured as the difference between positive and negative realized volatility components ($RV^+ - RV^-$); and (iv) liquidity and trading-cost measures, including the Amihud illiquidity measure, defined as the absolute return divided by dollar trading volume, and the average relative bid–ask spread (*Spread*). Detailed definitions, construction procedures, and timing conventions for all dependent variables are provided in Section IA.A. The key explanatory variable is the abnormal component of deep sleep on night $t-1$, that is, the night between the close of trading day $t-1$ and the open of trading day t. This variable is obtained by filtering the deep-sleep measure defined in equation (1) through equation (3). All regressions include the previous trading day's open-to-close return, the overnight return, lagged economic policy uncertainty (EPU_{t-1}), and the lagged dependent variable (y_{t-1}) as controls. All variables are standardized. The sample spans April 26, 2017 to May 26, 2023, excluding observations between February 2020 and April 2020, inclusive. t-statistics based on Newey and West (1987) standard errors are reported in brackets.

Minutes (τ)	60	120	180	300	Close
Return	0.07	0.07	0.05	0.04	0.05
	[2.97]	[2.82]	[2.42]	[1.57]	[2.02]
$\bar{R}^2$	0.00	0.00	0.01	0.01	0.00
RV	-0.03	-0.04	-0.04	-0.04	-0.03
	[-2.33]	[-2.93]	[-2.96]	[-2.83]	[-2.79]
$\bar{R}^2$	0.63	0.64	0.65	0.67	0.67
RV^+-RV^-	0.07	0.05	0.05	0.03	0.04
	[2.90]	[2.26]	[2.08]	[1.01]	[1.58]
$\bar{R}^2$	0.01	0.02	0.03	0.04	0.05
Amihud	-0.05	-0.05	-0.03	-0.03	-0.05
	[-2.04]	[-2.01]	[-1.27]	[-1.33]	[-1.92]
$\bar{R}^2$	0.04	0.02	0.02	0.02	0.02
AvgRelSpread	-0.05	-0.05	-0.05	-0.03	-0.02
	[-1.27]	[-1.65]	[-1.97]	[-1.57]	[-1.39]
$\bar{R}^2$	0.18	0.44	0.59	0.64	0.62
Controls	Yes	Yes	Yes	Yes	Yes
N	1491	1491	1491	1491	1491

Table IA.C.9: Deep Sleep and Intraday Market Responses Excluding Macro Announcement Days

This table reports regressions in which the dependent variables are intraday market outcomes measured from the market open on day t through to horizon τ on the same trading day, where $\tau \in \{60, 120, 180, 300\}$ minutes, as well as over the full open-to-close trading day, which corresponds to $\tau = 390$ minutes. The dependent variables capture several dimensions of intraday market quality: (i) intraday price dynamics, measured by cumulative returns over the corresponding window (*Return*); (ii) realized volatility constructed from high-frequency returns (RV); (iii) intraday volatility asymmetry, measured as the difference between positive and negative realized volatility components ($RV^+ - RV^-$); and (iv) liquidity and trading-cost measures, including the Amihud illiquidity measure, defined as the absolute return divided by dollar trading volume, and the average relative bid–ask spread (*Spread*). Detailed definitions, construction procedures, and timing conventions for all dependent variables are provided in Section IA.A. The key explanatory variable is the abnormal component of deep sleep on night $t-1$, that is, the night between the close of trading day $t-1$ and the open of trading day t. This variable is obtained by filtering the deep-sleep measure defined in equation (1) through equation (3). All regressions include the previous trading day's open-to-close return, the overnight return, lagged economic policy uncertainty (EPU_{t-1}), and the lagged dependent variable (y_{t-1}) as controls. All variables are standardized. The sample spans April 26, 2017 to May 26, 2023, excluding macro announcement days corresponding to GDP, CPI, and nonfarm payroll releases. t-statistics based on Newey and West (1987) standard errors are reported in brackets.

Minutes (τ)	60	120	180	300	Close
Return	0.06	0.07	0.07	0.05	0.06
	[2.51]	[2.81]	[2.65]	[1.87]	[2.30]
$\bar{R}^2$	0.01	0.03	0.01	0.01	0.00
RV	-0.02	-0.03	-0.03	-0.03	-0.02
	[-2.29]	[-3.26]	[-3.32]	[-2.96]	[-2.62]
$\bar{R}^2$	0.73	0.75	0.76	0.78	0.78
RV^+-RV^-	0.06	0.06	0.05	0.03	0.04
	[2.58]	[2.46]	[2.17]	[1.01]	[1.51]
$\bar{R}^2$	0.03	0.06	0.04	0.05	0.04
Amihud	-0.05	-0.05	-0.03	-0.03	-0.05
	[-1.99]	[-1.75]	[-0.91]	[-0.98]	[-1.56]
$\bar{R}^2$	0.04	0.02	0.03	0.02	0.02
AvgRelSpread	-0.06	-0.05	-0.05	-0.03	-0.03
	[-1.39]	[-1.81]	[-2.13]	[-1.95]	[-1.85]
$\bar{R}^2$	0.30	0.55	0.67	0.71	0.68
Controls	Yes	Yes	Yes	Yes	Yes
N	1364	1364	1364	1364	1364

Table IA.C.10: Deep Sleep and Intraday Market Responses Controlling for Absolute Overnight Returns

This table reports regressions in which the dependent variables are intraday market outcomes measured from the market open on day t through to horizon τ on the same trading day, where $\tau \in \{60, 120, 180, 300\}$ minutes, as well as over the full open-to-close trading day, which corresponds to $\tau = 390$ minutes. The dependent variables capture several dimensions of intraday market quality: (i) intraday price dynamics, measured by cumulative returns over the corresponding window (*Return*); (ii) realized volatility constructed from high-frequency returns (RV); (iii) intraday volatility asymmetry, measured as the difference between positive and negative realized volatility components ($RV^+ - RV^-$); and (iv) liquidity and trading-cost measures, including the Amihud illiquidity measure, defined as the absolute return divided by dollar trading volume, and the average relative bid–ask spread (*Spread*). Detailed definitions, construction procedures, and timing conventions for all dependent variables are provided in Section IA.A. The key explanatory variable is the abnormal component of deep sleep on night $t-1$, that is, the night between the close of trading day $t-1$ and the open of trading day t. This variable is obtained by filtering the deep-sleep measure defined in equation (1) through equation (3). All regressions include the previous trading day's open-to-close return, the overnight return, the absolute value of the overnight return, lagged economic policy uncertainty (EPU_{t-1}), and the lagged dependent variable (y_{t-1}) as controls. All variables are standardized. The sample spans April 26, 2017 to May 26, 2023. t-statistics based on Newey and West (1987) standard errors are reported in brackets.

Minutes (τ)	60	120	180	300	Close
Return	0.06	0.07	0.06	0.05	0.05
	[2.72]	[3.03]	[2.75]	[1.99]	[2.24]
$\bar{R}^2$	0.02	0.03	0.02	0.01	0.01
RV	-0.02	-0.03	-0.03	-0.03	-0.03
	[-2.10]	[-3.05]	[-3.32]	[-3.06]	[-2.88]
$\bar{R}^2$	0.72	0.75	0.76	0.78	0.79
RV^+-RV^-	0.06	0.06	0.05	0.03	0.03
	[2.77]	[2.52]	[2.13]	[1.11]	[1.45]
$\bar{R}^2$	0.04	0.08	0.06	0.07	0.08
Amihud	-0.06	-0.05	-0.04	-0.04	-0.06
	[-2.33]	[-2.18]	[-1.40]	[-1.49]	[-2.01]
$\bar{R}^2$	0.05	0.05	0.04	0.03	0.03
AvgRelSpread	-0.05	-0.05	-0.04	-0.03	-0.02
	[-1.38]	[-1.71]	[-2.03]	[-1.89]	[-1.85]
$\bar{R}^2$	0.33	0.56	0.67	0.71	0.68
Controls	Yes	Yes	Yes	Yes	Yes
N	1532	1532	1532	1532	1532

IA.D Additional Figures

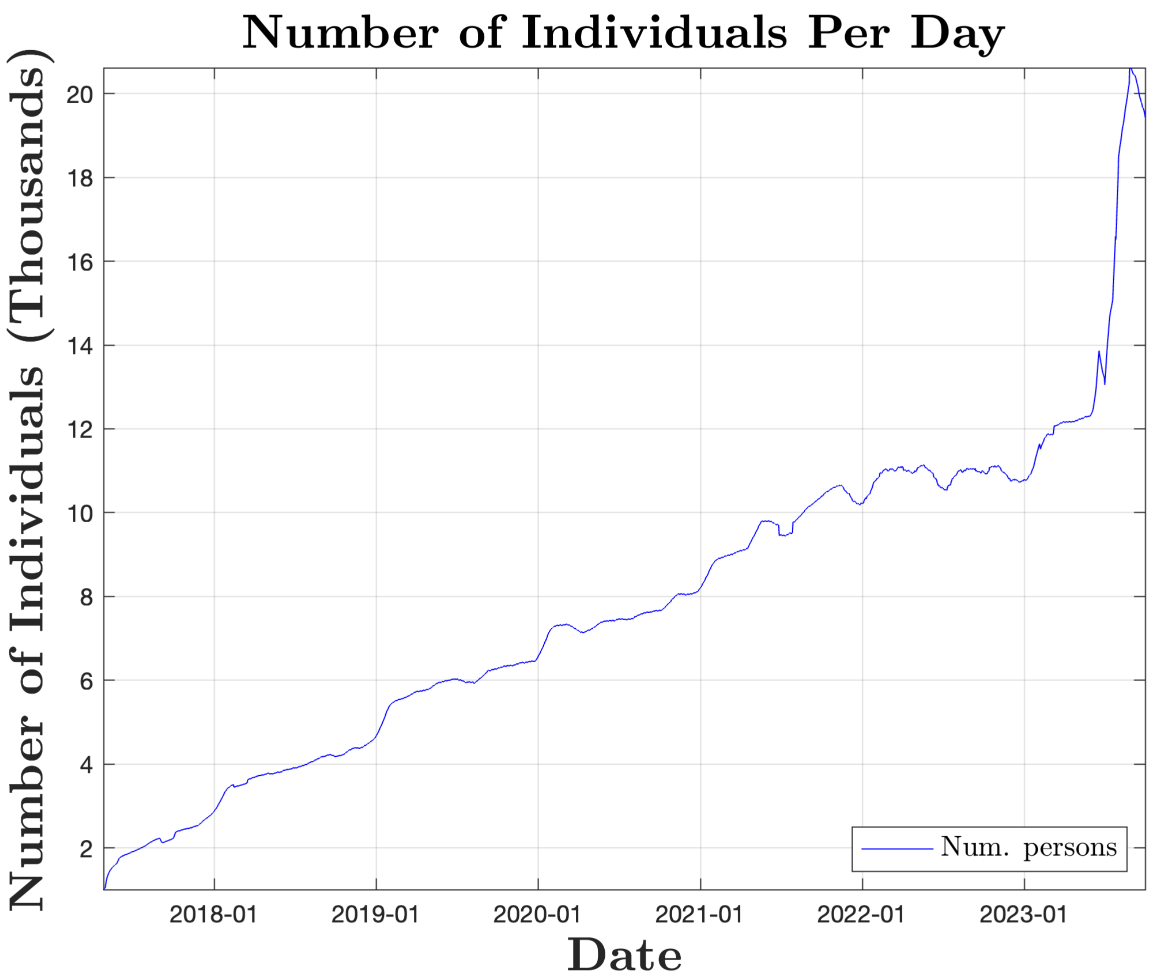

Figure IA.D.1: Unique individuals per day
The figure reports the number of unique individuals in the NIH *All of Us* Research Program on each day of the sample period. We retain only individual–day observations for which the "is_main_sleep" flag in the *All of Us* data is true and drop days with fewer than 1,000 individuals with valid data. For visual clarity, we plot the 30-day moving average of the daily counts. The resulting sample runs from April 26, 2017 through May 26, 2023.

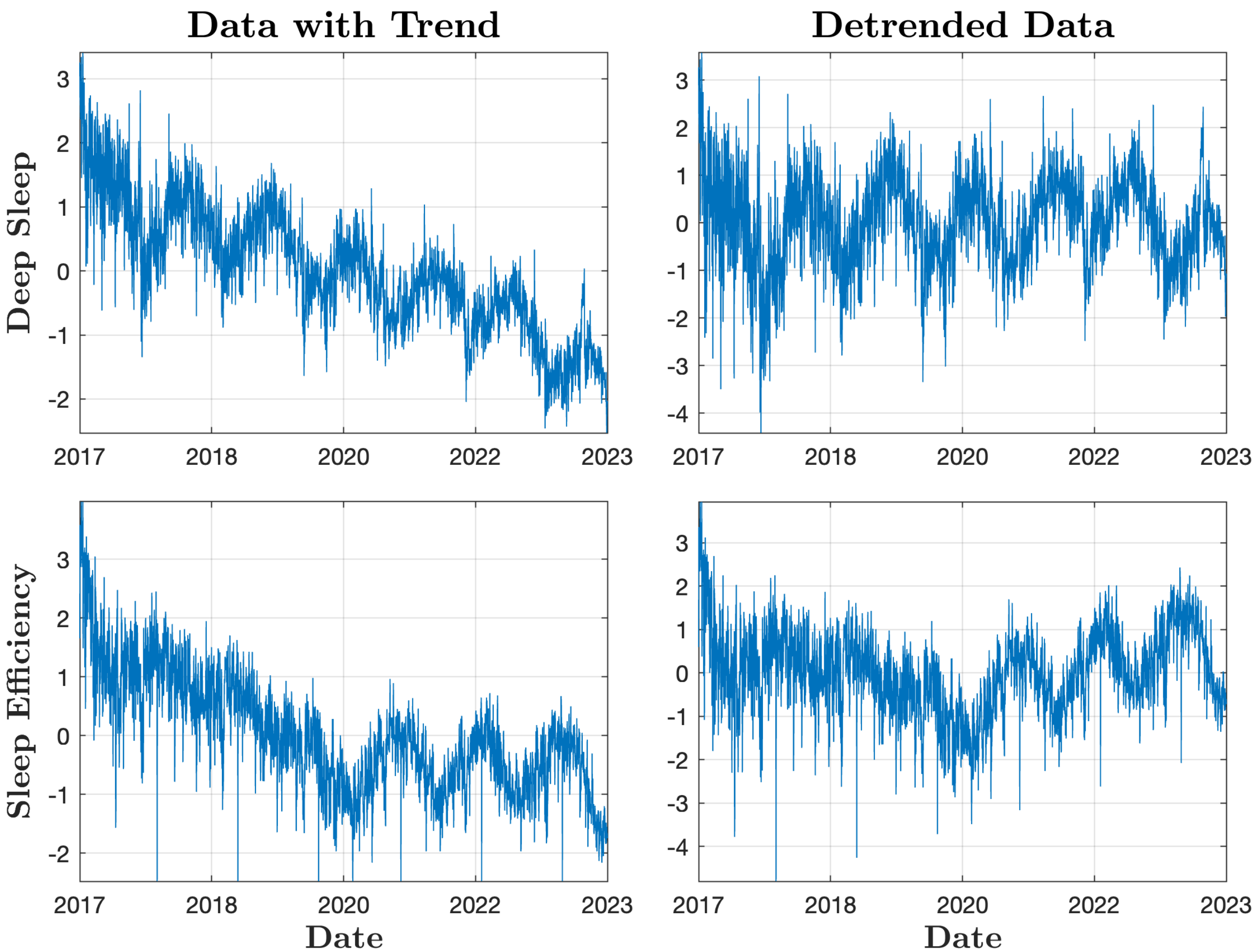

Figure IA.D.2: Aggregate sleep quality with and without linear time trend
The figure provides the daily time series of aggregate sleep quality, defined in Section 1.4.1, with and without removing a linear time trend. The top row of the figure displays the time series of the aggregate deep-sleep share, defined via equation (1), while the bottom row of the figure displays the time series of aggregate sleep efficiency, defined via equation (2). The left column of the figure shows the raw aggregate time series associated with each variable before removing day-of-the-week fixed effects and winsorization. The right column of the figure shows the linearly detrended aggregate time series of each variable. Specifically, the data is detrended by projecting the daily time series of each measure of sleep quality on a time index that takes on a value of one on the first day of the sample period, and is incremented by one on each subsequent day. The detrended series is obtained as the residual of this projection.

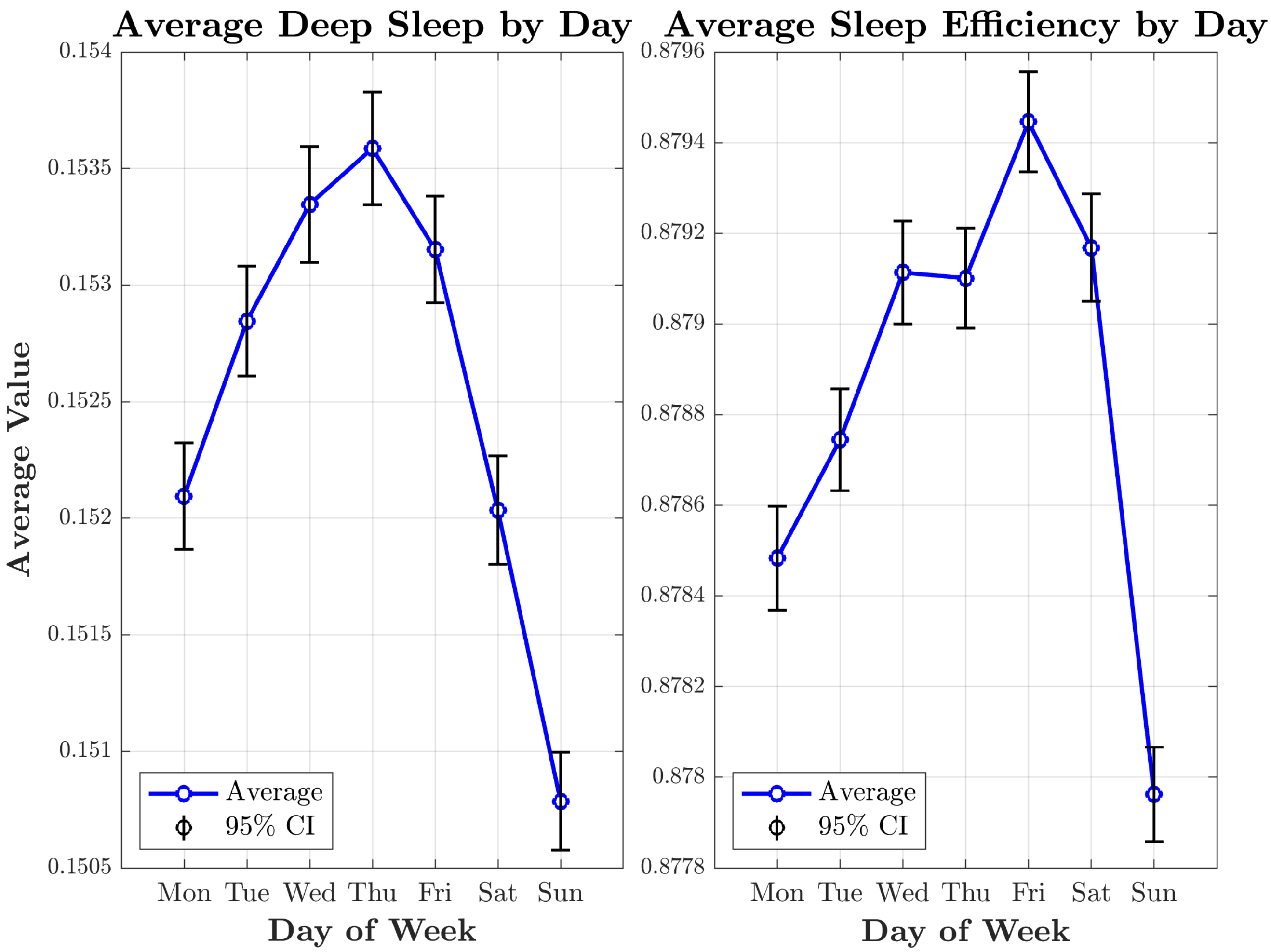

Figure IA.D.3: Aggregate sleep quality and day-of-the-week effects
The figure provides the average value of each measure of aggregate sleep quality, defined in Section 1.4.1, on each weekday of the sample period. The left column of the figure displays the average value of the aggregate deep-sleep share, defined via equation (1), on each day of the week across the entire sample period, while the right column displays the average value of aggregate sleep efficiency, defined via equation (2). Each point on the plot presents the average value on a given day of the week and the black bars present the 95% confidence interval associated with each mean.

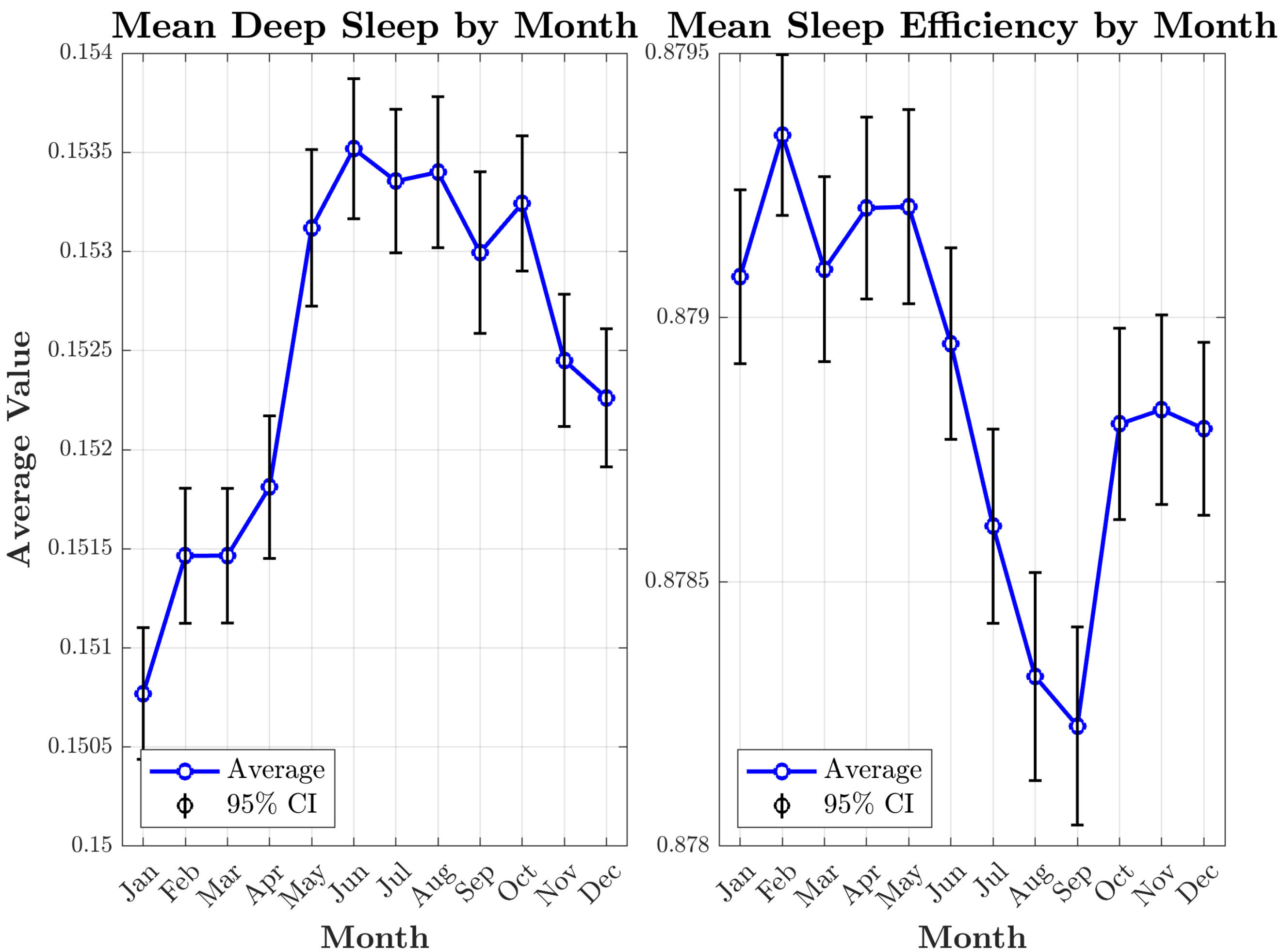

Figure IA.D.4: Aggregate sleep quality and month-of-the-year effects
The figure provides the average value of each measure of aggregate sleep quality, defined in Section 1.4.1, on each month of the sample period. The left panel of the figure displays the average value of the aggregate deep-sleep share, defined via equation (1), in each month of the year across the entire sample period, while the right panel displays the average value of aggregate sleep efficiency, defined via equation (2). Each point on the plot presents the average value in a given month of the year and the black bars present the 95% confidence interval associated with each mean.

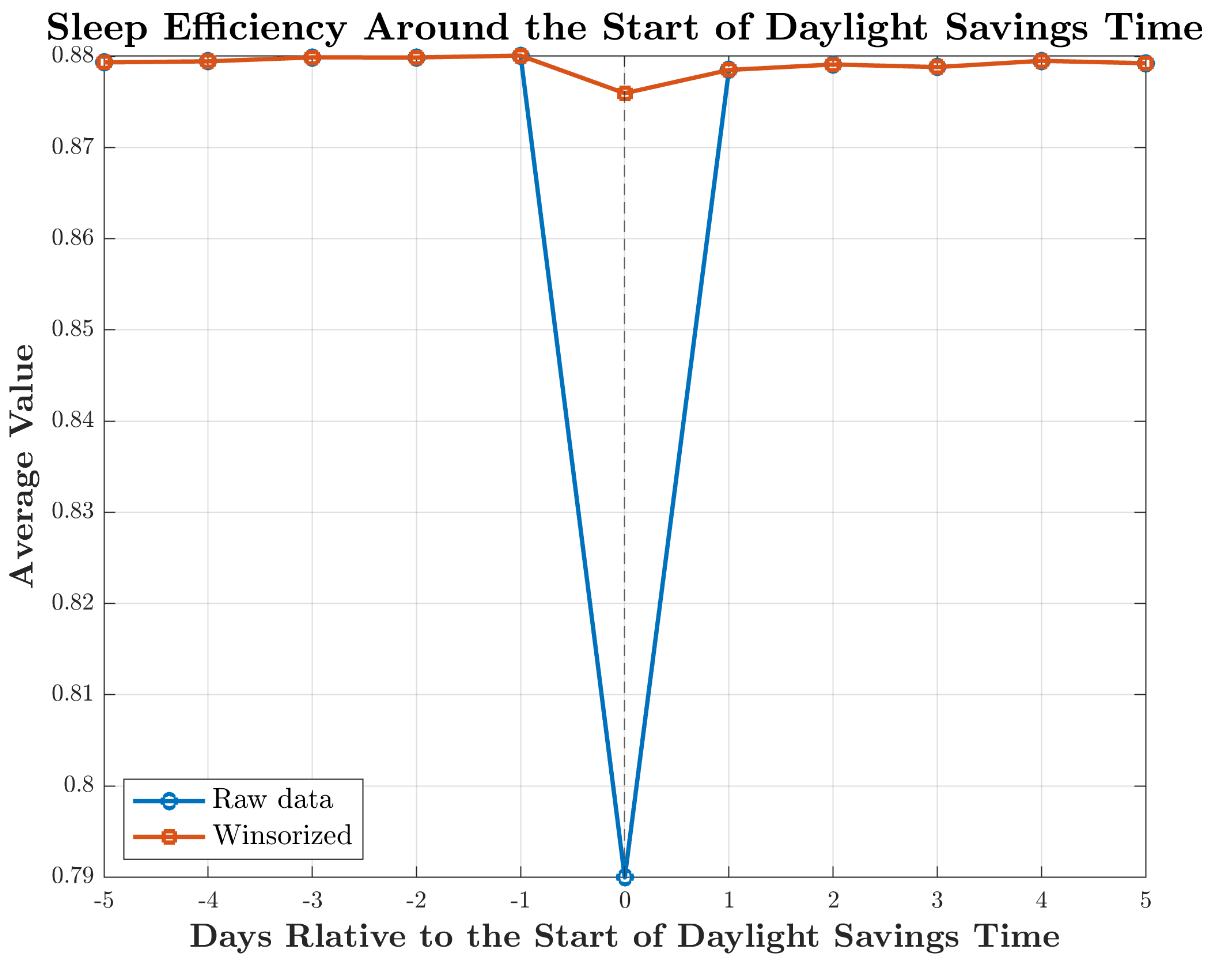

Figure IA.D.5: Aggregate sleep efficiency and the effects of winsorization
The figure provides the average value of aggregate sleep efficiency, defined via equation (2), in the 11-day event window surrounding each year's start of Daylight Saving Time (DST). For each event date, we compute the daily value of aggregate sleep efficiency, and then take the mean value of this time series across all six time changes during our sample period. The blue line reports the results of this analysis when we do not winsorize the sleep data at the 1% level, while the red line reports the results of this analysis after winsorizing the data.

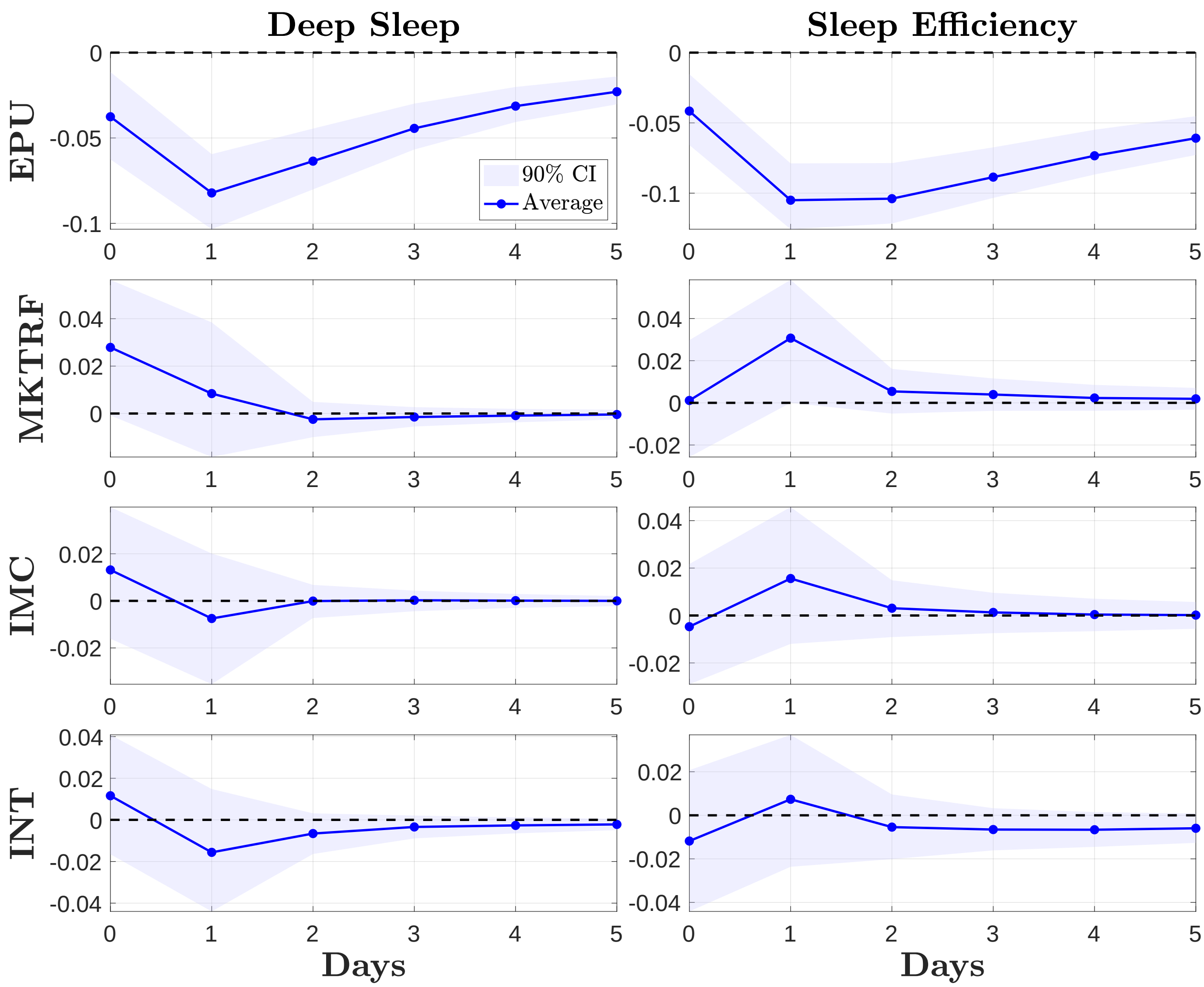

Figure IA.D.6: Impulse response functions: Additional first-moment controls
The figure reports impulse response functions (IRFs) that display how structural shocks to each of the economic variables, measured using the natural logarithm of the daily Economic Policy Uncertainty (EPU) index of Baker *et al.* (2016) and three additional first-moment controls, propagate to the proportion of deep sleep (left panel), measured via equation (1), and sleep efficiency (right panel), measured via equation (2). These IRFs are obtained by first augmenting the vector autoregression presented by equation (6) to include three extra variables. These three additional variables are included in the vector $\boldsymbol{y}_t$ immediately preceding the EPU index. The three variables are the daily excess market return, denoted by MKTRF, the daily return on the investment-minus-consumption spread of Papanikolaou (2011), denoted by IMC, and the daily return on the intermediary capital factor of He *et al.* (2017), denoted by INT. We obtain the IRFs by estimating the vector autoregression and employing the recursive (Cholesky-based) identification of each structural shock. The top row of the figure shows the IRFs associated with EPU, the second row shows the IRFs associated with MKTRF, the third row shows the IRFs associated with IMC, and the final row shows the IRFs associated with INT. The solid blue line in each panel represents the average effect, and the 90% confidence interval represented by the blue-shaded region is obtained using a residual bootstrap with one thousand draws from the estimated residuals. Finally, the analysis uses daily data that spans each trading day from April 26, 2017 through May 26, 2023.

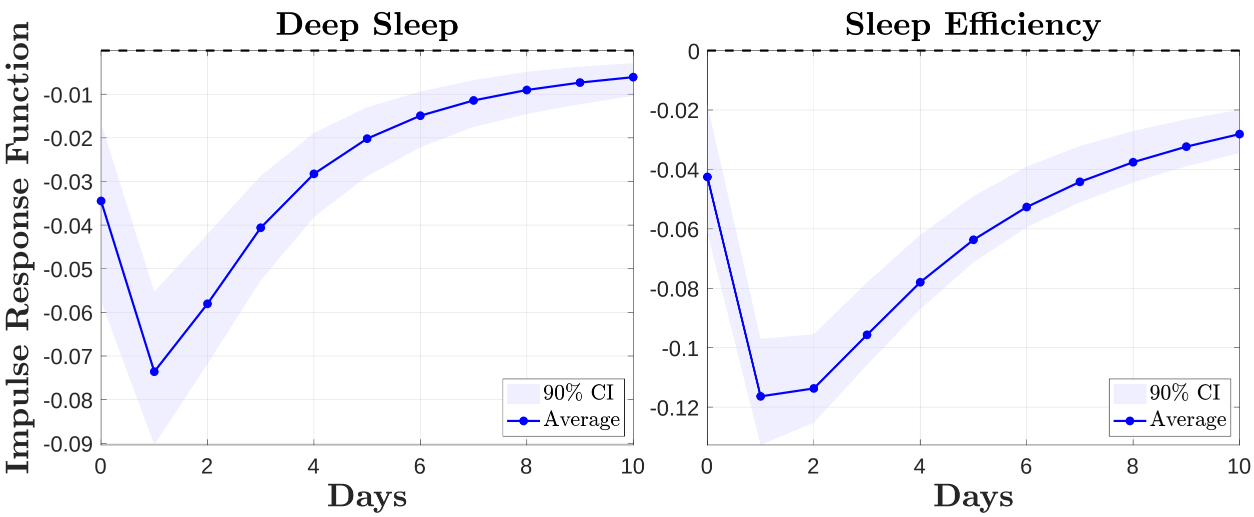

Figure IA.D.7: Impulse response functions: Generalized (order-invariant) responses The figure reports impulse response functions (IRFs) that display how a structural shock to economic uncertainty, measured using the natural logarithm of the daily Economic Policy Uncertainty (EPU) index of Baker *et al.* (2016), propagates to the proportion of deep sleep (left panel), measured via equation (1), and sleep efficiency (right panel), measured via equation (2). These IRFs are obtained by estimating the vector autoregression presented by equation (6) and employing the order-invariant generalized IRF identification scheme described by Pesaran and Shin (1998). The solid blue line in each panel represents the average effect, and the 90% confidence interval represented by the blue-shaded region is obtained using a residual bootstrap with one thousand draws from the estimated residuals. Finally, the analysis uses daily data and runs from April 26, 2017 through May 26, 2023.

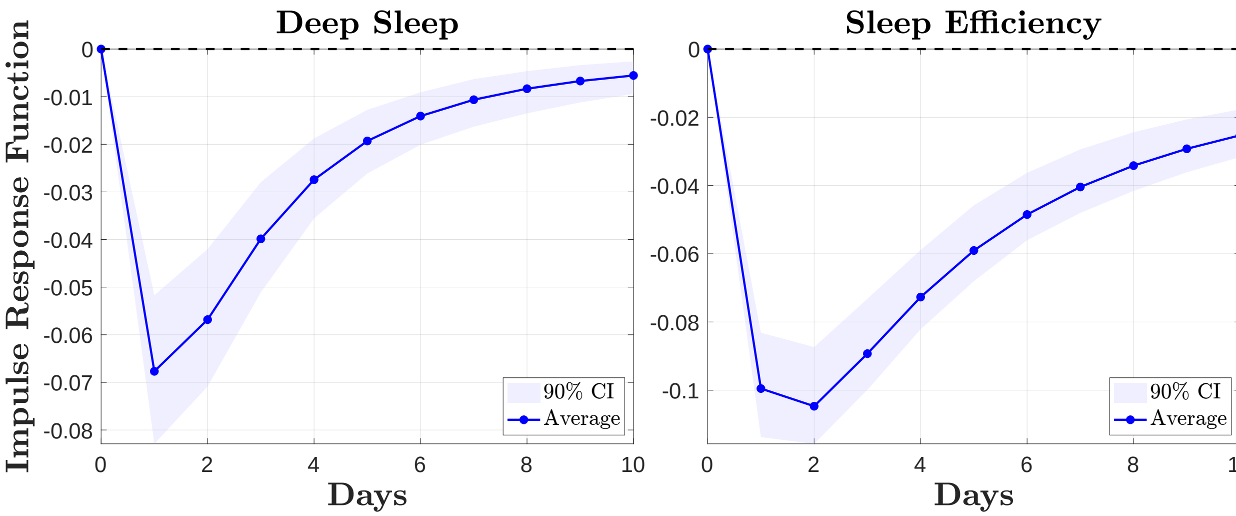

Figure IA.D.8: Impulse response functions: EPU last

The figure reports impulse response functions (IRFs) that display how a structural shock to economic uncertainty, measured using the natural logarithm of the daily Economic Policy Uncertainty (EPU) index of Baker *et al.* (2016), propagates to the proportion of deep sleep (left panel), measured via equation (1), and sleep efficiency (right panel), measured via equation (2). These IRFs are obtained by estimating the vector autoregression presented by equation (6) and employing the recursive (Cholesky-based) identification of structural shocks. However, in contrast to the baseline analysis, the EPU index is placed last in the vector of variables that enter the VAR. The solid blue line in each panel represents the average effect, and the 90% confidence interval represented by the blue-shaded region is obtained using a residual bootstrap with one thousand draws from the estimated residuals. Finally, the analysis uses daily data and runs from April 26, 2017 through May 26, 2023.

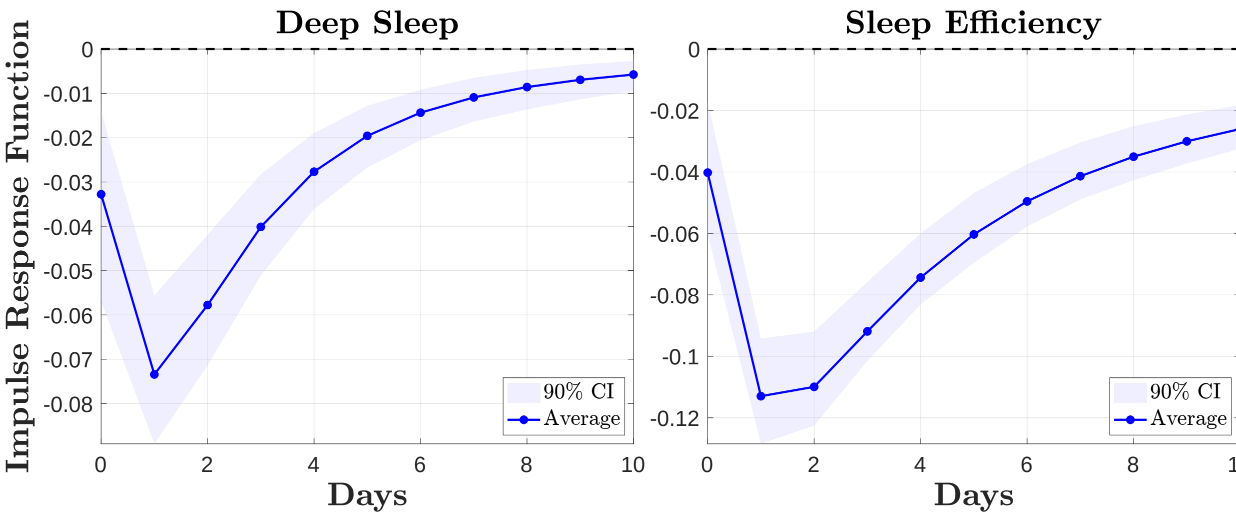

Figure IA.D.9: Impulse response functions: Sleep last
The figure reports impulse response functions (IRFs) that display how a structural shock to economic uncertainty, measured using the natural logarithm of the daily Economic Policy Uncertainty (EPU) index of Baker *et al.* (2016), propagates to the proportion of deep sleep (left panel), measured via equation (1), and sleep efficiency (right panel), measured via equation (2). These IRFs are obtained by estimating the vector autoregression presented by equation (6) and employing the recursive (Cholesky-based) identification of structural shocks. However, in contrast to the baseline analysis, the measure of sleep quality is placed last in the vector of variables that enter the VAR. The solid blue line in each panel represents the average effect, and the 90% confidence interval represented by the blue-shaded region is obtained using a residual bootstrap with one thousand draws from the estimated residuals. Finally, the analysis uses daily data and runs from April 26, 2017 through May 26, 2023.

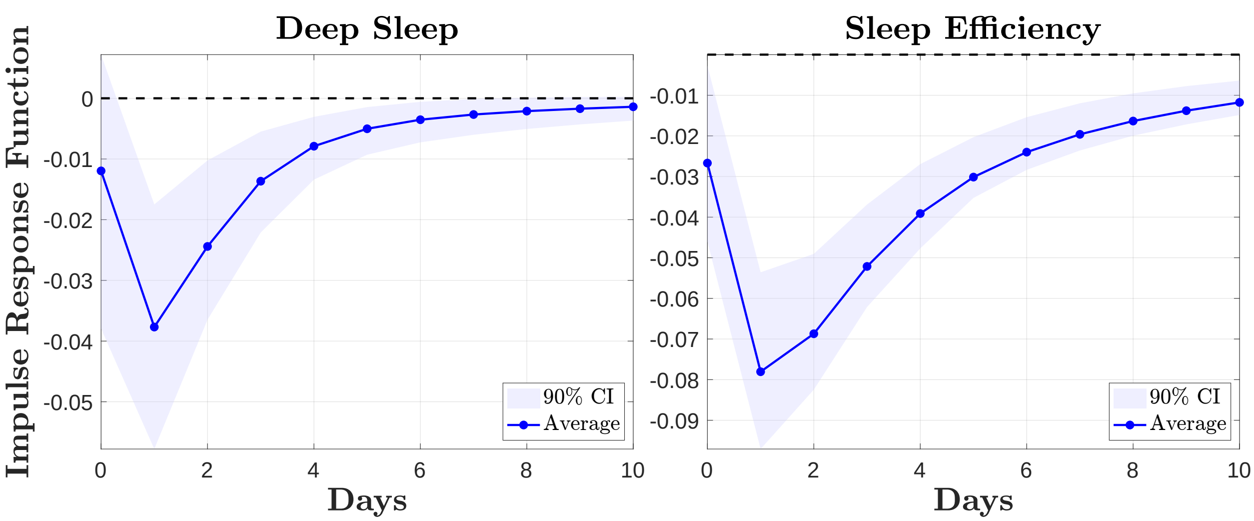

Figure IA.D.10: Impulse response functions: Equity market volatility
The figure reports impulse response functions (IRFs) that display how a structural shock to economic uncertainty, measured using the equity market volatility index, propagates to the proportion of deep sleep (left panel), measured via equation (1), and sleep efficiency (right panel), measured via equation (2). These IRFs are obtained by estimating the vector autoregression presented by equation (6) and employing the recursive (Cholesky-based) identification of structural shocks. The solid blue line in each panel represents the average effect, and the 90% confidence interval represented by the blue-shaded region is obtained using a residual bootstrap with one thousand draws from the estimated residuals. Finally, the analysis uses daily data and runs from from April 26, 2017 through May 26, 2023.

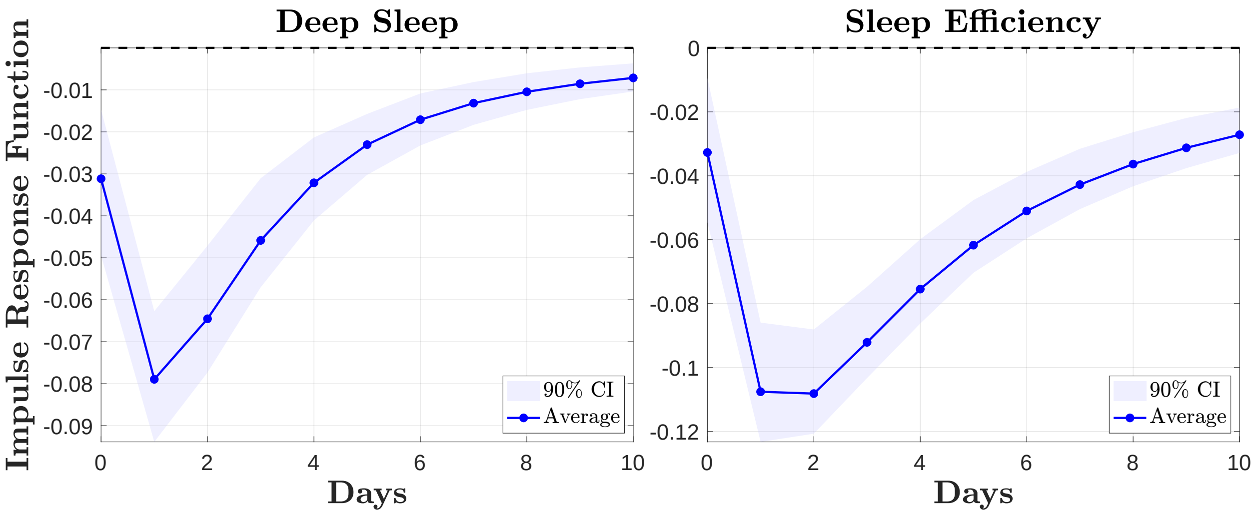

Figure IA.D.11: Impulse response functions: Cross-sectional average
The figure reports impulse response functions (IRFs) that display how a structural shock to economic uncertainty, measured using the natural logarithm of the daily Economic Policy Uncertainty (EPU) index of Baker *et al.* (2016), propagates to the proportion of deep sleep (left panel), measured via equation (1), and sleep efficiency (right panel), measured via equation (2). Unlike the baseline analysis that aggregates observations across individuals by taking the cross-sectional median value each day, the sleep quality data underlying this figure computes the daily cross-sectional average value. These IRFs are then obtained by estimating the vector autoregression presented by equation (6) and employing the recursive (Cholesky-based) identification of structural shocks. The solid blue line in each panel represents the average effect, and the 90% confidence interval represented by the blue-shaded region is obtained using a residual bootstrap with one thousand draws from the estimated residuals. The analysis uses daily data and runs from April 26, 2017 through May 26, 2023.

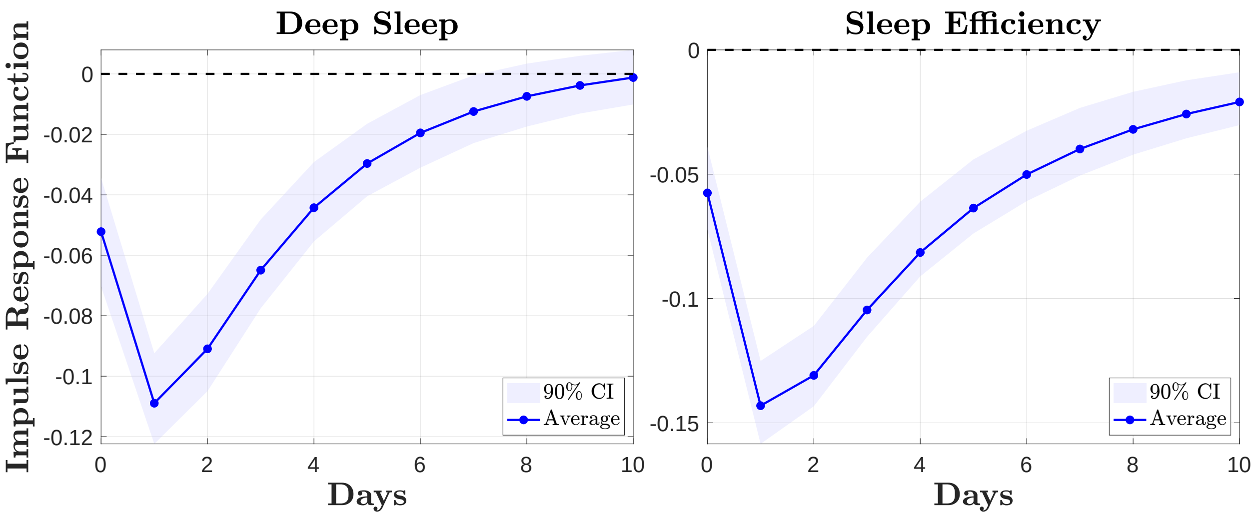

Figure IA.D.12: Impulse response functions: No time trend

The figure reports impulse response functions (IRFs) that display how a structural shock to economic uncertainty, measured using the natural logarithm of the daily Economic Policy Uncertainty (EPU) index of Baker *et al.* (2016), propagates to the proportion of deep sleep (left panel), measured via equation (1), and sleep efficiency (right panel), measured via equation (2). Unlike the baseline analysis that removes a time trend from the aggregate measures of sleep quality (as discussed in Section 1.4.1 of the main text), the sleep quality data underlying this figure is not detrended. These IRFs are then obtained by estimating the vector autoregression presented by equation (6) and employing the recursive (Cholesky-based) identification of structural shocks. The solid blue line in each panel represents the average effect, and the 90% confidence interval represented by the blue-shaded region is obtained using a residual bootstrap with one thousand draws from the estimated residuals. Finally, the analysis uses daily data and runs from April 26, 2017 through May 26, 2023.

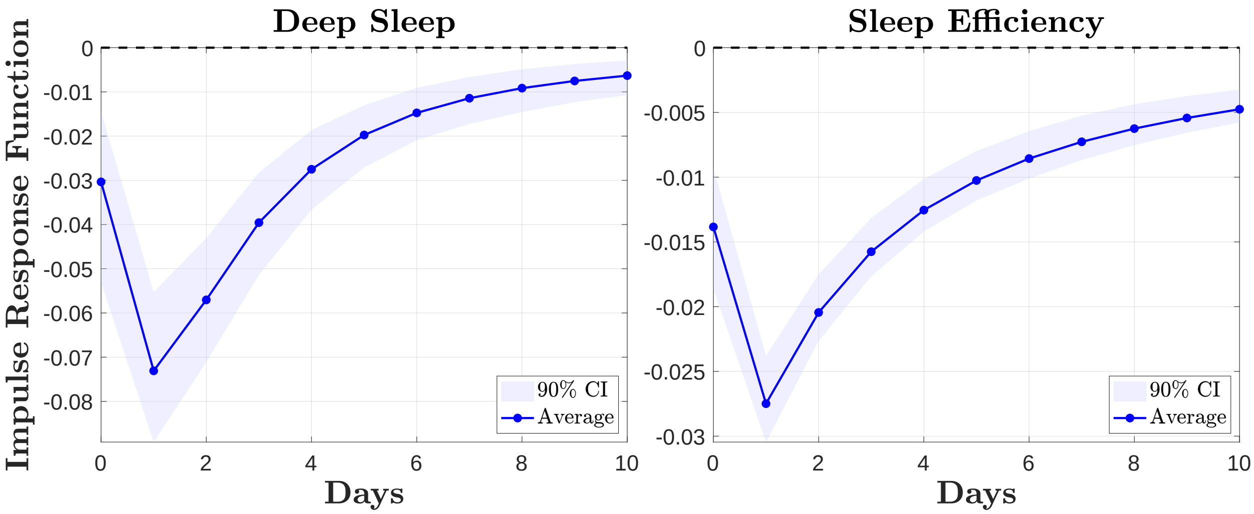

Figure IA.D.13: Impulse response functions: No winsorization and holiday fixed effects

The figure reports impulse response functions (IRFs) that display how a structural shock to economic uncertainty, measured using the natural logarithm of the daily Economic Policy Uncertainty (EPU) index of Baker *et al.* (2016), propagates to the proportion of deep sleep (left panel), measured via equation (1), and sleep efficiency (right panel), measured via equation (2). Unlike the baseline analysis that winsorizes the sleep quality measures at the 1% level (as discussed in Section 1.4.1 of the main text), the sleep quality data underlying this figure is not winsorized. However, the VAR also includes a comprehensive set of fixed effects that capture differences in sleep quality on (i) the days that Daylight Saving Time starts and ends, (ii) Federal holidays, (iii) Easter, (iv) Federal election dates, and (v) major holidays, including New Year, July 4, Christmas, Thanksgiving, and Labor Day. These IRFs are then obtained by estimating the vector autoregression presented by equation (6) and employing the recursive (Cholesky-based) identification of structural shocks. The solid blue line in each panel represents the average effect, and the 90% confidence interval represented by the blue-shaded region is obtained using a residual bootstrap with one thousand draws from the estimated residuals. Finally, the analysis uses daily data and runs from April 26, 2017 through May 26, 2023.

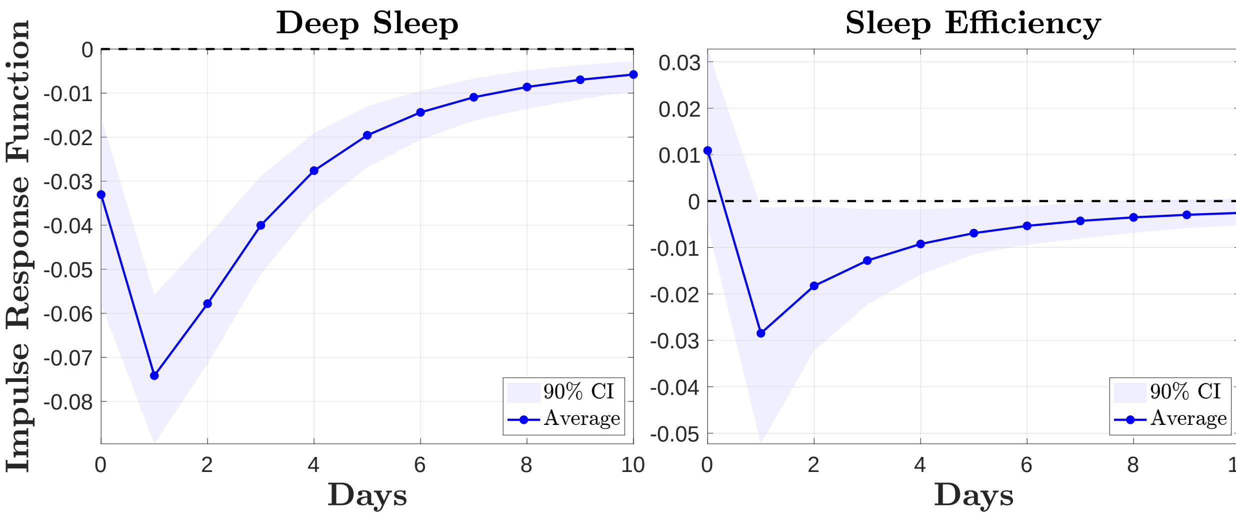

Figure IA.D.14: Impulse response functions: No winsorization
The figure reports impulse response functions (IRFs) that display how a structural shock to economic uncertainty, measured using the natural logarithm of the daily Economic Policy Uncertainty (EPU) index of Baker *et al.* (2016), propagates to the proportion of deep sleep (left panel), measured via equation (1), and sleep efficiency (right panel), measured via equation (2). Unlike the baseline analysis that winsorizes the sleep quality measures at the 1% level (as discussed in Section 1.4.1 of the main text), the sleep quality data underlying this figure is not winsorized. These IRFs are then obtained by estimating the vector autoregression presented by equation (6) and employing the recursive (Cholesky-based) identification of structural shocks. The solid blue line in each panel represents the average effect, and the 90% confidence interval represented by the blue-shaded region is obtained using a residual bootstrap with one thousand draws from the estimated residuals. Finally, the analysis uses daily data and runs from April 26, 2017 through May 26, 2023.

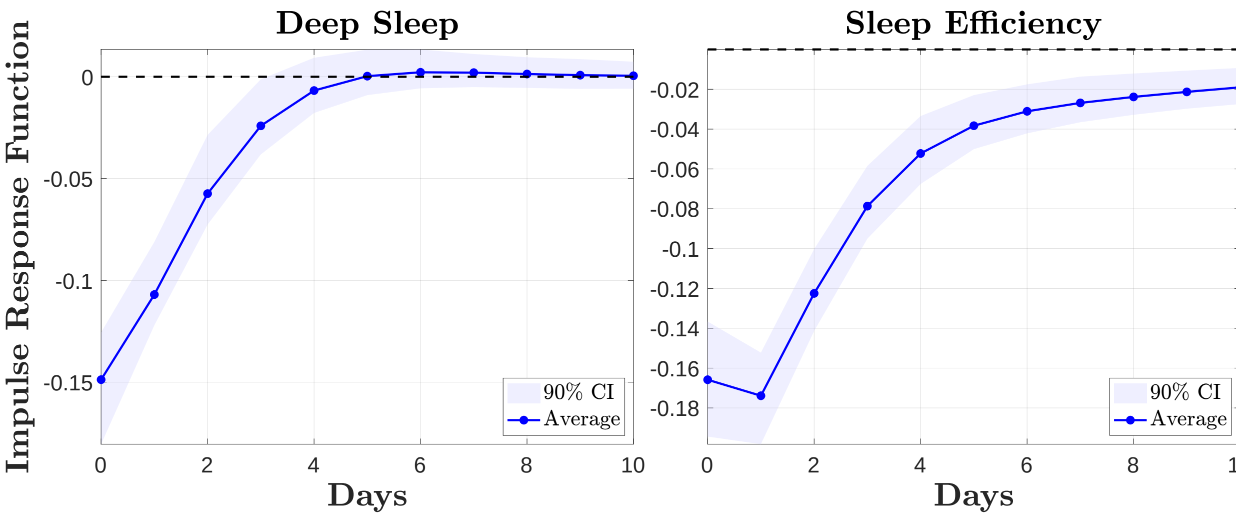

Figure IA.D.15: Impulse response functions: No calendar fixed effects

The figure reports impulse response functions (IRFs) that display how a structural shock to economic uncertainty, measured using the natural logarithm of the daily Economic Policy Uncertainty (EPU) index of Baker *et al.* (2016), propagates to the proportion of deep sleep (left panel), measured via equation (1), and sleep efficiency (right panel), measured via equation (2). Unlike the baseline analysis that removes intra-week variation in sleep quality by applying day-of-the-week fixed effects to the aggregate measures of sleep quality (as discussed in Section 1.4.1 of the main text), the sleep quality data underlying this figure is not adjusted for this intra-week seasonality. These IRFs are then obtained by estimating the vector autoregression presented by equation (6) and employing the recursive (Cholesky-based) identification of structural shocks. The solid blue line in each panel represents the average effect, and the 90% confidence interval represented by the blue-shaded region is obtained using a residual bootstrap with one thousand draws from the estimated residuals. Finally, the analysis uses daily data and runs from April 26, 2017 through May 26, 2023.

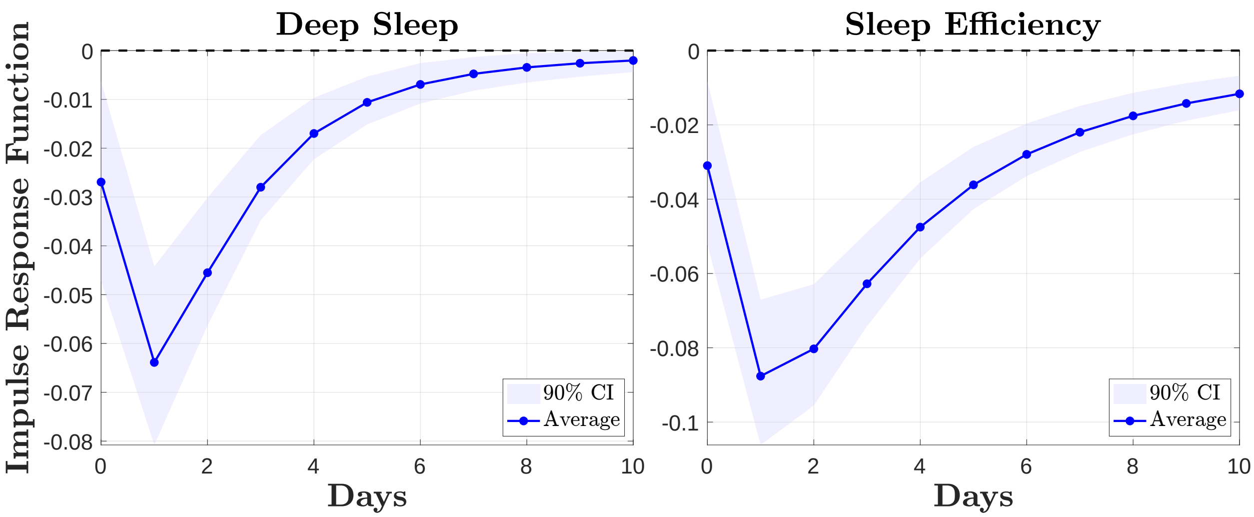

Figure IA.D.16: Impulse response functions: Baseline without COVID-19 recession The figure reports impulse response functions (IRFs) that display how a structural shock to economic uncertainty, measured using the natural logarithm of the daily Economic Policy Uncertainty (EPU) index of Baker *et al.* (2016), propagates to the proportion of deep sleep (left panel), measured via equation (1), and sleep efficiency (right panel), measured via equation (2). These IRFs are obtained by estimating the vector autoregression presented by equation (6) and employing the recursive (Cholesky-based) identification of structural shocks. The solid blue line in each panel represents the average effect, and the 90% confidence interval represented by the blue-shaded region is obtained using a residual bootstrap with one thousand draws from the estimated residuals. Finally, the data underlying this analysis is daily and runs from April 26, 2017 through May 26, 2023, excluding the NBER recession that ranged from February 2020 through April 2020.

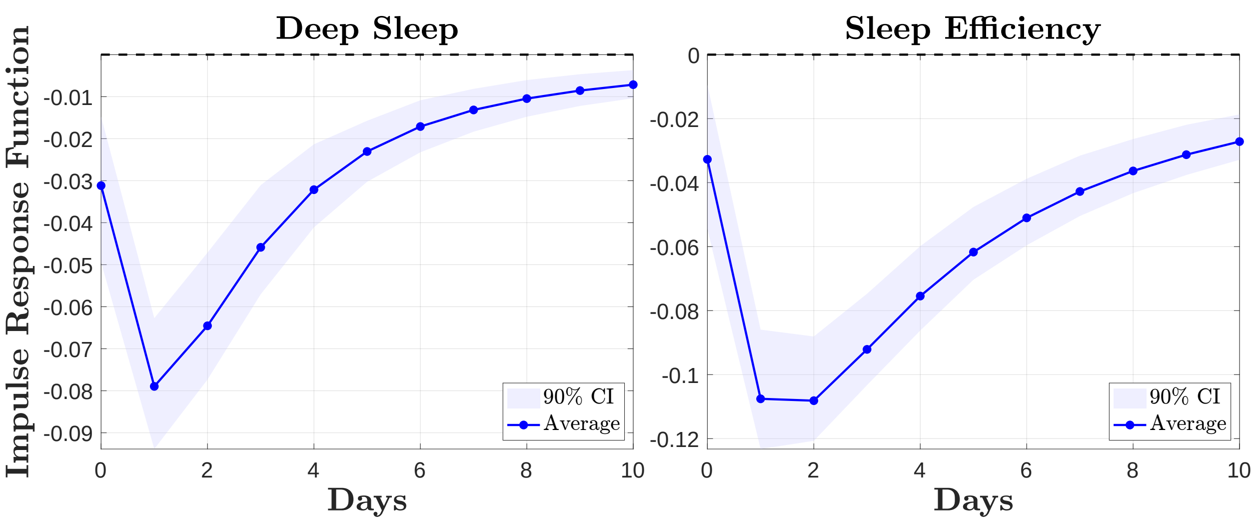

Figure IA.D.17: Impulse response functions: Baseline in recent subsample
The figure reports impulse response functions (IRFs) that display how a structural shock to economic uncertainty, measured using the natural logarithm of the daily Economic Policy Uncertainty (EPU) index of Baker *et al.* (2016), propagates to the proportion of deep sleep (left panel), measured via equation (1), and sleep efficiency (right panel), measured via equation (2). These IRFs are obtained by estimating the vector autoregression presented by equation (6) and employing the recursive (Cholesky-based) identification of structural shocks. The solid blue line in each panel represents the average effect, and the 90% confidence interval represented by the blue-shaded region is obtained using a residual bootstrap with one thousand draws from the estimated residuals. Finally, the analysis uses daily data and runs from May 10, 2020 through May 26, 2023.